ORNL-5775

ornl

OAK
RIDGE
NATIONAL
LABORATORY

UNION
CARBIDE

Preparation and Characterization of Cesium—137 Aluminosilicate Pellets for Radioactive Source Applications

F. J. Schultz
J. A. Tompkins
K. W. Haff
F. N. Case

OPERATED BY
UNION CARBIDE CORPORATION
FOR THE UNITED STATES
DEPARTMENT OF ENERGY

ORNL-5775
Distribution
Category UC-23

Contract No. W-7405-eng-26

OPERATIONS DIVISION

Space Nuclear Systems
Terrestrial Radioisotopes Applications Development
(FTP/A No. 001367)

PREPARATION AND CHARACTERIZATION OF CESIUM-137 ALUMINOSILICATE PELLETS FOR RADIOACTIVE SOURCE APPLICATIONS

F. J. Schultz
J. A. Tompkins
K. W. Haff
F. N. Case

Date Published: July 1981

OAK RIDGE NATIONAL LABORATORY
Oak Ridge, Tennessee 37830
operated by
UNION CARBIDE CORPORATION
for the
U. S. DEPARTMENT OF ENERGY

CONTENTS

FIGURE TITLES

PREPARATION AND CHARACTERIZATION OF CESIUM-137 ALUMINOSILICATE PELLETS FOR RADIOACTIVE SOURCE APPLICATIONS*

F. J. Schultz, J. A. Tompkins, K. W. Haff, and F. N. Case

Radioisotope Department

ABSTRACT

Twenty-seven fully loaded ^{137}Cs aluminosilicate pellets were fabricated in a hot cell by the vacuum hot pressing of a cesium carbonate/montmorillonite clay mixture at 1500°C and 570 psig. Four pellets were selected for characterization studies which included calorimetric measurements, metallography, scanning electron microscope and electron backscattering (SEM-BSE), electron microprobe, X-ray diffraction, and cesium ion leachability measurements. Each test pellet contained 437 to 450 curies of ^{137}Cs as determined by calorimetric measurements. Metallographic examinations revealed a two-phase system: a primary, granular, gray matrix phase containing large and small pores and small pore agglomerations, and a secondary fused phase interspersed throughout the gray matrix. SEM-BSE analyses showed that cesium and silicon were uniformly distributed throughout both phases of the pellet. This indicated that the cesium-silicon-clay reaction went to completion. Aluminum homogeneity was unconfirmed due to the high background noise associated with the inherent radioactivity of the test specimens. X-ray diffraction analyses of both radioactive and non-radioactive aluminosilicate pellets confirmed the crystal lattice structure to be pollucite. Cesium ion quasi-static leachability measurements determined the leach rates of fully loaded ^{137}Cs sectioned pollucite pellets to date to be 4.61 to 34.4 $\times 10^{-10}$ kg $m^{-2}s^{-1}$, while static leach tests performed on unsectioned fully loaded pellets showed the leach rates of the cesium ion to date to be 2.25 to 3.41 $\times 10^{-12}$ kg $m^{-2}s^{-1}$. The cesium ion diffusion coefficients through the pollucite pellet were calculated using Fick's first and second laws of diffusion. The diffusion coefficients calculated for three tracer level ^{137}Cs aluminosilicate pellets were $1.29 \times 10^{-16} m^2 s^{-1}$, $6.88 \times 10^{-17} m^2 s^{-1}$, and $1.35 \times 10^{-17} m^2 s^{-1}$, respectively.

INTRODUCTION

The demonstrated benefits that can be derived from the use of gamma-ray irradiation of sewage sludge[1,2] to further reduce pathogens,[3]

*Research sponsored by the Division of Nuclear Energy, U.S. Department of Energy under contract W-7405-eng-26 with the Union Carbide Corporation.

and of food to extend shelf life,[4,5,6] has provided incentive for the characterization of ^{137}Cs sealed sources used in process irradiation. While byproduct ^{137}Cs as cesium chloride has been used for a number of years in relatively small sealed sources, containing up to 2,500 Ci without source failure, the high solubility of the chloride has a potential for release of ^{137}Cs if the capsule fails. Investigation of low solubility compounds to overcome this problem has been carried out[7] and cesium pollucite prepared by high temperature reaction of aluminosilicate clay and ^{137}Cs carbonate has been prepared and characterized. While the gamma ray production per unit of cesium pollucite is lower than that of cesium chloride and costs are higher, the added safety of a low solubility compound is available if needed. This report describes the preparation and testing of cesium pollucite.

CESIUM POLLUCITE PELLET PRODUCTION

Experimental Procedure

The process steps involved in producing the ^{137}Cs aluminosilicate pellets are illustrated in Fig. 1. The major process steps included the following.

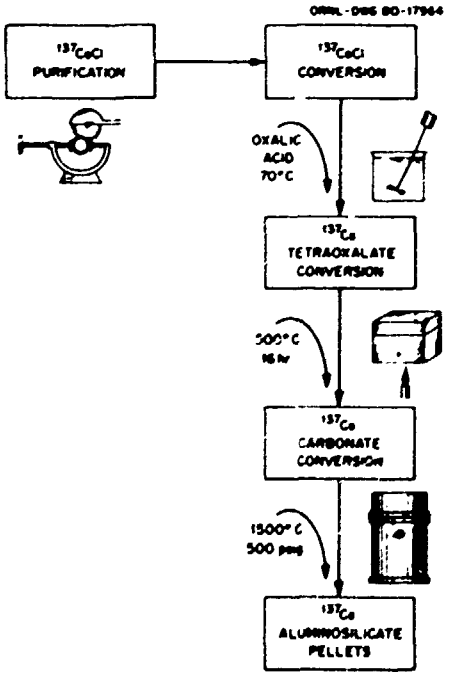

Fig. 1. Cesium-137 Aluminosilicate Pellet Production Process Steps

1. The purification of the $^{137}CsCl$ to remove impurities such as ^{137}Ba and rubidium.
2. The coprecipitation of oxalic acid crystals and cesium in the form of cesium tetraoxalate [$CsH_3(C_2O_4)_2 \cdot 2H_2O$].
3. The calcining of the cesium tetraoxalate to form cesium carbonate (Cs_2CO_3).
4. The mixing of the Cs_2CO_3 with a montmorillonite clay to form a pre-pollucite powder.
5. The vacuum hot pressing of the Cs_2CO_3/clay mixture to produce pollucite ($CsAlSi_2O_6 \cdot nH_2O$).

These steps are discussed in greater detail below.

Cesium-137 Chloride Purification

Cesium-137 chloride was received from Hanford, Washington in a shielded shipping cask (Fig. 2). The cask can hold up to two Hanford waste encapsulation and storage facility capsules in which the hot cast, solid cesium chloride is contained (Fig. 3). After removal of the cesium chloride from the capsule, it was purified[8] to remove the ^{137}Ba and rubidium impurities according to the following procedure.

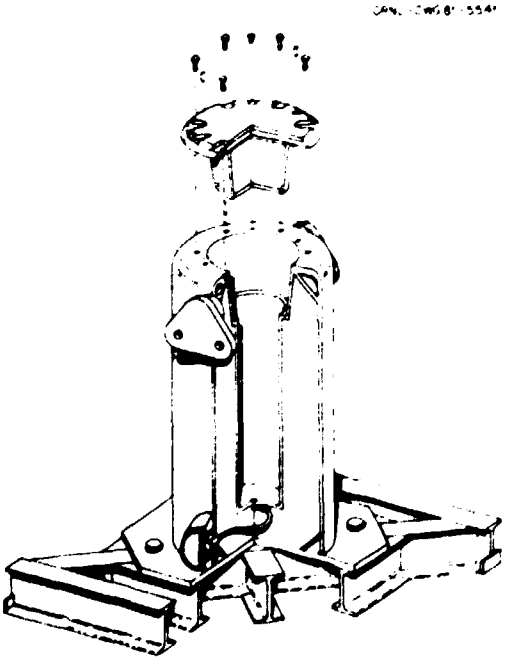

Fig. 2. Hanford Shielded Shipping Cask

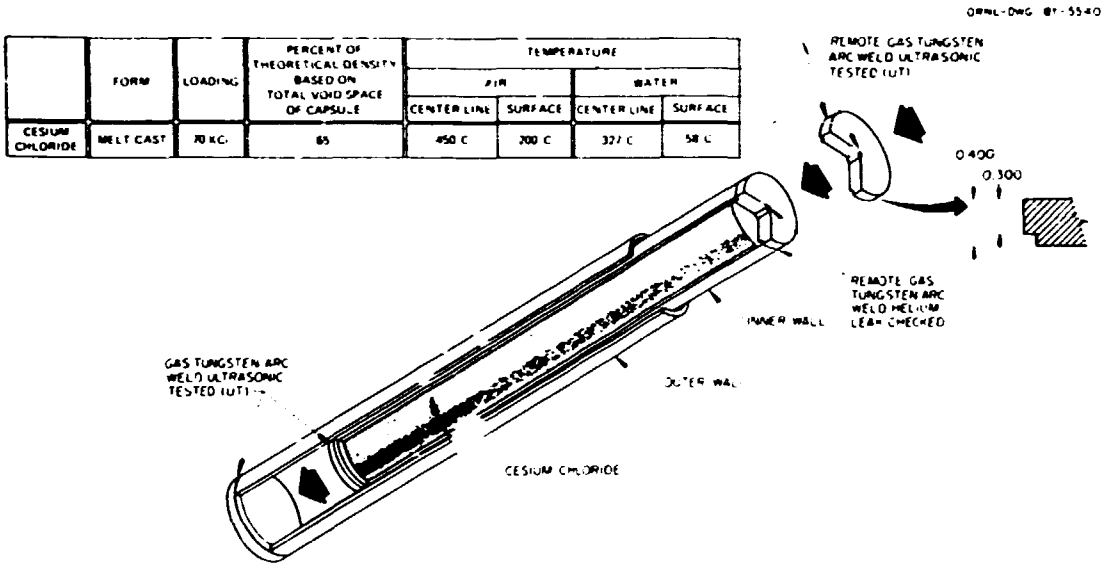

	FORM	LOADING	PERCENT OF THEORETICAL DENSITY BASED ON TOTAL VOID SPACE OF CAPSULE	TEMPERATURE			
				AIR		WATER	
				CENTER LINE	SURFACE	CENTER LINE	SURFACE
CESIUM CHLORIDE	MELT CAST	70 KG	85	450 C	200 C	327 C	58 C

	CAPSULE									
	INNER					OUTER				
	MATERIAL	WALL THICKNESS	OUTSIDE DIAMETER	TOTAL LENGTH	TOTAL CAP THICKNESS	MATERIAL	WALL THICKNESS	OUTSIDE DIAMETER	TOTAL LENGTH	TOTAL CAP THICKNESS
CESIUM CHLORIDE	316L STAINLESS STEEL (UT)	0.095 (UT)	2.250	19.725	0.400	316L AINLESS STEEL (UT)	0.109 (UT)	2.675	20.775	0.400

NOTE: ALL DIMENSIONS ARE IN INCHES — NOVEMBER 1972

Fig. 3. Hanford Waste Encapsulation and Storage Facility Capsule

1. Add 500 ml 0.10 *N* HCl to 200 g of ground cesium chloride powder.
2. Digest solution at 90°C with agitation for 1 hour. The pH is adjusted by adding 10 ml aliquots of 0.10 *N* HCl until the pH is 6 to 7.
3. Filter the digested solution through a medium porosity fritted glass filter into a vacuum flask.
4. Pour the filtered material into a tantalum beaker and boil to dryness.
5. Add 500 ml distilled water to the dried powder and stir until dissolved. Solution pH should be 6 to 7.
6. Filter the solution through a Millipore filter and transfer to the tantalum beaker.
7. Heat the solution to dryness on a hot plate set on medium heat. Constantly stir the solution to avoid caking.
8. Bake the powder on medium heat for 1 to 2 hours.

9. Weigh and store the powder in a stainless steel beaker.
10. Sample for ^{137}Cs, ^{134}Cs, ^{137}Ba, and Rb to assure product purity.

Nine 200 g batches of $^{137}CsCl$ each were processed and 1,777.5 g of pure $^{137}CsCl$ was recovered (a 98.8% recovery). A neutron activation analysis of the $^{137}CsCl$ product showed it contained 23.4 Ci/g of ^{137}Cs, giving a total of 41.6 kCi of ^{137}Cs processed. [Neutron activation analysis involves the production of a radioisotope through an (n,γ) reaction with analysis of the concomitant gamma rays as a measure of the kind and quantity of isotope present in the sample.]

Cesium-137 Chloride Conversion

The purified $^{137}CsCl$ is first converted to $CsH_3(C_2O_4)_2 \cdot 2H_2O$ through digestion with oxalic acid and the resultant solid is calcined at 500°C for 16 hours to yield Cs_2CO_3. The procedure[9] presented below was used to convert the cesium chloride to Cs_2CO_3.

1. Dissolve 570 g oxalic acid in 2.7 liters of distilled water at 70°C.
2. Dissolve 150 g purified $^{137}CsCl$ in 300 ml distilled water and mix with oxalic acid solution.
3. Digest the solution mix for 1 hour at 70°C.
4. Cool the digested solution to 14°C and hold for 30 minutes.
5. Filter crystals of $CsH_3(C_2O_4)_2 \cdot 2H_2O$ and unreacted oxalic acid through a 500 ml coarse porosity fritted glass filter and wash with 0.5 liters of saturated oxalic acid solution.
6. Transfer crystals to a glass beaker and dry at 200°C for 2 hours. Store in desiccator for combination with future batches.
7. Recycle filtrate from step 5 back to process vessel.
8. Dissolve 107 g $^{137}CsCl$ in recycle filtrate to increase cesium concentration.
9. Add 200 g oxalic acid crystals to filtrate solution and heat with gentle agitation at 70°C.
10. Repeat steps 3 through 6 and combine dry crystals with first batch produced.
11. Recycling of filtrate is repeated until a total of 4 batches of $CsH_3(C_2O_4)_2 \cdot 2H_2O$ is prepared.

12. The combined dry $CsH_3(C_2O_4)_2 \cdot 2H_2O$ containing free oxalic acid crystals is dried at 150°C for 2 hours. This procedure sublimes the oxalic acid without entrainment of the cesium and subsequent loss of product.
13. The dried $CsH_3(C_2O_4)_2 \cdot 2H_2O$ is calcined at 500°C for 16 hours. The temperature should not exceed 500°C so as to avoid cesium oxide volatility.
14. Cool the Cs_2CO_3 product, grind, and store it in a desiccator for use in pollucite preparation. Weigh and sample for determination of ^{137}Cs content and elemental impurities.

The procedure outlined above produced the quantities of Cs_2CO_3 listed in Table 1.

Table 1. Cesium Carbonate Production Yields

Type of Cs_2CO_3	Quantity of Cs_2CO_3 produced (g)	Curie content (Ci)
Full level $^{137}Cs_2CO_3$	328.4	8,177
Full level $^{137}Cs_2CO_3$	489.1	11,445
Tracer level $^{137}Cs_2CO_3$ [a]	200	4×10^{-3}
Stable Cs_2CO_3	~500	nil

[a] Approximately 200 g of tracer level Cs_2CO_3 containing 4 mCi of ^{137}Cs was produced according to the chloride conversion procedure. This powder was combined with stable Cs_2CO_3 in a 1:3 ratio to produce the 25 to 75% tracer level Cs_2CO_3 powder.

An attempt was made to minimize possible cesium oxide (Cs_2O) volatilization by reducing the calcining temperature employed in converting the $CsH_3(C_2O_4)_2 \cdot 2H_2O$ to Cs_2CO_3 from 500°C to 450°C. Also, the calcining time was reduced from 16 hours to 8 hours. Previous operating experience in producing Cs_2CO_3 suggested that the temperature and time reductions would not adversely effect the Cs_2CO_3 production. However, an earlier experiment conducted by our group had indicated that the conversion from the tetraoxalate to the carbonate was both temperature and time dependent (Table 2). The weight percent of cesium in the pure carbonate is 81.6%. The precise effect of the temperature lowering on the $CsH_3(C_2O_4)_2 \cdot 2H_2O$ conversion, however, required further elucidation. Approximately 50 g of stable (non-radioactive) Cs_2CO_3 was produced by

calcination at 450°C for varying lengths of calcining time. Three batches of powder were calcined at 450°C for 6.5, 10, and 24 hours, respectively. This range of calcining times should indicate the length of time required for full conversion to the carbonate at the reduced temperature. The results are presented in Table 3.

Table 2. Cesium Tetraoxalate Conversion Data — Part I

Sample I.D.	Calcination temperature (°C)	Duration of calcination (h)	Cesium (wt %)	Carbonate (wt %)	Oxalate (wt %)	Oxides (meq/g)
TERRA ST-2P	425	16	72.5	2.42	22.4	0.075
TERRA ST-3P	450	16	74.8	4.27	13.7	0.28
TERRA ST-9P	450	18	80.2	16.5	1.93	2.43

Table 3. Cesium Tetraoxalate Conversion Data — Part II

Sample I.D.	Calcination temperature (°C)	Duration of calcination (h)	Cesium (wt %)	Carbonate (wt %)	Oxalate (wt %)	Oxides (meq/g)
TERRA SUP 1	450	6.5	71.1	1.28	23.8	<0.05
TERRA SUP 2	450	24	72.2	16.8	2.41	<0.05
TERRA SUP 3	450	10	67.9	3.28	21.62	<0.05

The results from the calcination of the tetraoxalate at 450°C using varying lengths of calcining time indicate that ~36 to 48 hours would be required at the reduced temperature to convert an acceptable quantity of the tetraoxalate to the carbonate. The calcination time of 36 to 48 hr was determined to be excessive since 4 1/2 to 6 worker shifts (8 hr/shift) would be required to attend the calcination at the reduced temperature, while only two shifts would be necessary at the elevated temperature. The powder which had been calcined at 450°C was recalcined at 500°C for 16 hours.

Metal stirrers and process vessels were avoided during the $CsH_3(C_2O_4)_2 \cdot 2H_2O$ conversion in order to minimize possible contamination of the final product with iron, chromium, etc. Iron disrupts the $CsAlSi_2O_6 \cdot nH_2O$ crystal lattice and thus tends to weaken the aluminosilicate pellet. As a consequence glass stirrers and beakers were used

during the crucial digestion and calcination steps. Chemical analyses* for iron content in seven pollucite pellets are given in Table 4.

Table 4. Iron Content of Cesium Pollucite Pellets

Sample I.D.	Iron Content (ppm)
TERRA 3	247
TERRA 4	382
TERRA 5	277
TERRA 6	305
TERRA 7	252
TERRA 8	235
TERRA 9	210

Cesium Carbonate/Clay Conversion

The final step in the production of pollucite pellets is the conversion of a Cs_2CO_3/clay mixture to pollucite by vacuum hot pressing. Prior to the vacuum hot pressing the Cs_2CO_3 is dissolved in water to make a solution which is 2.5 to 3.0 *M* in Cs_2CO_3. The aluminosilicate clay is then added to the carbonate solution in small batches. The following procedure was used in producing the pre-pollucite mixture of Cs_2CO_3 and aluminosilicate.

1. Weigh out 100 g of dry Cs_2CO_3 powder.
2. Measure 105 ml of distilled water into a mixing bowl. This will make a solution that is 2.5 to 3.0 *M* in Cs_2CO_3.
3. Pour the Cs_2CO_3 slowly into the mixing bowl containing the distilled water. Mix thoroughly. The dissolution of Cs_2CO_3 is exothermic.
4. Calculate the quantity of montmorillonite clay [gel White L (GWL)] required to produce the pre-pollucite mixture.

   Wt GWL = (1.667)(wt fraction Cs)(wt of Cs_2CO_3 powder)

   For the 100 g of Cs_2CO_3 powder there should be ~130 g of GWL. The clay should be dry.
5. Pour the GWL into the Cs_2CO_3 solution in small batches while mixing thoroughly.

*All chemical analyses were performed by the ORNL Analytical Chemistry Division.

6. Spread the resulting paste on the walls of the drying container and cut vertical grooves in the paste. The grooves facilitate removal of the dried paste from the container.
7. Dry the paste for 8 hours at 150°C.
8. Grind the dry solid in a blender.
9. Sieve the powder through a 30 mesh sieve tray. Recycle unpassed powder back to the blender. Repeat until all the powder passes through the 30 mesh sieve.
10. Store the powder in a desiccator. The powder is hygroscopic.

The aluminosilicate clay material used in the production of $CsAlSi_2O_6 \cdot nH_2O$ is a purified, low iron content, montmorillonite clay known as gel White L (supplied by Georgia Kaolin Company). Gel White L[10] is a white, microgranular montmorillonite with a moisture content of ~10%. Montmorillonite minerals[11] are a group of secondary minerals derived from the breakdown of ferro-magnesium rich igneous rock. Other members of the secondary clay minerals include kaolin, chlorites, vermiculites, and hydrous micas. They are of variable composition containing aluminum, silicon, magnesium, and other elements. The ideal montmorillonite has the following chemical formula: $Al_2(Si_4)O_{10}(OH)_2X \cdot H_2O$. Montmorillonites, beidellite, and nontronite form one series of minerals where silica, alumina, magnesia, iron oxide, and water are the principal components. The general name given to clays which contain appreciable quantities of montmorillonite minerals is bentonite. The structural formula for GWL is

$$(Si_{7.65}Al_{0.35})(Al_{3.20}Fe_{0.09}{}^{3+}Mg_{0.74})O_{20}(OH)_4(Ca_{0.34}K_{0.01}Na_{0.31})$$

Gel white L disperses readily in water to form a colloidal suspension and a 15 wt % quantity of GWL is required before a gel consistency colloidal suspension is produced. This characteristic is illustrated in Table 5 where viscosities of water dispersions with varying GWL weight percents are listed.[10]

Table 5. Viscosities of Aqueous Gel White L Dispersions

Gel white L (wt %)	Brookfield helipath viscosity (cps @ 5 rpm)
5	20
7	24
9	70
11	550
13	4,400
15	18,600

The results of an ORNL elemental chemical analysis of GWL are given in Table 6.

Table 6. Elemental Chemical Analysis of Gel White L

Sample I.D.	Aluminum (wt %)	Silicon (wt %)	Iron (wt %)	Oxide (wt %)
TERRA GWL 2	8.70	29.1	0.50	60.0

The amount of GWL added to the Cs_2CO_3 slurry to fabricate the correct pre-pollucite mixture is obtained from Eq. (1).*

$$\text{Weight of GWL in grams} = (1.667)(\text{wt-fraction of Cs in } Cs_2CO_3 \text{ powder}) \times (\text{weight in grams of } Cs_2CO_3 \text{ powder}) \quad (1)$$

Actually the powder is not pure Cs_2CO_3 since the weight fraction would be a constant 0.816 as mentioned previously. The powder, however, contains oxalate due to the incomplete conversion of the tetraoxalate and oxide due to the further conversion of a small amount of the carbonate to Cs_2O and cesium superoxide (CsO_2)(Table 7).

Table 7. Cesium Carbonate Chemical Analysis Results

Sample I.D.	Cesium (wt %)	Carbonate (wt %)	Oxalate (wt %)	Oxides (wt %)
TERRA ST-5P	77.6	18.8	0.67	<0.05
TERRA ST-6P	81.8	18.8	0.03	<0.05
TERRA ST-7P	83.2	18.4	0.26	<0.05

*See Appendix B for derivation and discussion of Eq. (1).

After the GWL clay has been combined with the Cs_2CO_3 in the proper proportions, it must be loaded into the graphite die for the conversion to pollucite. Three procedures for loading the charge of pre-pollucite powder into the die were devised and tested with subsequent analysis of the pellet produced by each technique to determine the method's efficacy. Two methods involved wetting the carbonate/clay mixture with distilled water to form a paste and then forming the paste into a cylinder by pressing in a die (Method 1, Appendix A), or by centrifuging (Method 2, Appendix A). After drying the rod or cylinder of pre-pollucite powder it is then loaded into the die for vacuum hot pressing. The third method simply involves pouring the powder through a funnel into the bore hole of the hot press die.

Optical microscopy, BSE, SEM, and EDX analyses of the aluminosilicate pellets produced by Methods 1 and 2 revealed that these processes produced pellets which were plagued by Cs^+ migration towards the pellet's outer surface and by severe phase separations.

An SEM and EDX analysis across a 12 mm slice (center to periphery of pellet) of a sample pellet produced using Method 2 indicated an inhomogeneous cesium concentration profile (Table 8).

Table 8. Elemental Mole and Weight Fractions of a Cesium Aluminosilicate Pellet[12]

	Mole fraction			Weight percent		
	Cesium	Aluminum	Silicon	Cesium	Aluminum	Silicon
Point 1 (near center of pellet face)	0.1440	0.0798	0.1838	52.68	5.93	14.19
Point 1A	0.1446	0.0760	0.1868	52.81	5.63	14.40
Point 2	0.1417	0.0771	0.1875	51.21	5.76	14.58
Point 3	0.1454	0.08	0.1799	52.90	6.00	13.82
Point 4	0.1551	0.0742	0.1820	54.86	5.33	13.59
Point 5	0.1705	0.0667	0.1825	57.77	4.59	13.05
Point 6 (edge of pellet)	0.2132	0.0733	0.1524	64.32	4.48	9.71

The above sample pellet contained a minimum of 25% more cesium than the stoichiometric quantity of cesium in the pollucite crystal lattice

structure. The weight percent of cesium in the unhydrated pollucite is 42.6% compared to the 52 to 64 wt % cesium in the above sample. This excess cesium in the carbonate, oxide, or superoxide form would be more susceptable to any leaching agents such as water since cesium is less tightly bonded in these forms than it is in the pollucite crystal lattice.

The cesium concentration profile depicted in Table 8 may be explained by the rotating action of the centrifuge which caused the slight excess of water existing in the pre-pollucite paste to migrate towards the surface. This excess water would have dissolved some of the more soluble cesium-containing compounds (mostly Cs_2CO_3 with small amounts of $CsH_3(C_2O_4)_2 \cdot 2H_2O$ and Cs_2O) in the paste and thus would have caused a moderate increase in the cesium concentration on the pellet surface when the water was forced to the surface.

Optical micrograph and BSE studies of the aluminosilicate pellets produced using Method 1 show a phase separation into light (solid, possibly fused masses) and dark (finely divided particles with high porosity). Count data obtained from these two phases yield elemental weight when compared with known standards (Table 9).

Table 9. Electron Backscattering Elemental Composition Comparison of Grain and Boundary Phases of a Cesium Aluminosilicate Pellet

Element	Grain (dark area) (wt %)	Boundary (light area) (wt %)
Aluminum	3	1
Silicon	10	14
Cesium[a]	1.5	1

[a]No cesium standard was available and, therefore, the numbers reported for cesium are relative intensities and not absolute weight percents.

The relative intensities obtained for the cesium show a one-third decrease in the amount of cesium in the light (boundary) phase compared to the quantity of cesium in the dark (grain) phase. This inhomogeneity is an undesirable characteristic for a cesium source compound. Due to these cesium inhomogeneities Methods 1 and 2 were discontinued and Method 3 was readopted. Although optical micrograph and X-ray diffraction analyses of a non-radioactive pollucite pellet produced early in

the program using Method 3 indicated the existence of light and dark areas, there was no elemental or chemical composition difference detected.[13] Method 3 for pre-pollucite powder mixture loading was used for the remainder of the pellet production runs.

The final procedure for vacuum hot pressing the pre-pollucite powder mixture (Cs_2CO_3/montmorillonite clay) is given below. This procedure outlines the die loading, furnace loading, heating and pressing, cooling, furnace unloading, pellet ejection, and pellet storage steps involved in producing a $CsAlSi_2O_6 \cdot nH_2O$ pellet.

A. Die Loading

1. Insert the prerolled grafoil sleeves into the die body.
2. Insert the bottom punches (with the punch head pointing up) into the die body. Position each punch carefully over the bore hole and using the protruding grafoil as a guide drop the bottom punches into the die body. Check the grafoil for visible tears.
3. Insert the first grafoil disc into each bore hole of the die body. Check that the discs are seated properly on top of the bottom punch.
4. Lift the die body and slowly transfer it to the die loading stand.
5. Transfer the fuel increment (a 45 g charge of the Cs_2CO_3/clay mixture) from the fuel container into the die body using a spoon and a funnel. The density of the pre-pollucite charge is $\sim$1.5 to 1.7 g/cm^3.
6. After assuring that the powder is level place the remaining grafoil disc on top of the powder. Check that the discs are seated properly.
7. Carefully insert the top punches into the die. Check the grafoil for visible tears.

B. Furnace Loading

1. Carefully lift the loaded die and position it onto the furnace baseplate.
2. After the die is in place inspect the alignment of the assembly to insure that there is no contact between the die and heating element, and the element and heat shield.

3. Install the heat shield cover.
4. Slowly lower the vacuum hot press bonnet onto the base and guide it until the two sections are seated properly.
5. Extend the hydraulic ram until the powder-pellet pressure gage corresponds to a pressure of approximately 500 psig.
6. Check the VHP power unit for proper operation.
7. Open the vacuum block valve and turn on the vacuum pump. Evacuate the furnace to (-) 24 inches Hg.
8. Purge the hot press six times with argon and vacuum. Evacuate the furnace to (-) 24 inches Hg.
9. Turn the water on to the cooling circuits (base, electrodes, bellows, and the bonnet).
10. Turn the main power switch on the VHP power unit to the on position. Set the voltage and amperage controls to give 1000 watts. Begin recording date, time, volts, amps, vacuum, hydraulic ram pressure, and ram travel at 5 minute intervals.
11. After one hour has elapsed, increase the voltage control to maximum setting (47 volts). DO NOT exceed 22,000 watts of power.

C. Heating and Pellet Pressing

1. Maintain power pressure and vacuum settings throughout the course of the run.
2. Continue pressing until no ram travel is registered for six successive readings.

D. Cooling

1. Turn the VHP power supply off.
2. Maintain the 500 psig and cooling water flow rate to the furnace for at least two hours.
3. Open the argon line to the VHP valve and allow Ar(g) to flow into the VHP until the pressure reaches (-) 2 inches Hg. Release the pressure on the hydraulic ram. Turn off the cooling water.
4. Open the vent valve to the VHP.

E. Furnace Unloading and Pellet Ejection

1. Move the hydraulic pump to retract and retract the ram until the bonnet raises off the base. Continue raising the bonnet until it clears the die's top punch.
2. Remove the heat shield cover.
3. Remove the die to the cell floor.
4. Remove the pellets from the die body.

F. Pellet Storage

1. Record the weight of the pellet using the double beam balance.
2. Measure the height of the pellet using the 0–2 in. micrometer.
3. Measure the diameter of the pellet using the 0–2 in. micrometer.
4. Place the pellet in the pellet storage tray.

Experimental Equipment

The $CsAlSi_2O_6 \cdot nH_2O$ pellets were fabricated employing a device called a vacuum hot press (VHP)[14] (Fig. 4). A VHP consists of the following major components: a water cooled upper and lower 304L stainless steel housing which encloses the area to be heated; a stainless steel bellows assembly which transmits the pressure supplied by a hydraulic ram to the pollucite pellet; ATJ graphite power terminals which supply the electricity required to heat the pellet charge; an ATJ graphite heating element used to convert the electricity to resistance heating and radiantly transmit it to the pellet charge; a molybdenum heat shield which reflects the radiant heat from the heating element and die back towards the die for maximum heating of the pollucite charge; an ATJ graphite die used to contain and form the pollucite charge; and a Carbosil 45 graphite base plate used to support the die, heating element, and heat shield.

See Fig. 5 for a sketch of the VHP components. Two VHPs were utilized during the development and production stages of the $CsAlSi_2O_6 \cdot nH_2O$ program: one small VHP housing a one-hole (one pellet) die and a larger VHP housing a three-hole (three pellets) die. Some of the details of the VHP's major components will be discussed later in this section.

ORNL PHOTO–0626-71A

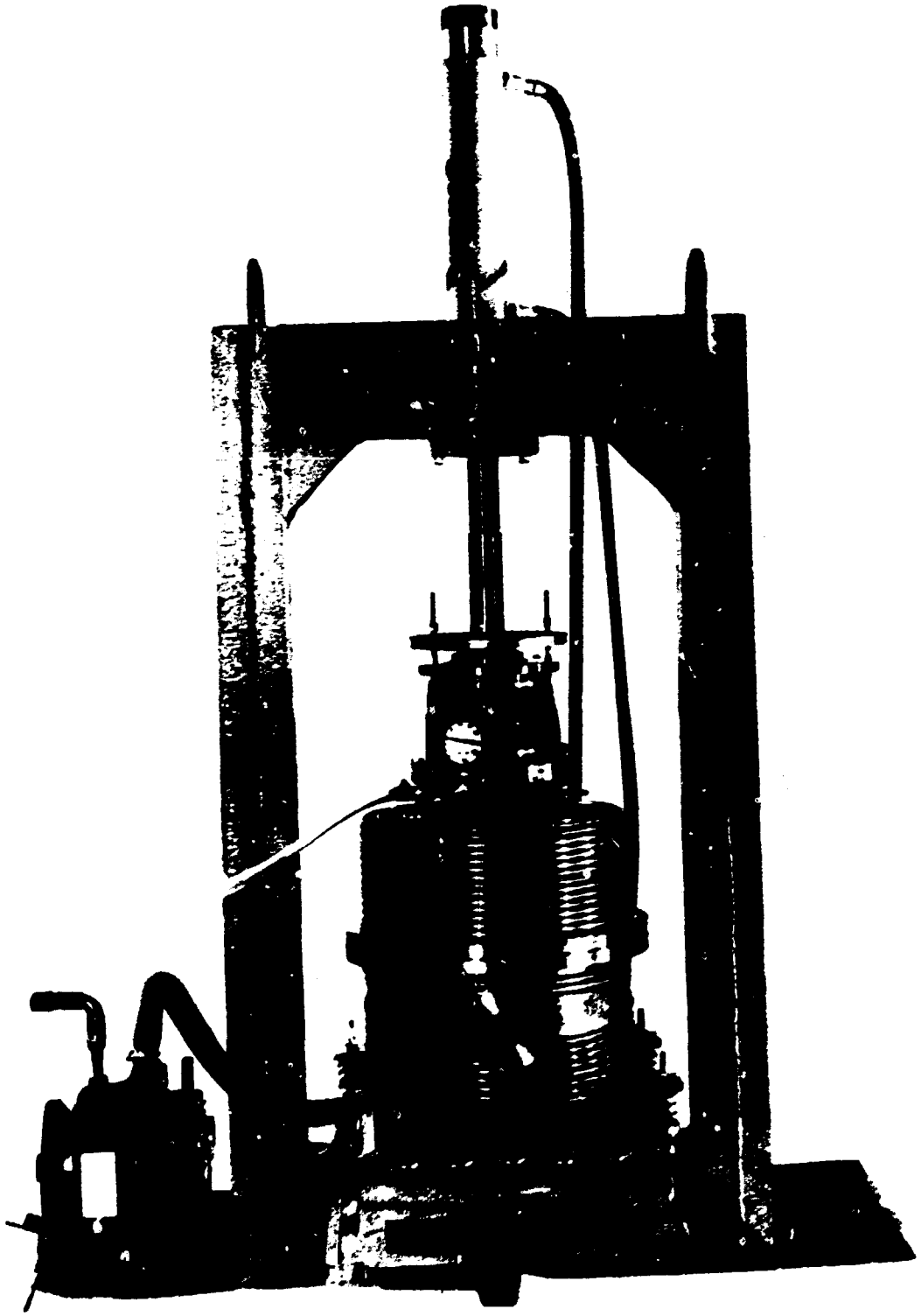

Fig. 4. Vacuum Hot Press

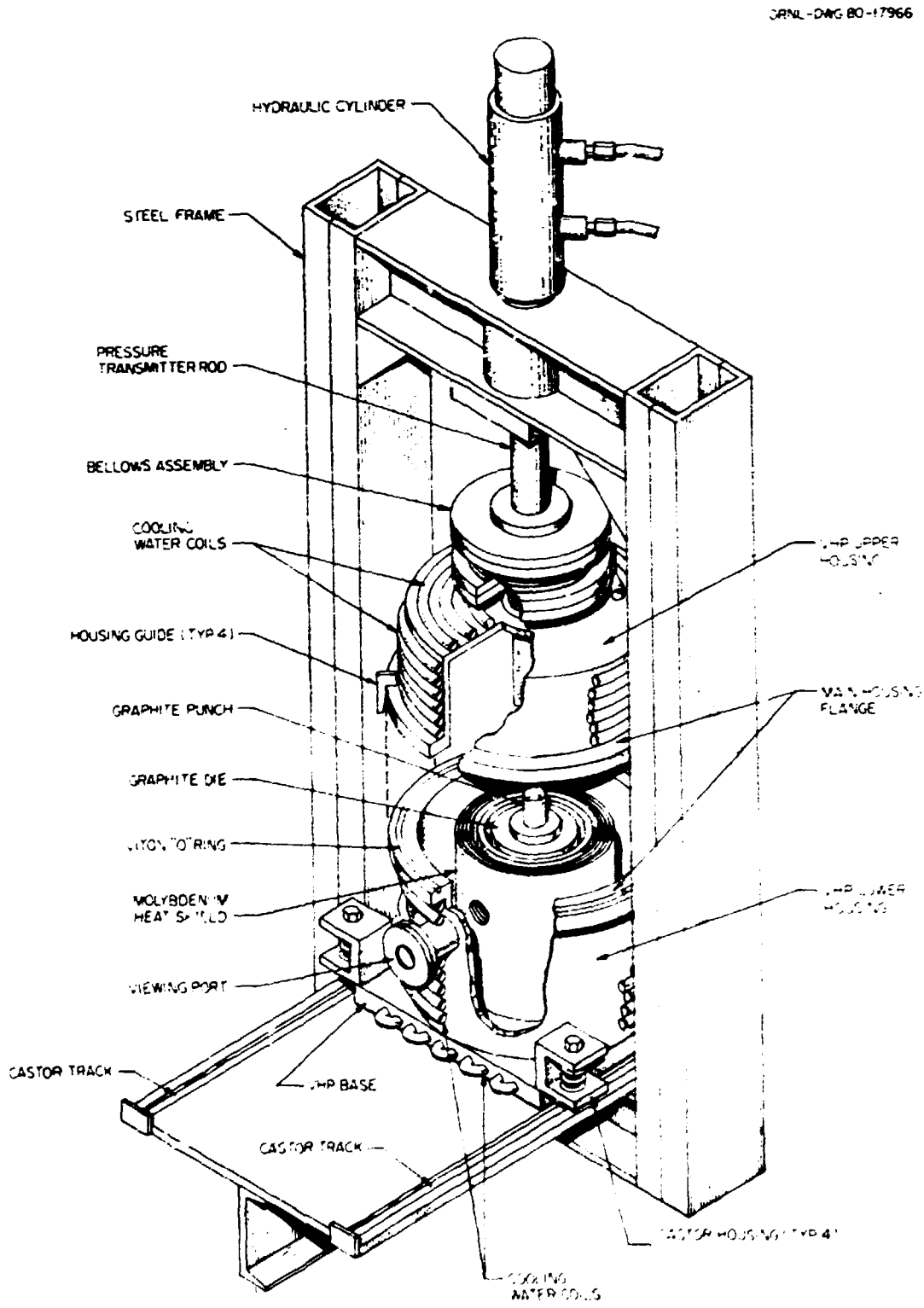

Fig. 5. Vacuum Hot Press Components

The two parameters involved in controlling the production of pollucite were temperature and pressure. A pressure of 500 to 570 psig was applied to the pre-pollucite powder before the power to the heating element was initiated, during the transformation of the powder to pollucite, and after the formation of the pellet was completed. This pressure cycle assured the conversion of the Cs_2CO_3/clay mixture to the desired $CsAlSi_2O_6 \cdot nH_2O$. The pressure was easily controlled and monitored by a manually operated hydraulic press which was coupled to the pollucite pellet via the VHP bellows and transmitter rod assemblies.

Temperature was the more difficult parameter to control in terms of both achieving the required conversion temperature and monitoring the precise temperature. Sandia Laboratories had suggested that a temperature range of 1500°C to 1550°C (as well as a pressure of ~500 psig) would be necessary to convert the Cs_2CO_3/clay mixture to pollucite. To assure that this temperature was being achieved several techniques for temperature measurement were employed. First, a graph of "pellet" temperature vs VHP input power was constructed to obtain a useful correlation which would simplify hot cell operation. The graph was obtained by allowing the graphite die in which the thermocouple was imbedded (the temperature sensitive junction was separated from the pellet by 0.64 cm [1/4 in.] of graphite and alumina tubing [Fig. 6]) to attain thermal equilibrium at a corresponding power setting. The temperature was then recorded yielding a point on the temperature vs power curve.

A platinum-platinum (rhodium) thermocouple, which had been calibrated at a lower temperature range (up to 1200°C) using a chromel-alumel thermocouple, was used to obtain the "pellet" temperature. However, the emf produced at the Pt-Pt(Rh) junction was not an accurate representation of the pellet's temperature since the thermocouple was surrounded by an alumina tube and separated from the pellet by 0.32 cm (1/8 in.) of ATJ graphite. The alumina tube (melting point 2045°C) was necessary to protect the sensitive thermocouple material from graphite attack during the heating cycle. To account for the temperature gradient across the graphite and alumina, early temperature calibration experiments utilized pyrometric cones[15] and temperature sensitive paints and crayons which were

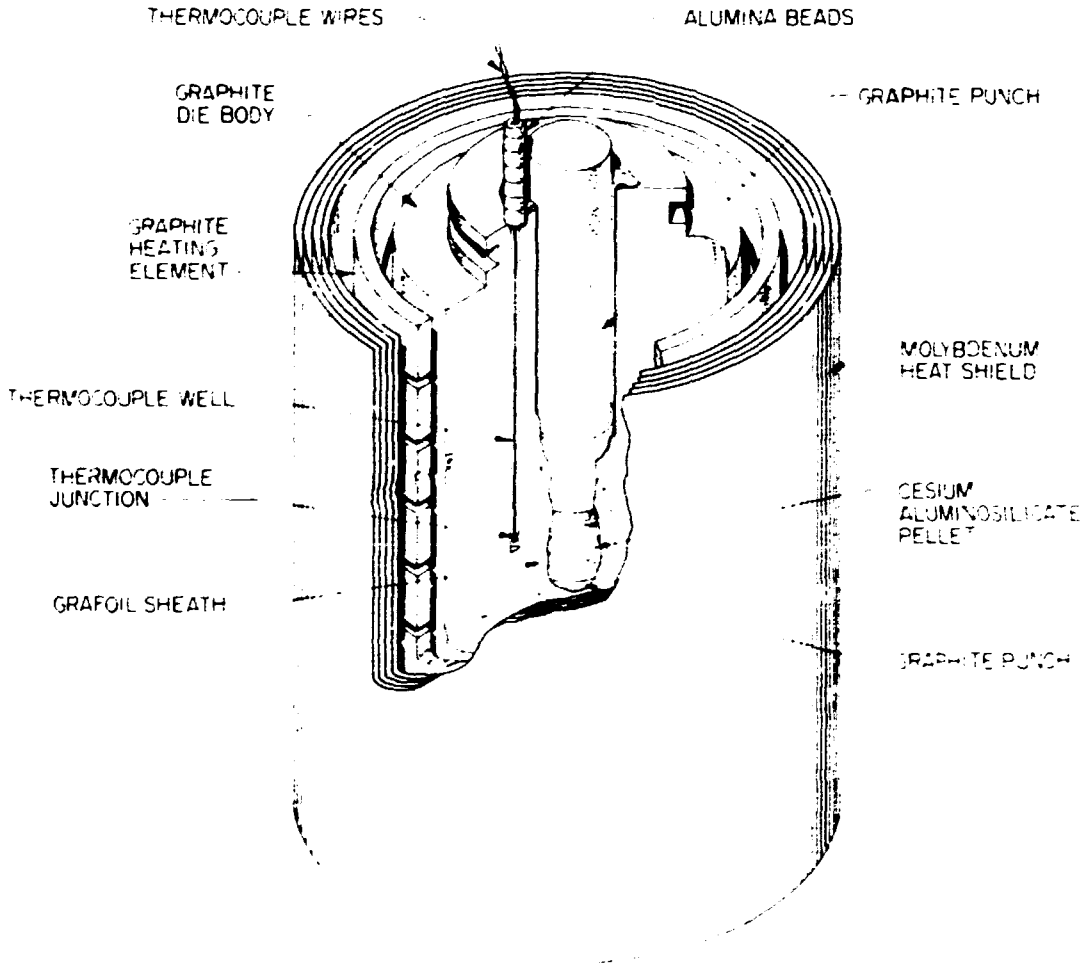

Fig. 6. Detail of Heat Shield Heating Element and Die

placed in the die's bore hole prior to the heating cycle and examined afterwards to determine the temperature attained and thus the actual "pellet" temperature. Figure 7 shows a graph of temperature vs VHP input power. The dashed line indicates the true "pellet" temperature as determined by pyrometric cones, whereas the solid line gives a chromel-alumel thermocouple's output voltage (converted to °C). The graph clearly displays the effect of the graphite and alumina on the temperature readings of the thermocouple in that the readings are low by ~200°C.

A tungsten (rhenium)-tungsten (rhenium) thermocouple's emf was also measured and compared to the temperature readings of a chromel-alumel thermocouple (up to 1200°C) and linearly extrapolated to 1600°C (Fig. 8).

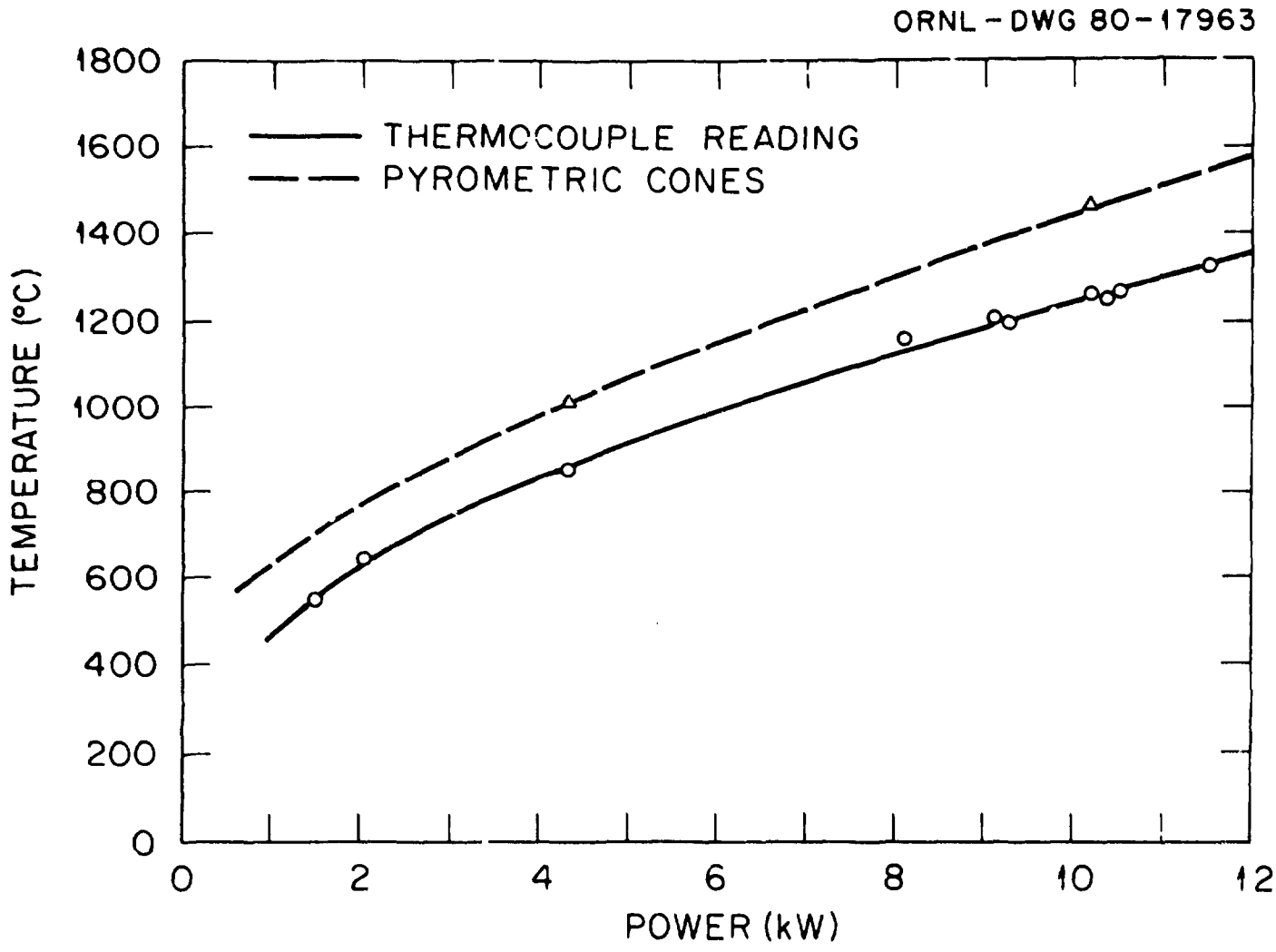

Fig. 7. Graph of Temperature vs VHP Input Power

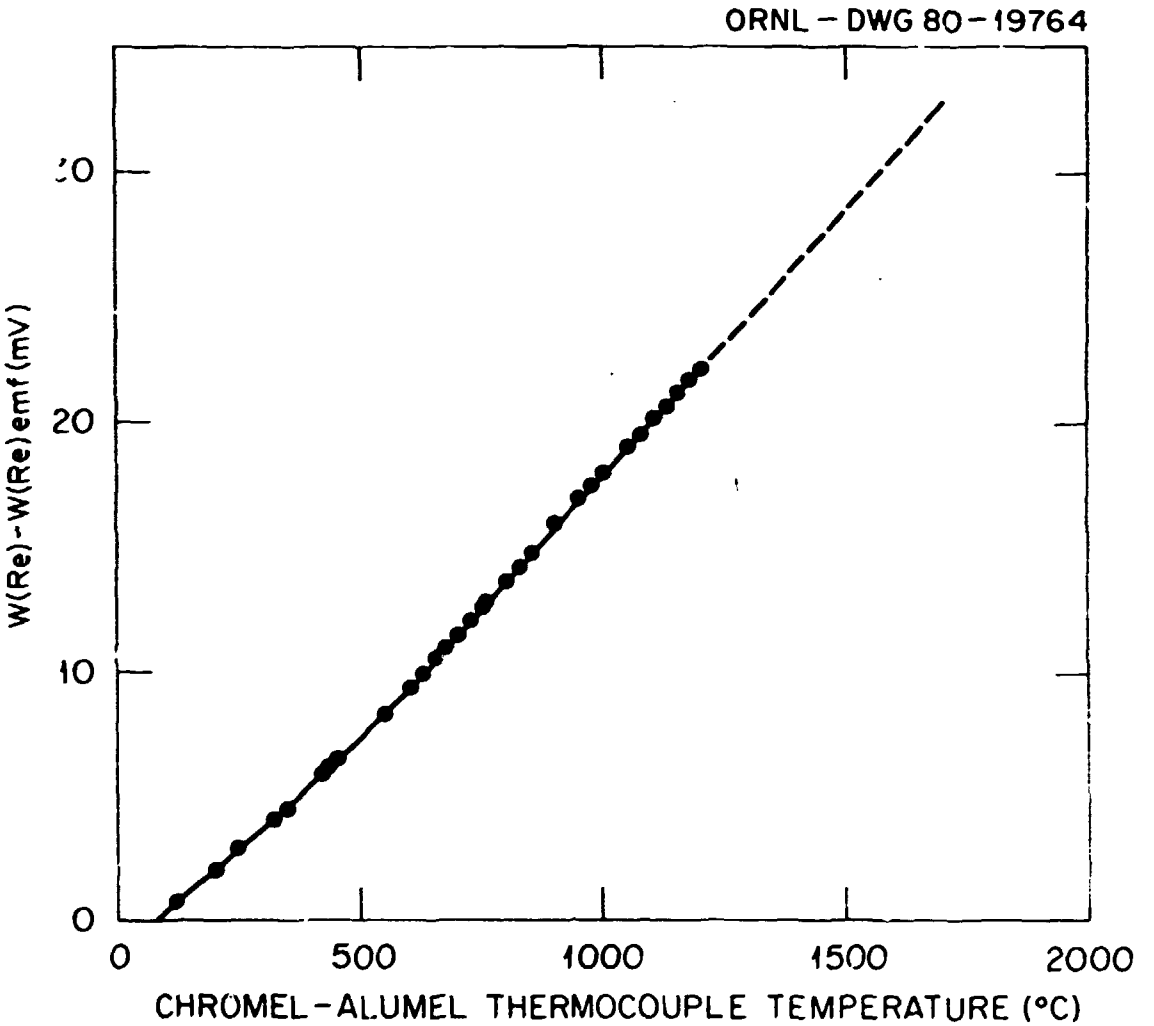

Fig. 8. A Graph of W(Re)-W(Re) emf(mV) vs Chromel-Alumel emf(°C) for Small VHP

The W(Re)-W(Re) thermocouple was chosen because of its higher maximum measurable temperature of 1800°C as compared to the maximum measurable temperature of 1600°C for the Pt-Pt(Rh) thermocouple. This higher maximum temperature assured a linear response in the operating range of 1500°C to 1550°C. During the temperature calibration runs, as well as for all subsequent pellet production runs, the same power source was used; that is, a Nobatron DCR40-500A. This assured power continuity to the VHP heating element. The power source's maximum power rating was 22,000 watts (~49 volts × 450 amps), while the normal operating range was 47 volts × (405-430) amps (19.04 kW-20.21 kW).

As mentioned previously two VHPs were used during the course of pollucite process development and production: one termed small and the other large. The small hot press was 82.55 cm (32 1/2 in.) high by 55.88 cm (22 in.) diameter, while the large hot press was 127.0 cm (50 in.) high by 55.88 cm (22 in.) diameter (dimensions of steel support frame). The small VHP contained a one-hole graphite die and was used in process design and development. The large VHP housed a three-hole graphite die which was used in the actual production of the fully loaded ^{137}Cs aluminosilicate pellets.

The VHP as originally designed (it was to be used in ^{90}Sr pellet production) was unable to achieve the temperatures required for manufacturing pollucite. However, two sources of heat leakage were discovered and altered to enable attainment of the desired temperature. The original base plate supporting the die was composed of ATJ graphite, the same material which comprised the power electrodes, heating element, and the die body itself. When replaced by a base plate made of Carbosil 45, a graphite with one-fifth the thermal conductivity of ATJ graphite, the maximum theoretical temperature of the VHP was significantly increased. To further increase the VHP maximum temperature a Carbosil 45 pressure distribution plate (plate between the ram transmitter rod and the die's graphite punches) was substituted for the ATJ graphite plate. These two material alterations, as well as a decrease in the size and, therefore, bulk of the die body, enabled the VHP to achieve the operating temperature of 1500°C to 1550°C.

Water lines jacketing the bottom and top housings, as well as the bellows assembly of the VHP, were used to regulate the temperature of the outer stainless steel skin. Temperature probes indicated that during the hot press heating cycle the main flange between the upper and lower housings attained a temperature of ∿120°C, the power electrodes reached ∿38°C, while the bellows were only slightly above room temperature. A water flow rate of 3 to 5 gal/min (∿10 to 20 liters/min) was maintained throughout the hot pressing procedure.

The dies used in containing and forming the pre-pollucite powder into pollucite were composed of a graphite called ATJ (Fig. 9). A three-hole

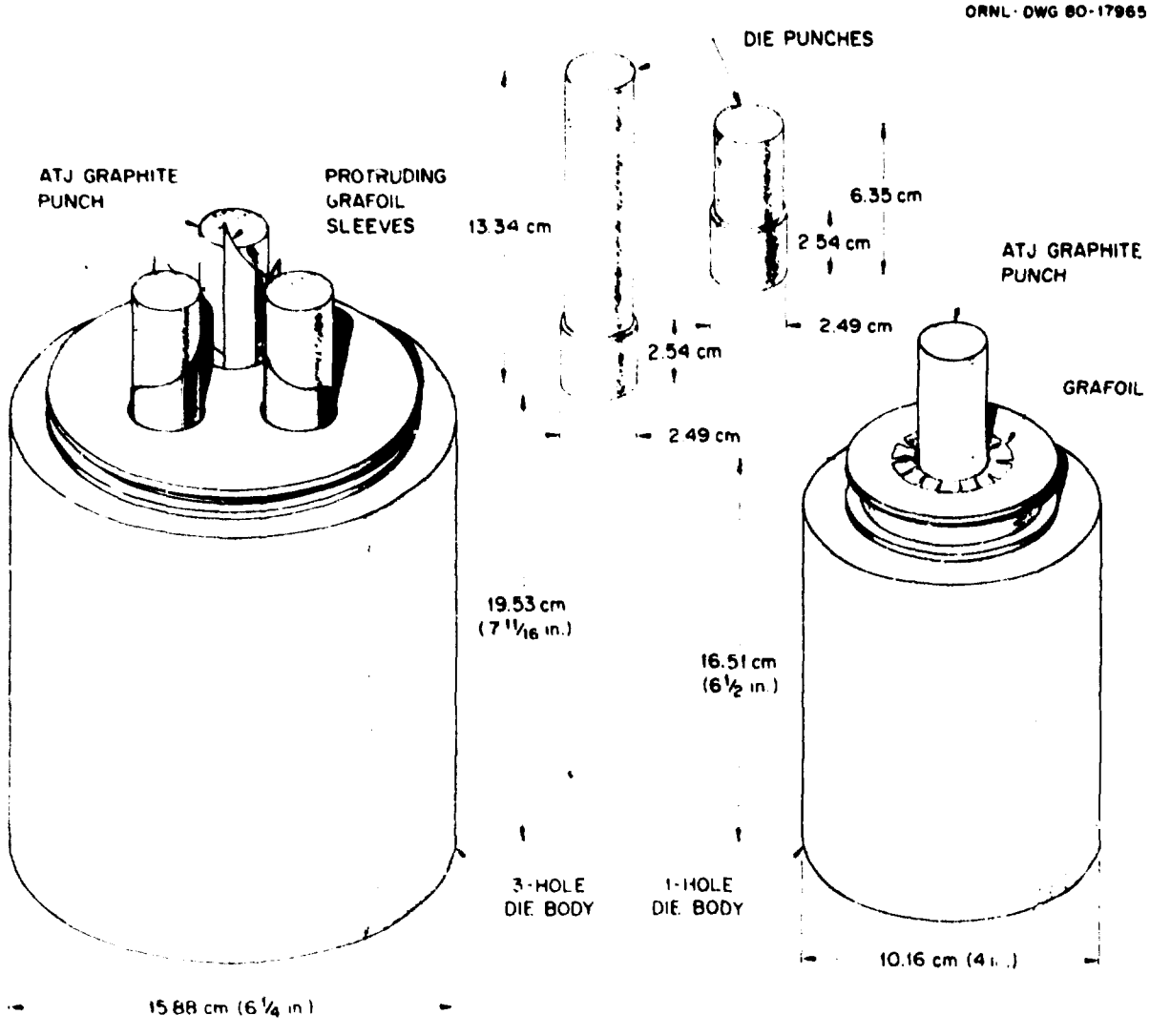

Fig. 9. Three-Hole and One-Hole ATJ Graphite Dies

version of the die was employed in the large VHP for producing the full level ^{137}Cs aluminosilicate pellets in the hot cell, whereas a one-hole version was utilized in the development and testing stages of the cesium source compound application program.

A grafoil sleeve (Figs. 6 and 9) running the entire length of the die bore was used as a lubricating agent between the forming pollucite pellet and the graphite bore hole. Powdered graphite and a MoS_2-acetone spray were also tried as lubricants but were found not to be as successful in preventing the pellet from adhering to the bore hole wall and were, therefore, discontinued. Grafoil discs were also placed between the pellet and the graphite punches to prevent sticking. Without the grafoil serving as a lubricant the graphite die was cracked during pellet extraction.

The design of the punches was altered from a simple cylinder of one diameter to one where the punch was tapered somewhat at one end to facilitate loading into the die when using master slave manipulators (Fig. 9).

A coiled ATJ graphite heating element (Fig. 6) was used to generate the amount of heat required for the Cs_2CO_3/clay conversion to pollucite. Special orientation of the layers of carbon atoms in the graphite converts electrical energy to heat by resisting the flow of electrons. molybdenum heat shield surrounds the graphite heating element and die to reflect the heat generated by the heating element and heat reflected from the die back to the die and consequently the pollucite pellet. This retards any dissipation of heat from the primary heating zone (i.e., heating element plus die) and thereby increases the total quantity of heat focused on the die and pellet.

Results and Discussion

A 45 g charge of pre-pollucite (Cs_2CO_3/clay mixture) powder was loaded into each bore hole of the graphite die and vacuum hot pressed. The resulting aluminosilicate pellet contained ~400 to 450 curies of ^{137}Cs* with the following dimensions:

*Estimated from known activity and isotopic composition of starting material (CsCl) and weight of cesium aluminosilicate pellet.

Height:	2.86 cm (1 1/8 in.)
Diameter:	2.54 cm (1 in.)
Weight:	40 to 42 g .

A total of 27 full level ^{137}Cs pellets with th above dimensions were produced in the hot cell by the large VHP. The production run conditions used to hot press the aluminosilicate pellets are given in Table 10.

Table 10. Full Level Cesium-137 Aluminosilicate Vacuum Hot Pressing Run Conditions

Production run number	Vacuum Hot Press: Power level at maximum ram travel (kW)	Pressing ram pressure (psig)	Pressing ram pressure (kPa)	Length of time power applied after completion of ram travel (min)
79CsP-4	19.78	575	4070	45
79CsP-5	20.68	570	4030	30
79CsP-6	20.45	570	4030	20
79CsP-7	20.30	575	4070	10
79CsP-8	19.98	575	4070	30
79CsP-9	19.83	595	4200	45
79CsP-10	19.74	570	4030	40
79CsP-11	18.86	570	4030	90
79CsP-12	19.98	595	4200	40

The last column in Table 10 depicts the length of time the power to the hot press remained on after the last recorded ram movement (i.e., after the pellet had been fully compressed). This "curing" step with a minimum duration of 15 minutes was found by experience to be necessary for the production of good quality pellets. The curing step duration was varied to determine its effect on the pellets' physical characteristics such as density and leach rate.

The measured densities of the recovered full level ^{137}Cs aluminosilicate pellets produced in the hot cell are reported in Table 11.

One pellet each from runs 79CsP-6, 79CsP-7, 79CsP-8, 79CsP-9, 79CsP-11, and 79CsP-12 were selected and stored for further pellet characterization studies. These studies will be discussed in detail in the next section, "Cesium Aluminosilicate Pellet Characterization."

Table 11. Cesium-137 Aluminosilicate Pellet Densities

Run No.	Average density[a] (g/cm^3)
79CsP-4	2.90[b]
79CsP-5	2.97 ± 0.09
79CsP-6	2.75 ± 0.08
79CsP-7	2.94 ± 0.03
79CsP-9	3.00[b]
79CsP-10	2.89 ± 0.09
79CsP-11	2.94 ± 0.05
79CsP-12	3.00 ± 0.02

[a]The range of densities presented is simply the standard deviation of the average of three pellets' densities and does not reflect the error associated with the actual pellet measurements.

[b]Only one pellet was measured.

A total of 50 development stage hot press temperature calibration and aluminosilicate production runs (both stable and tracer level) were completed outside the hot cell using both the large VHP (before insertion into the hot cell) and the small VHP. The control parameters of temperature and pressure, as well as run duration, powder charge composition, heating rate, punch-die lubrication, etc., were varied to note their affect on pellet production and quality. Approximately 40 stable and tracer level pellets were fabricated during the developmental stage of the cesium source compound applications program and the results obtained were used in formulating the full level ^{137}Cs aluminosilicate pellet process steps and controls. Table 12 gives a partial listing of the experimental run conditions for the pellet production runs completed during this stage of the program.

The densities of the pellets recovered from the pellet production runs listed in Table 12 are given in Table 13.

An interrogation of the aluminosilicate pellet based on density, correct color, and color homogeneity was employed in preliminary determinations of the success of a pellet production run. Also, as mentioned earlier, optical microscopy, SEM, and EDX analytical methods were used to

Table 12. Cesium-Aluminosilicate Small Hot Press Experimental Production Run Conditions

Run No.	Final input power level (kW)	Pressure ram pressure (psig)	Pressure ram pressure (kPa)	Duration of run (min)	Final temperature[a] (°C)
22	10.18	500	3550	90	1465
24	10.18	500	3550	60	1465
25	10.18	500	3550	53	1465
28	11.29	500	3550	60	1530
32	11.78	500	3550	60	1565
33	11.78	500	3550	79	1565
36	11.10	460	3270	60	1515
37	10.83	500	3550	48	1500
39	10.64	460	3270	60	1490
40	11.17	500	3550	52	1520
41	11.65	500	3550	50	1490
42	12.27	500	3550	66	1595
47	12.15	460	3270	53	1585(1470)[b]
49	11.70	460	3270	63	1555(1450)[b]
50	12.96	460	3270	104	1620

[a]The temperatures attained by the small VHP for each of the above runs was obtained from the temperature vs VHP input power graph previously discussed (Fig. 7).

[b]The temperatures given in parentheses were obtained directly from an imbedded W(Re)-W(Re) thermocouple.

Table 13. Cesium Aluminosilicate Pellet Densities

Run No.	Uncorrected densities[a] (g/cm^3)
22	3.02
24	2.77
25	2.73
28	3.10
32	3.08
33	3.00
36	3.16
37	3.09
39	3.04
40	3.06
41	2.97
42	3.06
47	3.02
49	2.92
50	3.04

[a]Not corrected for weight and volume surrounding grafoil sheath.

determine the precise physical and chemical composition and phase homogeneity of a pellet sample. These investigations directed the course of the next pellet production run by suggesting appropriate experimental conditions to be applied in manufacturing a pellet having the optimum physical and chemical characteristics.

CESIUM ALUMINOSILICATE PELLET CHARACTERIZATION

Pellet Characterization Studies

During the developmental stage of the ^{137}Cs source compound program optical microscopy, SEM-EDX, activation analysis, leaching tests, and standard analytical chemistry analyses (e.g., cesium concentration determination) were employed to provide information concerning the chemical and physical properties of the experimental aluminosilicate pellets. Some of these same analytical methods, as well as others, were again used to characterize the full level ^{137}Cs product aluminosilicate pellets fabricated in the large VHP. As mentioned previously, six full level production pellets were selected from various pellet production runs and stored for further characterization studies. These studies and their objectives are outlined in Table 14.

Table 14. Cesium-137 Aluminosilicate Production Pellet Characterization Studies

Analytical Technique	Objective
1. Calorimetry.	1. To determine ^{137}Cs curie content.
2. Metallography (optical microscopy).	2. To determine phase homogeneity.
3. SEM and electron microprobe.	3. To determine relative elemental composition.
4. X-ray diffraction.	4. To determine crystal lattice structure — is it pollucite?
5. Cesium ion leachability measurements.	5. To determine the leachability of the cesium cation out of the pollucite crystal lattice.

Each of the analytical techniques listed in Table 14 will be discussed in greater detail and attainment of their stated objectives evaluated.

Calorimetry Studies

An accurate assaying of the ^{137}Cs content of the aluminosilicate pellets was desired to provide needed information for future pellet characterization studies (such as the leach testing). Calorimetry is an established method for the curie content determinations of major constituent radioisotopes in radioactive sources.[16] A suitably designed calorimeter can measure the rate of heat production (measured in watts) of the radioactive source sample to an accuracy of 0.2% (95% confidence limit). Since the heat produced is proportional to the curie content of the sample one can determine the number of curies of ^{137}Cs in the sample after the calorimeter has been carefully calibrated.

The calorimeter employed was designed for an optimum operating range of 2 to 3 watts, which was the calculated heat generation of a sample full level production pellet. The calorimeter consisted of a 12.06 cm by 11.68 cm solid lead cup which surrounded a 2.86 cm by 3.49 cm hollow stainless steel sample container. This lead cup (15.9 kg of lead) absorbed greater than 99% of the total energy produced by the radioactive decay of ^{137}Cs (Figs. 10 and 11). The lead absorber rested on a 3-in. Sch. 40 stainless steel pipe which served as the heat transferral medium to a water-tight compartment containing a water-ethylene glycol mixture at the bottom of the calorimeter shaft. A temperature differential of 2 to 3°C was obtained between the hot and cold junctions of an attached chromel-alumel thermopile.

Fiberglas and polyurethane foam were used to insulate the shaft of the calorimeter. A large Dewar flask which encompassed the entire calorimeter maintained a near constant temperature environment. A constant temperature circulating bath supplied the cooling solution to the water-tight compartment located at the base of the shaft. The bath regulated the solution's temperature to within ±0.02°C in the operating region of interest (18°C–25°C) under a flowrate of ~1800 cc/min. A strip chart recorder plotted the thermopile signal output voltage vs time.

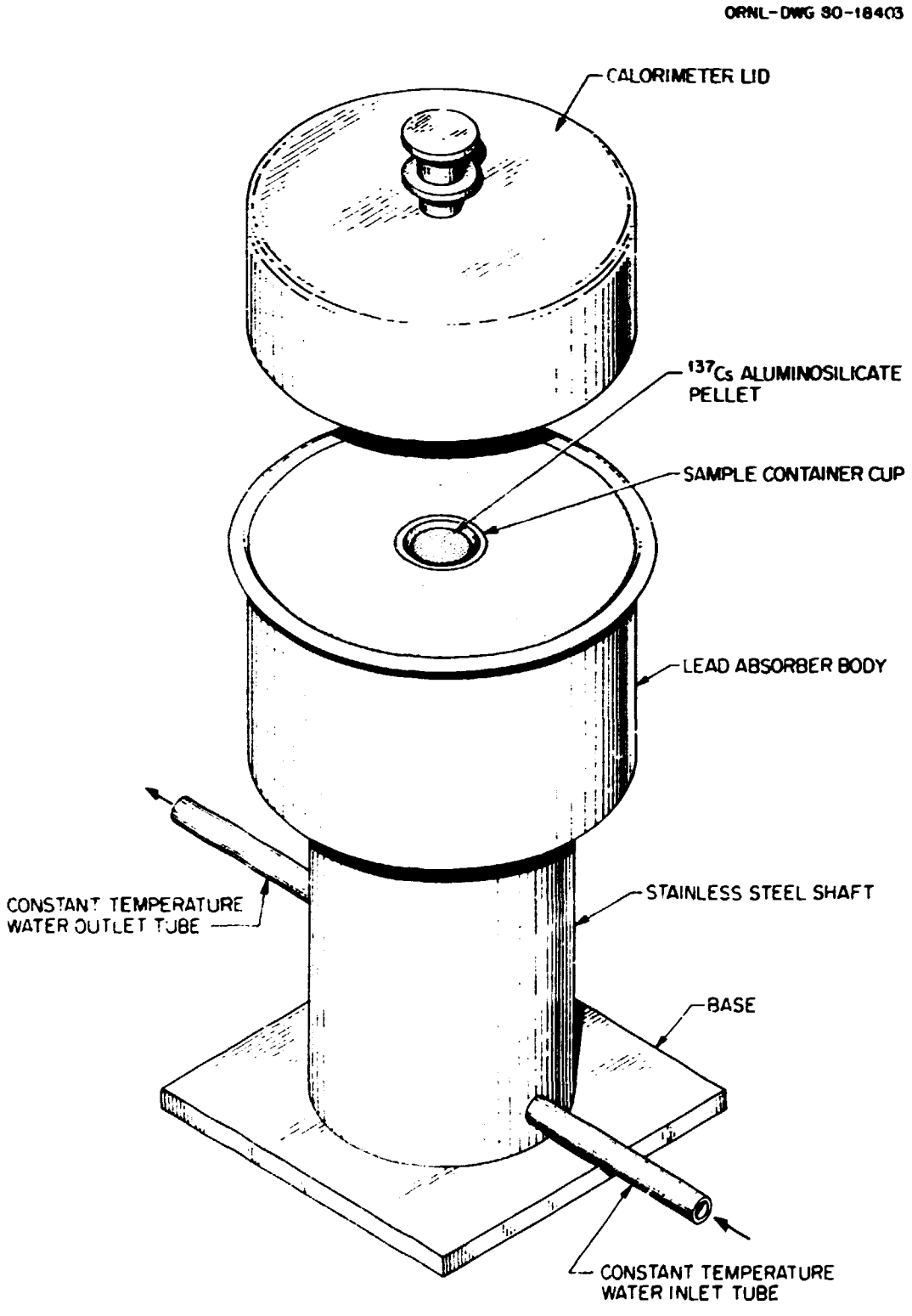

Fig. 10. Cesium-137 Aluminosilicate Pellet Calorimeter

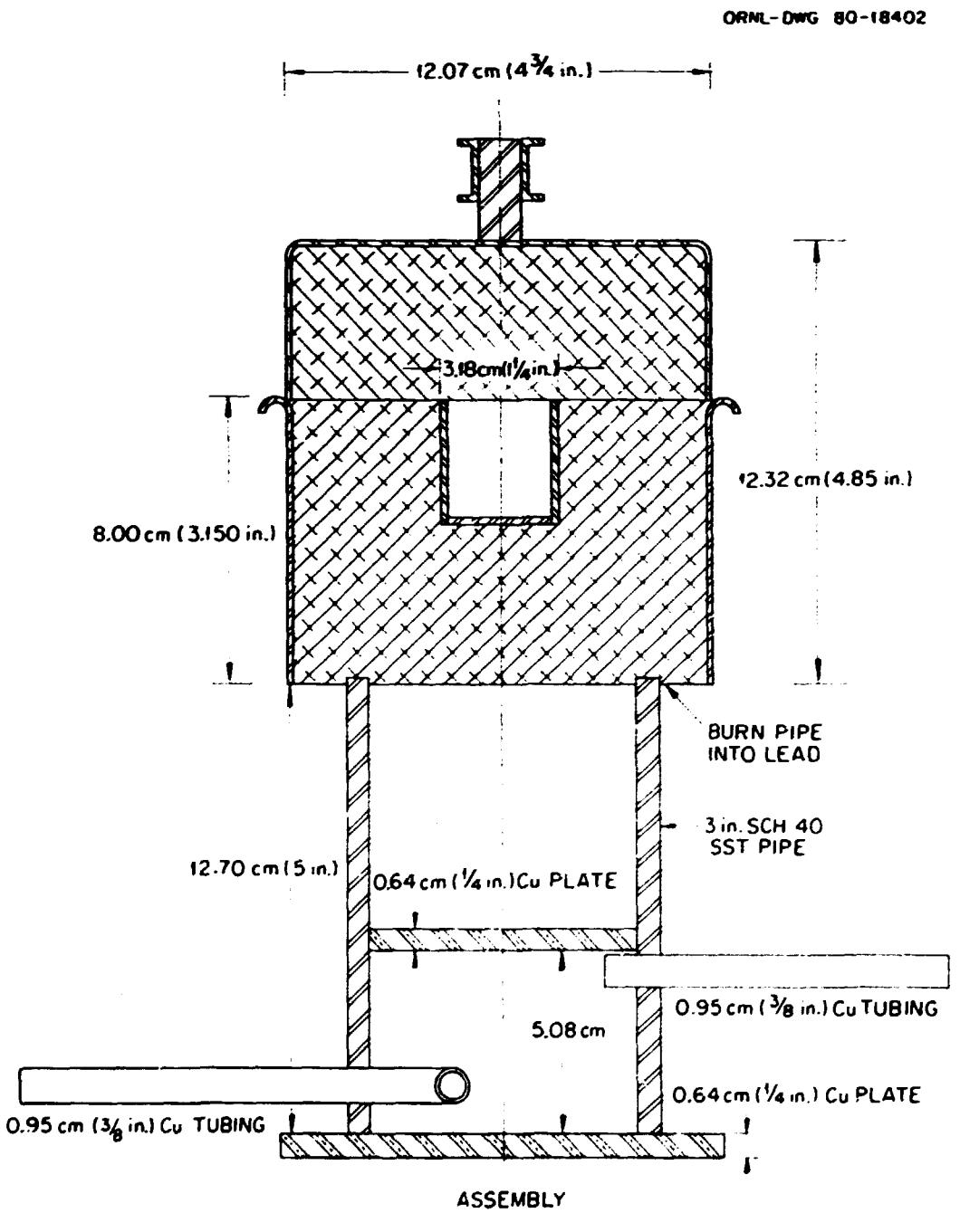

Fig. 11. Cesium-137 Aluminosilicate Pellet Calorimeter Schematic

The calorimeter was calibrated at temperatures of 18°C and 25°C using a high accuracy, low power resistance heater. Input power supplied to the calibration heater located in the calorimeter's sample cup (the cup was filled with distilled water to hasten the heat transfer to the surrounding lead) ranged from 0.5 watts to 5 watts. This range covered the anticipated output of 2 to 3 watts expected from the pollucite pellets. Table 15 presents the data obtained for construction of the calorimeter's calibration curve.

Table 15. Calorimeter Calibration Data for Liquid Temperature of 18.02°C

Input power (watts)	Thermopile output voltage (mV)
0.495	0.83
1.063	1.68
1.499	2.25
2.035	3.00
2.504	3.66
3.009	4.39
3.504	5.10
4.993	7.21

The equation of the straight line resulting from a general least squares fit of the data is given by Eq. (2).

$$y = (0.1371 \pm 0.0144) + (1.4147 \pm 0.0052)x \ , \qquad (2)$$

where

y = thermopile output in mV,

x = input power in watts .

The sample correlation coefficient, r, which is the expression of the tendency for x and y to be linearly related, obtained for the above data was 0.99996 (a value of 1.00000 for r indicates perfect linearity for two variables). During an actual calorimeter measurement of a pollucite pellet an inverse interpolation of a given thermopile voltage output will yield the number of watts generated by the sample. From the measured heat output and the known conversion factor for ^{137}Cs relating watts and curies one can then calculate the curie content of the pellets.

The heat outputs of four ^{137}Cs aluminosilicate pellets were measured and the calculated curie contents are shown in Table 16.

Table 16. Curie Content of Cesium-137 Aluminosilicate Pellets as Measured by Calorimetry

Pellet No.	Weight[a] (g)	Heat output (watts)	Curie content (Ci)
C1	41.24	2.18	450
C2	40.40	2.15	444
C3	40.35	2.15	444
C4	39.00	2.12	437

[a]Corrected for surrounding grafoil sheath.

The curie content of each pellet was calculated from the measured heat output of the sample and utilizing the following conversion factor.[17]

$$1 \text{ kCi} = 4.84 \text{ watts} .$$

Metallography (Optical Microscopy) Studies

Metallographic examinations of the aluminosilicate pellets provided information on phase homogeneity and other pellet physical characteristics such as porosity and density gradients.

The sectioned aluminosilicate pellet specimens were ground and polished before mounting on a metallographic specimen holder. The sample sections were examined by a modified Shielded Bausch and Lomb Metallograph employing a high intensity xenon lamp (450 w) for sample illumination. The pollucite specimens examined were recovered from two distinct areas of the pellet; the periphery or edge and the approximate geometric center. These two pellet areas were examined by both metallographic and SEM-electron microprobe techniques to determine if any elemental inhomogeneities existed across the pellet as well as porosity (density) gradients.

Figures 12 through 15 are metallographic photographs of selected pellet sections.

Figure 12 presents a sequence of photomicrographs depicting a density gradient from the center to the outer edge of the sample pellet. An

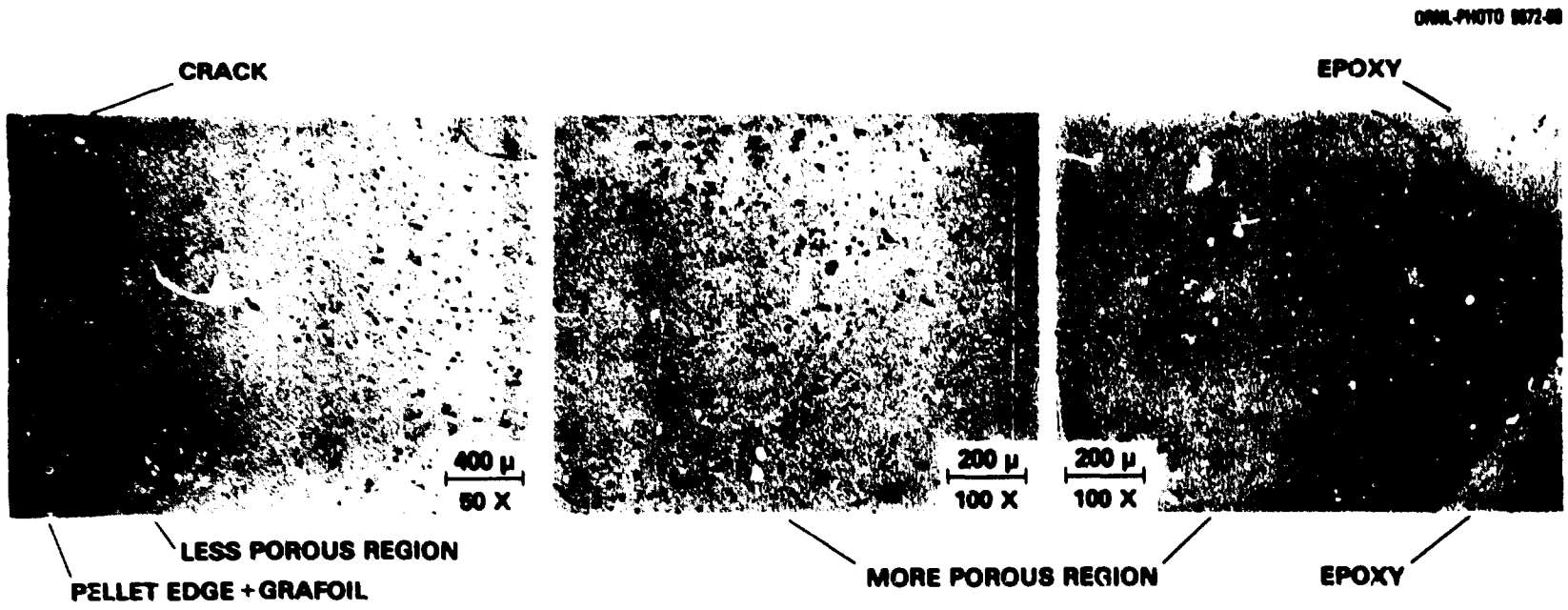

Fig. 12. Cesium-137 Aluminosilicate Pellet Photomicrographs Depicting Density Gradient

approximately 0.16 cm annulus located at the pellet's edge contains noticeably fewer voids (pores) than does the remainder of the pellet sections examined. This phenomenon suggests that less outgassing occurred at the pellet's edge than occurred in the interior regions during the vacuum hot pressing cycle. A possible explanation for the above would be the utilization of a preheat cycle wherein the pre-pollucite powder is heated at a reduced power setting (~1 kW) for one hour to ensure nonbonded water evaporation. Apparently, only the outer 0.16 cm of the pellet is affected by the preheating process step.

As mentioned earlier the pellet samples were ground and polished in preparation for metallographic mounting. Both alumina and silica were used in the sample preparation. Examination of Figs. 13 and 14 revealed residual alumina and silica which had been trapped in the large and small pores or depressions contained in the aluminosilicate pellets. The high reflectivity of alumina and silica accounts for the frequent occurrence of large and small bright white areas in the photomicrographs.

The major physical characteristic displayed in the photomicrographs was the existence of a primary and a secondary phase; the primary phase being a gray matrix containing large and small pores, some granular surfaces, and small pore agglomerations (Fig. 15), while the secondary phase consisted of small gray-white flecks sparsely interspersed throughout the gray matrix. Earlier studies of nonradioactive aluminosilicate pellets had indicated that the secondary, white phase consisted of fused cesium, aluminum, and silicon as opposed to the primary matrix grain phase.

A comparison of Figs. 13 and 14 highlights the porosity and consequently the density difference between the two pellets. The pellet section shown in Fig. 14 (pellet C2) contains significantly fewer pores (or voids) than does the pellet section shown in Fig. 13 (pellet C4). The lower density (higher porosity) of pellet C4 would account for the ease of removal of the grafoil sheath which had surrounded the pellet.*

*During the pellet extraction step the grafoil sheath was easily torn away from the pellet surface. Usually the grafoil sheath adheres tightly to the pellet and will not become dislodged even under extreme thermal stress.

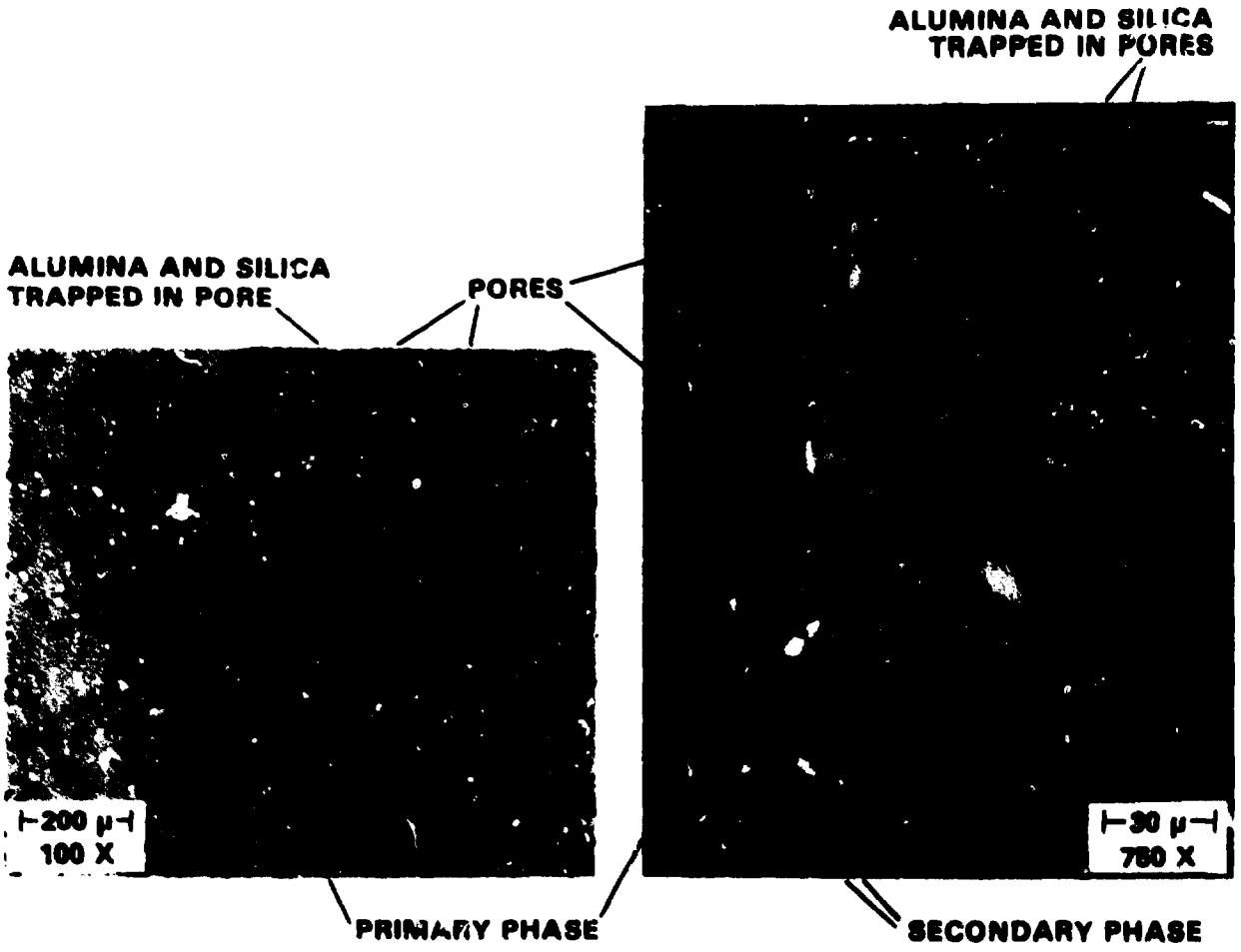

Fig. 13. Cesium-137 Aluminosilicate Pellet Photomicrograph Depicting Trapped Alumina and Silica

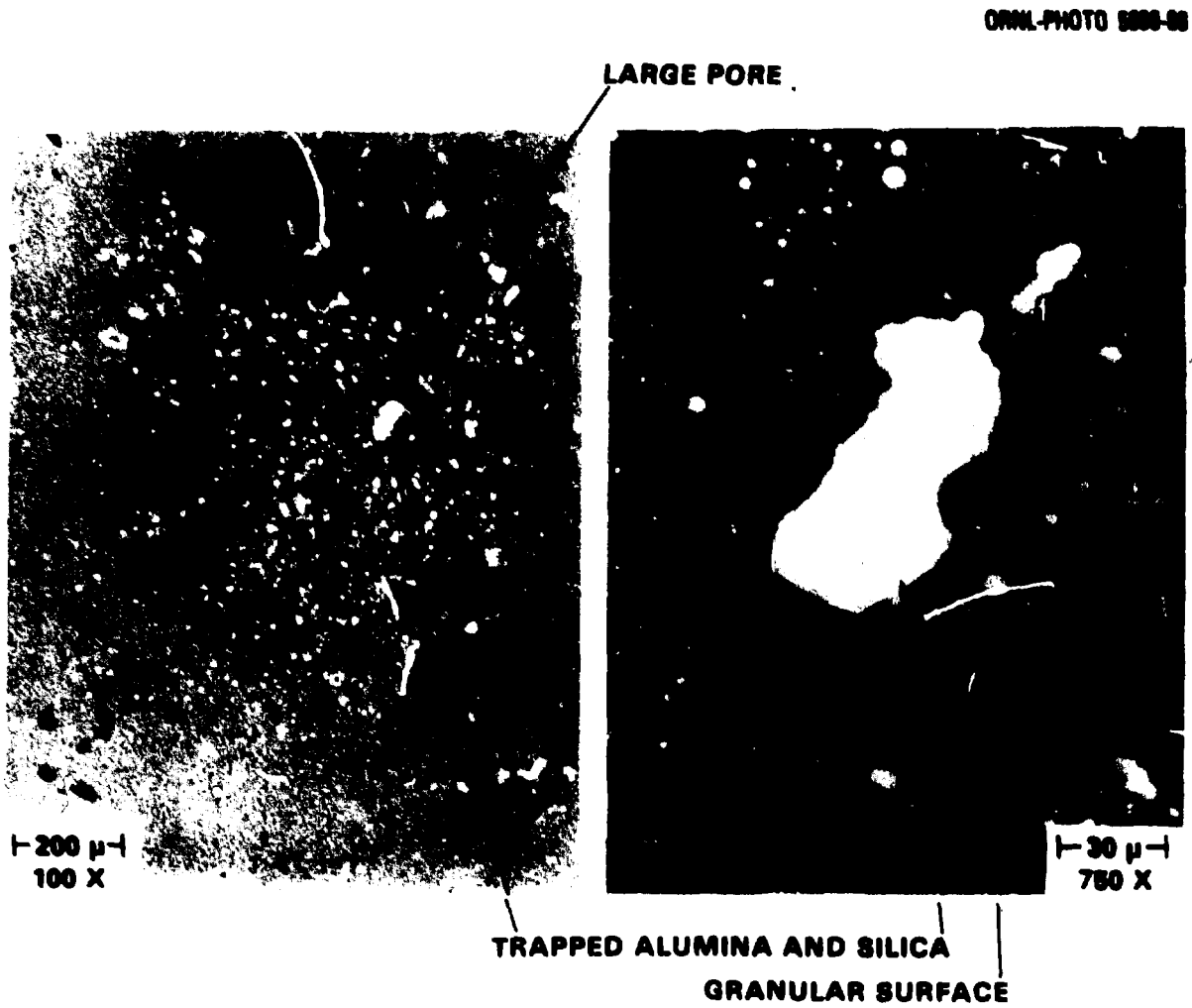

Fig. 14. Cesium-137 Aluminosilicate Pellet Photomicrograph Depicting Trapped Alumina and Silica

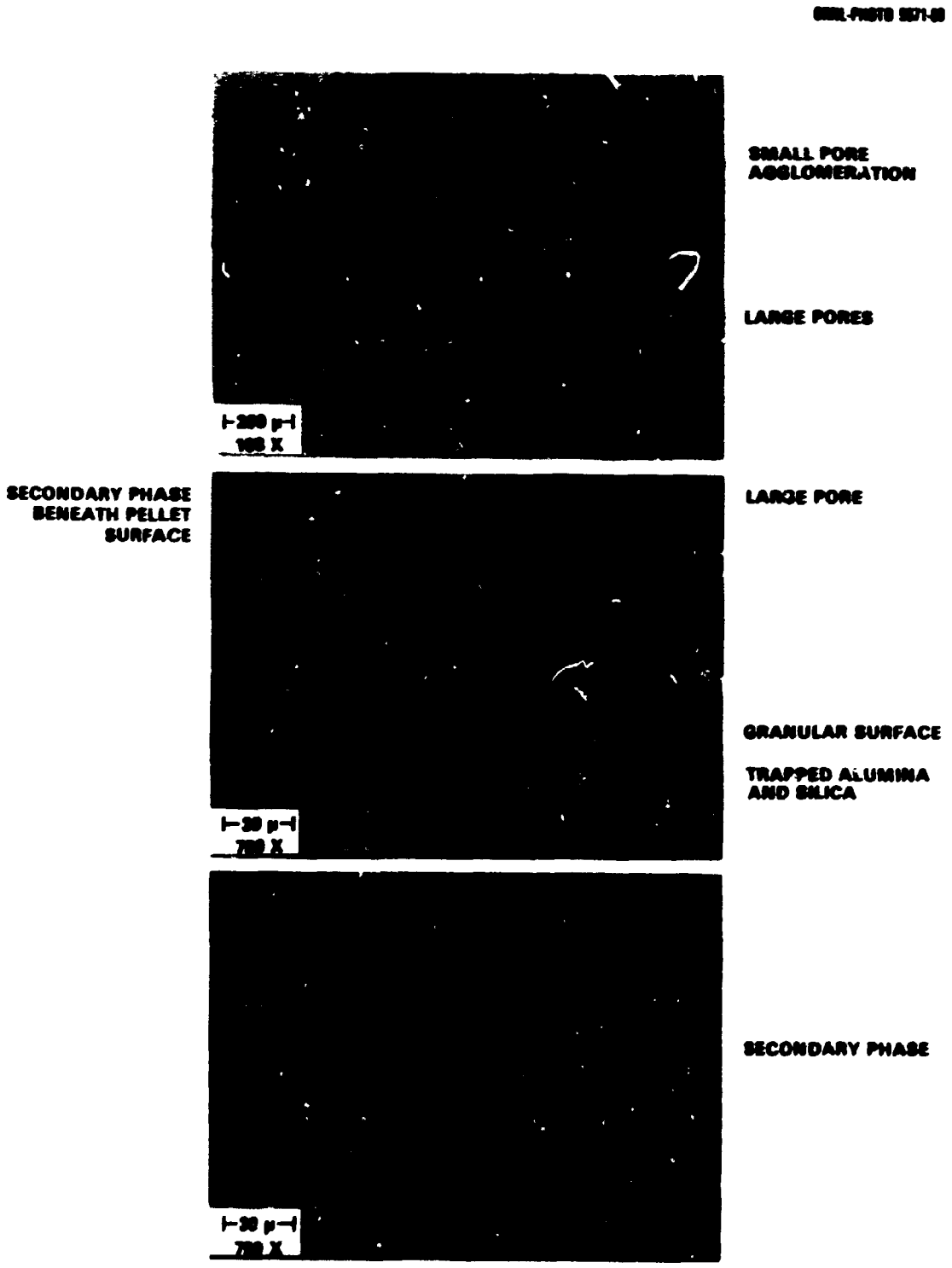

Fig. 15. Cesium-137 Aluminosilicate Pellet Photomicrograph Depicting Major Physical Characteristics

The production history of each full level ^{137}Cs aluminosilicate pellet which had been characterized is given in Table 17.

Table 17. Production History of the Full Level Cesium-137 Aluminosilicate Sample Pellets

Pellet No.	Clay-carbonate batch No.	VHP production run No.	VHP power at maximum ram travel (kW)	VHP maximum applied pressure (psig)	VHP maximum applied pressure (kPa)	"Curing" step duration	Corrected density[a] (g/cm^3)
C1	79CsP-1,2,3,4	6	20.45	575	4070	20	3.21
C2	79CsP-9	12	19.98	575	4200	40	3.15
C3	79CsP-5,6,7	11	18.86	640	4500	90	3.14[b]
C4	79CsP-1,2,3,4	7	20.30	575	4070	10	3.04[b]
F1	79CsP-5,6,7	8	19.98	575	4070	30	3.17
F2	79CsP-5,6,7	9	19.83	575	4200	45	3.22

[a]Corrected for weight and volume of surrounding grafoil sheath.

[b]Grafoil sheath had been removed during pellet extraction and, therefore, final weight of pellet was measured directly.

Using density as a first criterion defining pellet quality, an examination of Table 17 and, in particular, the VHP power applied and "Curing" durations, one can conclude that the "Curing" step duration is the critical factor controlling the aluminosilicate pellet production. The power applied to the pellet during its formation is not as crucial to pellet quality as is evidenced by VHP production runs 7 and 8. Both production runs were made under similar conditions of pressure and power, but the "curing" step duration time in run 8 was three times longer than that applied to the pellet produced in run 7. The density of the pellet produced in run 8 was 4.3% greater than the density of the pellet produced in run 7. Also, a comparison of VHP production runs 6 and 7, which were run under nearly identical power (temperature) and pressure conditions, but again significantly different "curing" step durations, underscores the importance of the duration of the "curing" step in the production of $CsAlSi_2O_6 \cdot nH_2O$. Run 6, which employed a "curing" duration twice as long as that used in run 7, produced a pellet having a density 5.6% greater than the pellet recovered from production run 7. However, no linear relationship between the "curing" step duration and density exists, but at sufficient power levels (>18.9 kW) a minimum "curing" step duration of 20 minutes should be allotted to ensure production of quality aluminosilicate pellets.

Scanning Electron Microscopy and Electron Microprobe Studies

SEM and electron microprobe analyses were used during the experimental stage of the project to assist in formulating optimum operating conditions for the production of the full level ^{137}Cs aluminosilicate pellets.

SEM-EDX studies of early experimental nonradioactive pellets had indicated an inhomogeneous concentration of cesium, aluminum, and silicon across the width (center to edge) of the pellet. Also, in the light, fused phase a cesium concentration 1.5 times that of the dark, grain phase was uncovered. However, SEM-BSE examinations of full level production pellets showed cesium and silicon to be homogeneously distributed throughout the pellet, including both the fused and grain phases (secondary and primary phases, respectively)(Fig. 16). Aluminum homogeneity was unconfirmed as a result of the high background noise caused by the inherent radioactivity of the pellet specimen. These results indicated that the cesium/silicon reaction during hot pressing was complete.

X-Ray Diffraction Studies

X-ray diffraction analyses of fully loaded ^{137}Cs and nonradioactive aluminosilicate pellet samples were employed to confirm the pollucite crystal lattice structure. A comparison of the three most intense sample lines measured with the three most intense known pollucite spectral lines given in Table 18 confirm the pollucite crystal lattice structure.

Table 18. Comparison of Sample Cesium Aluminosilicate and Cesium Pollucite Crystal Lattice Spacing[18]

Sample crystal lattice spacing (nm)	Pollucite crystal lattice spacing (nm)	Normalized intensities (I/I_1)
0.291	0.2913	45
0.342	0.342	100
0.365	0.365	30

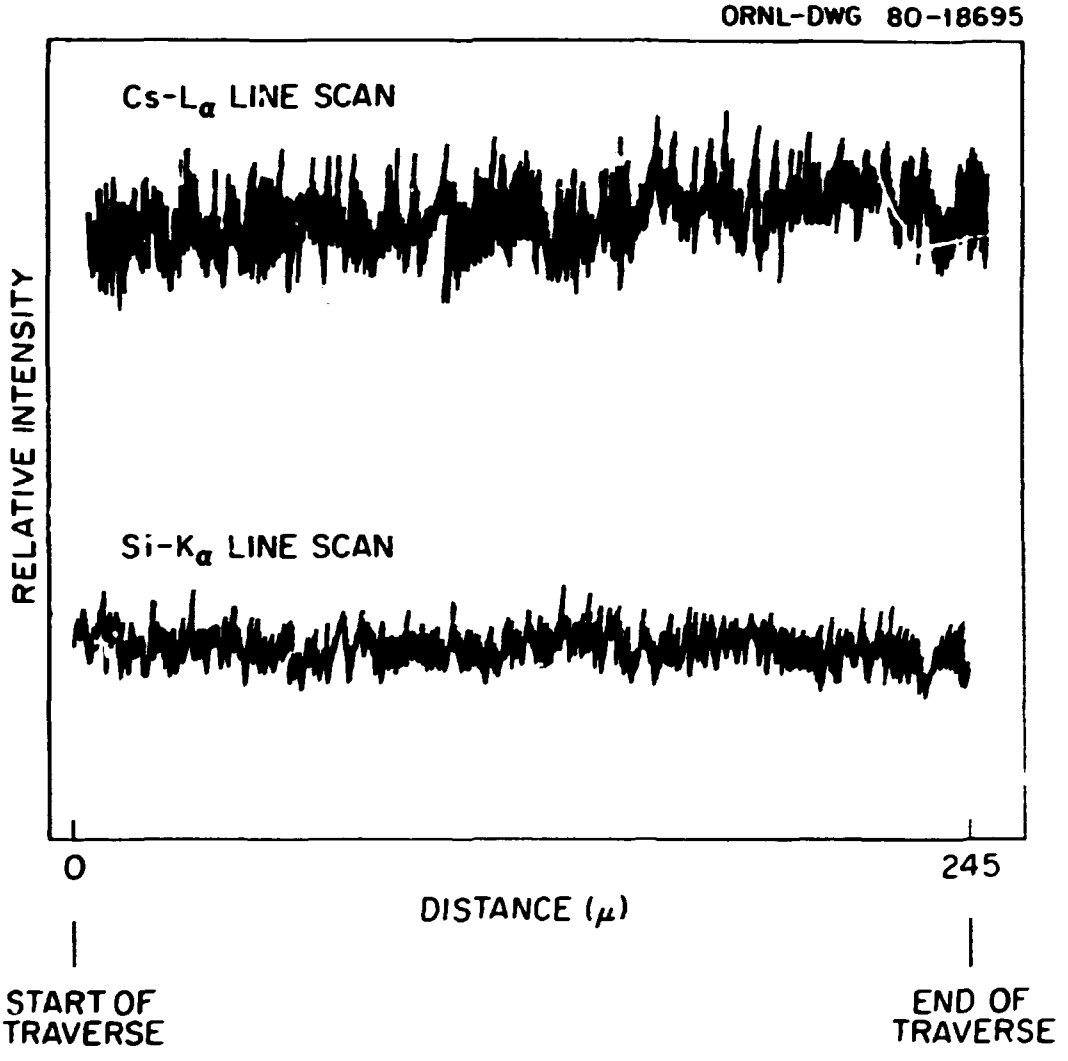

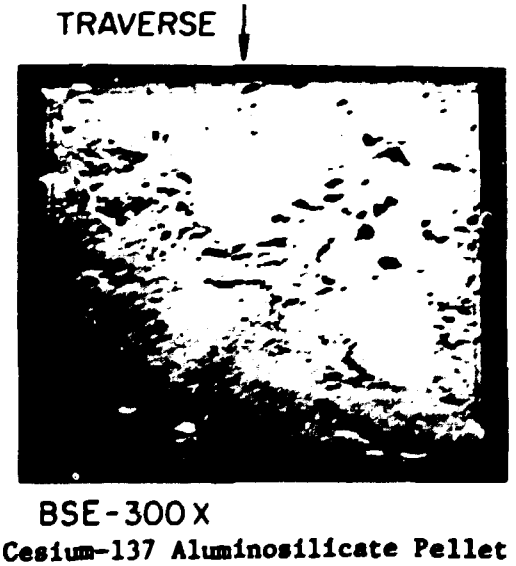

Fig. 16. Cesium-137 Aluminosilicate Pellet SEM-BSE Scan Depicting Cesium and Silicon Homogeneity

An X-ray diffraction pattern of a nonradioactive aluminosilicate pellet is shown in Fig. 17. Since a small, solid piece of pellet was analyzed, recognizing its diffraction pattern was more difficult due to the solid sample having a preferred orientation. Also, the high level of radioactivity emitted by the full level ^{137}Cs pollucite sample complicated the X-ray diffraction pattern measurement and interpretation.

Cesium Ion Leachability Measurements

Leachability measurements of the ^{137}Cs pollucite pellets was conducted in the four phases listed in Table 19.

Table 19. Leachability Measurement Phases

Phase	Leachability Measurements
1	Quasi-static leaching of tracer level ^{137}Cs pollucite pellet sections in distilled water [T = 94°C (367K)]
2	Quasi-static leaching of gamma-irradiated tracer level ^{137}Cs pollucite pellet sections in distilled water [T = 94°C (367K)]
3	Quasi-static leaching of full level ^{137}Cs pollucite pellet sections in distilled water [T = 94°C (367K)]
4	Static leaching of full level, unsectioned ^{137}Cs pollucite pellets in distilled water [T = 32°C (305K)]

The leaching of the sectioned ^{137}Cs pollucite pellets was conducted employing a Soxhlet extractor (Figs. 18–21).[19,20] The pellets were sectioned by a diamond-tipped saw blade to the approximate dimensions of 0.70 cm × 0.70 cm × 0.50 cm. The pellet was held in place by a specially designed vise (Fig. 22).

The Soxhlet extractor was an all glass quasi-static leaching apparatus having an overall length of approximately 3 ft (91 cm) consisting of a 1000-ml round bottom boiling flask which contains the leachate. The leachate, which in these experiments was distilled water, was heated to boiling with an encircling mantle. The water vapors passed through a vent to a reflux condenser. The condensate descends through the coils where it is preheated before falling dropwise into the sample cup. Every 9 to 12 minutes the leachant drains through a syphon leg to the distilled water

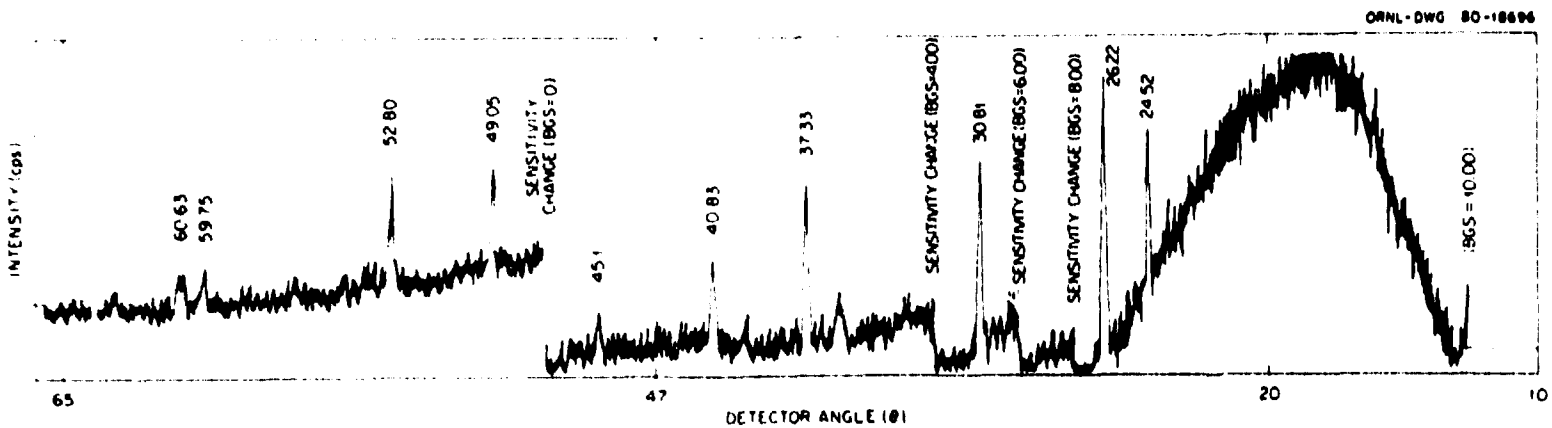

Fig. 17. Cesium Aluminosilicate Pellet X-Ray Diffraction Pattern

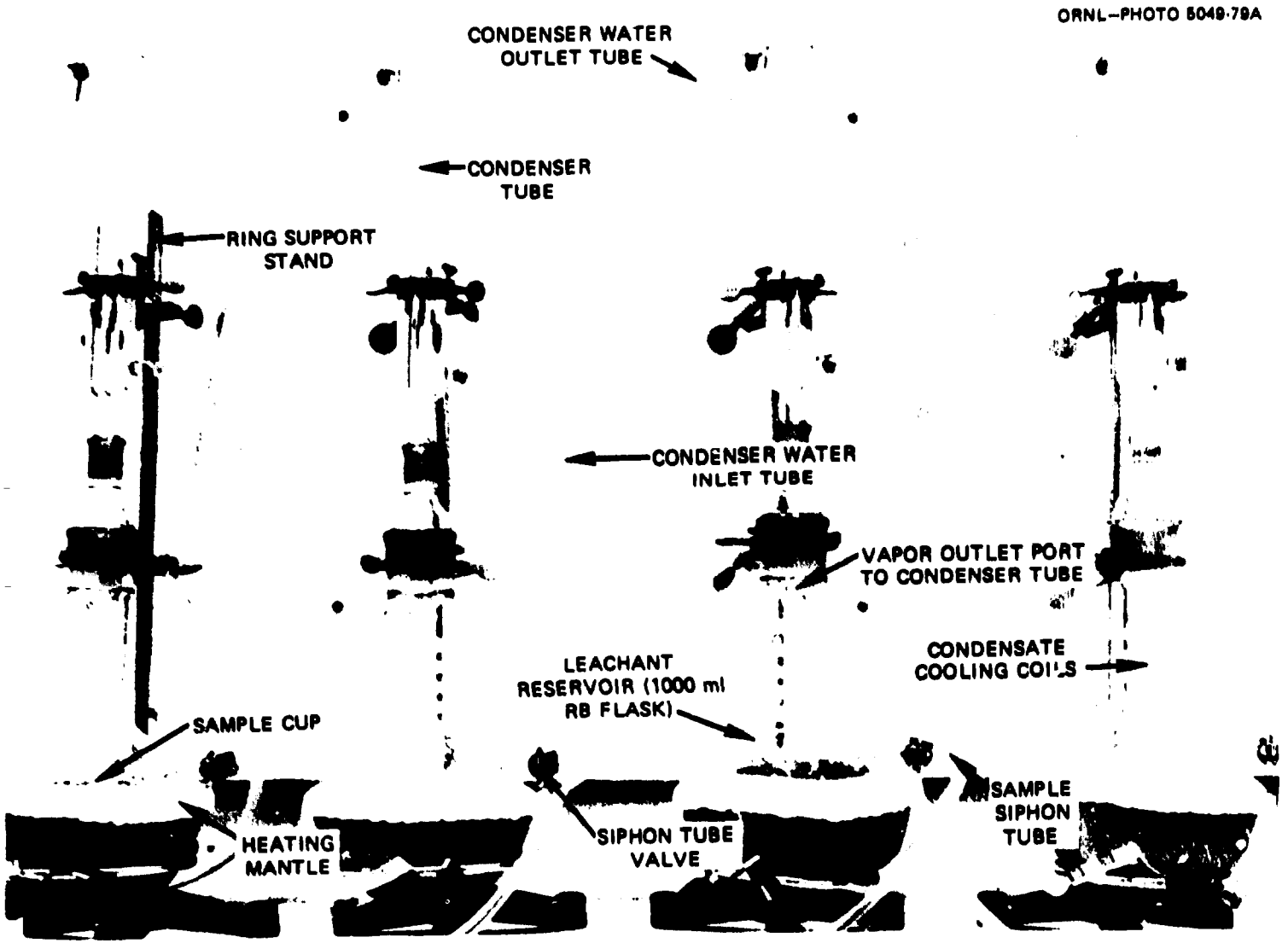

Fig. 18. Soxhlet Extractors

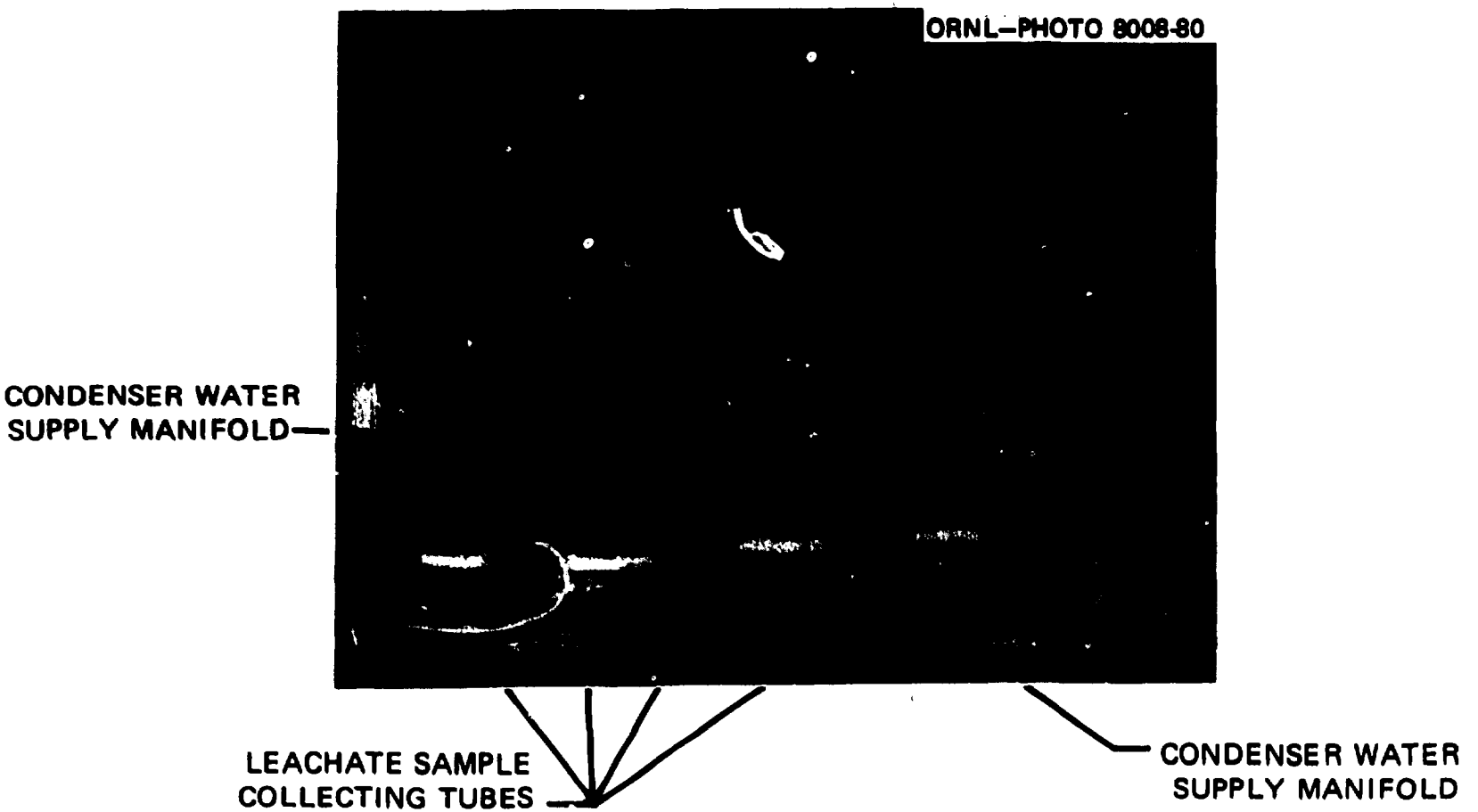

Fig. 19. Soxhlet Extractors in Hot Cell

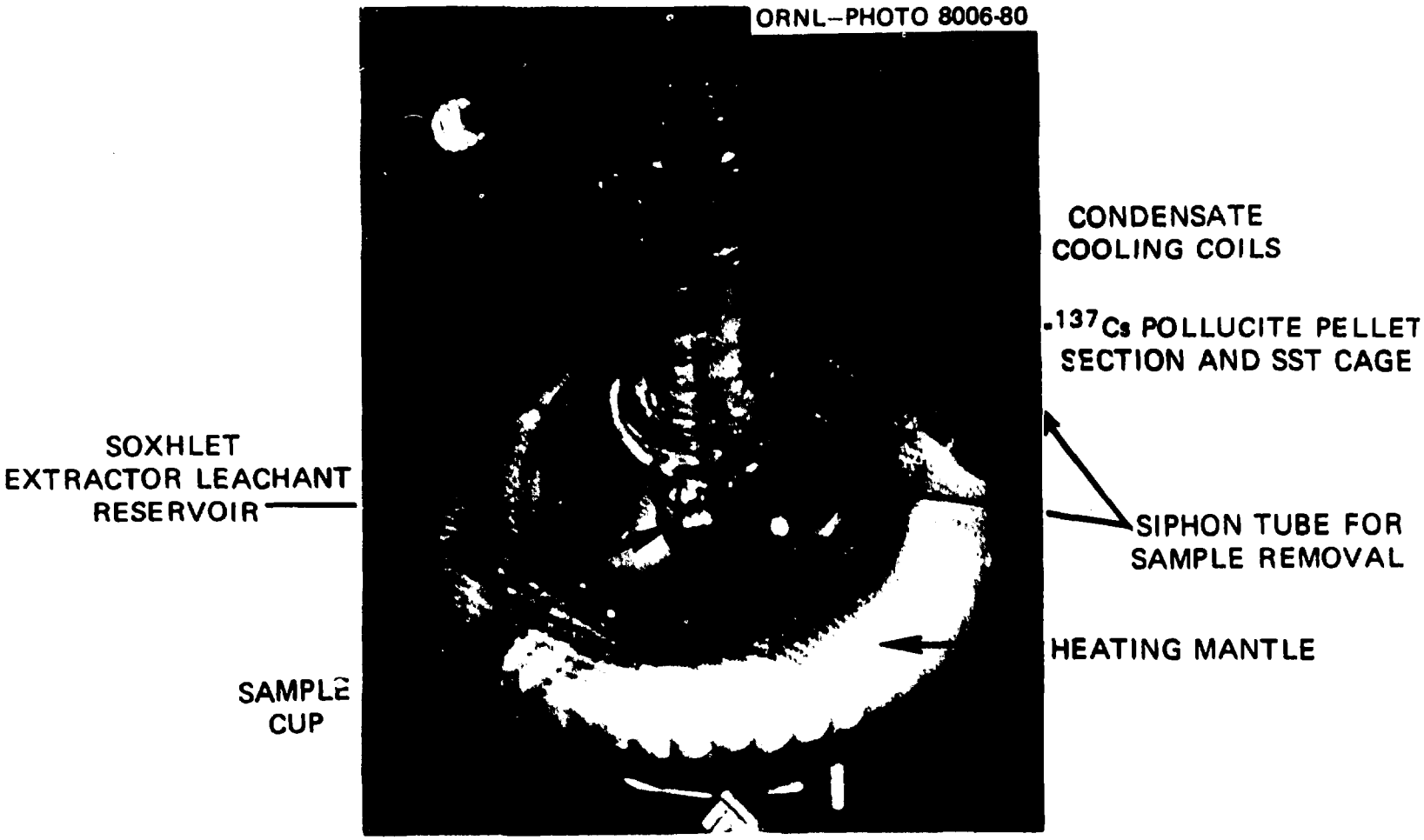

Fig. 20. Close-Up View of Soxhlet Extractor in Hot Cell

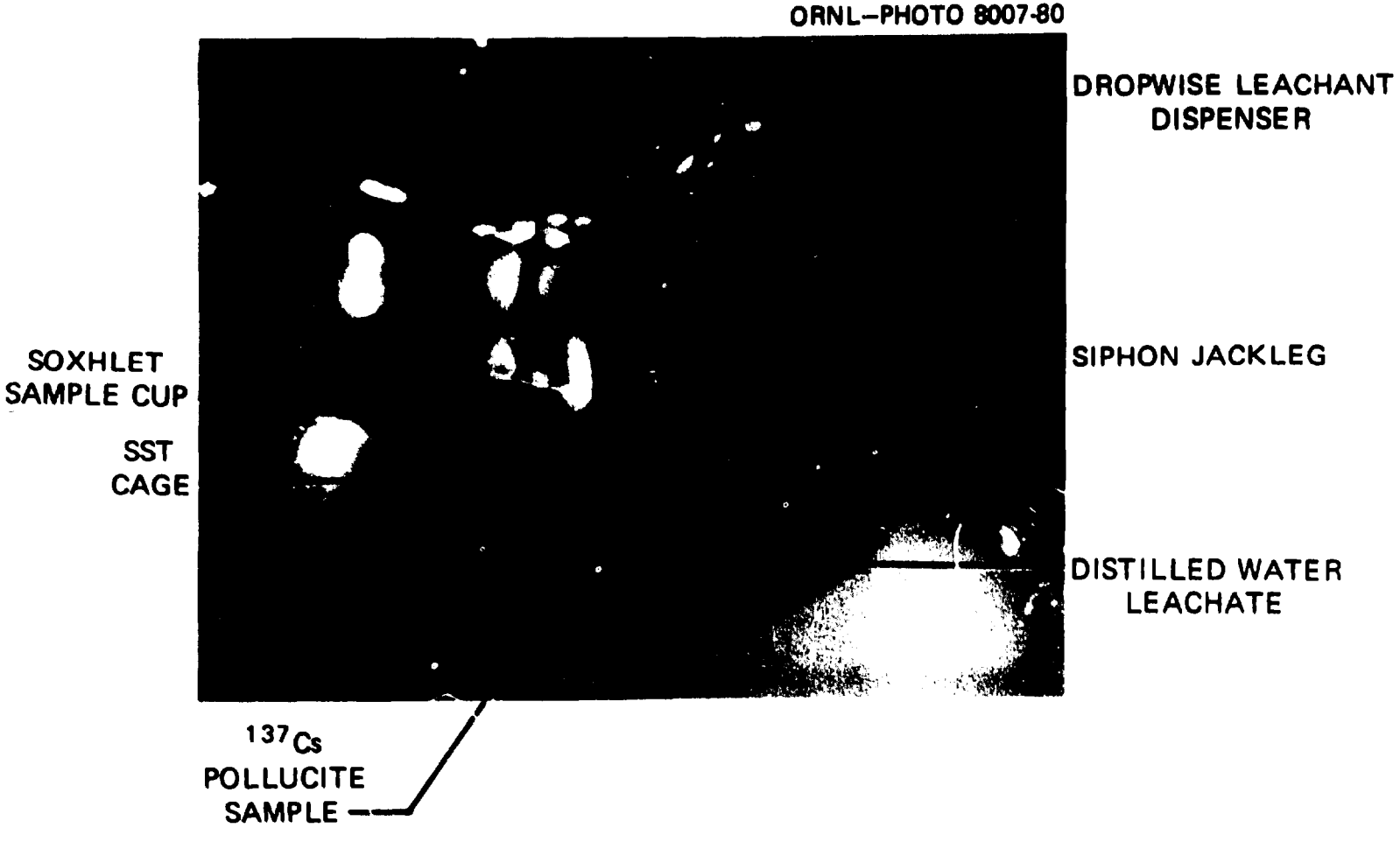

Fig. 21. Detail View of In-Cell Soxhlet Extractor's Sample Cup

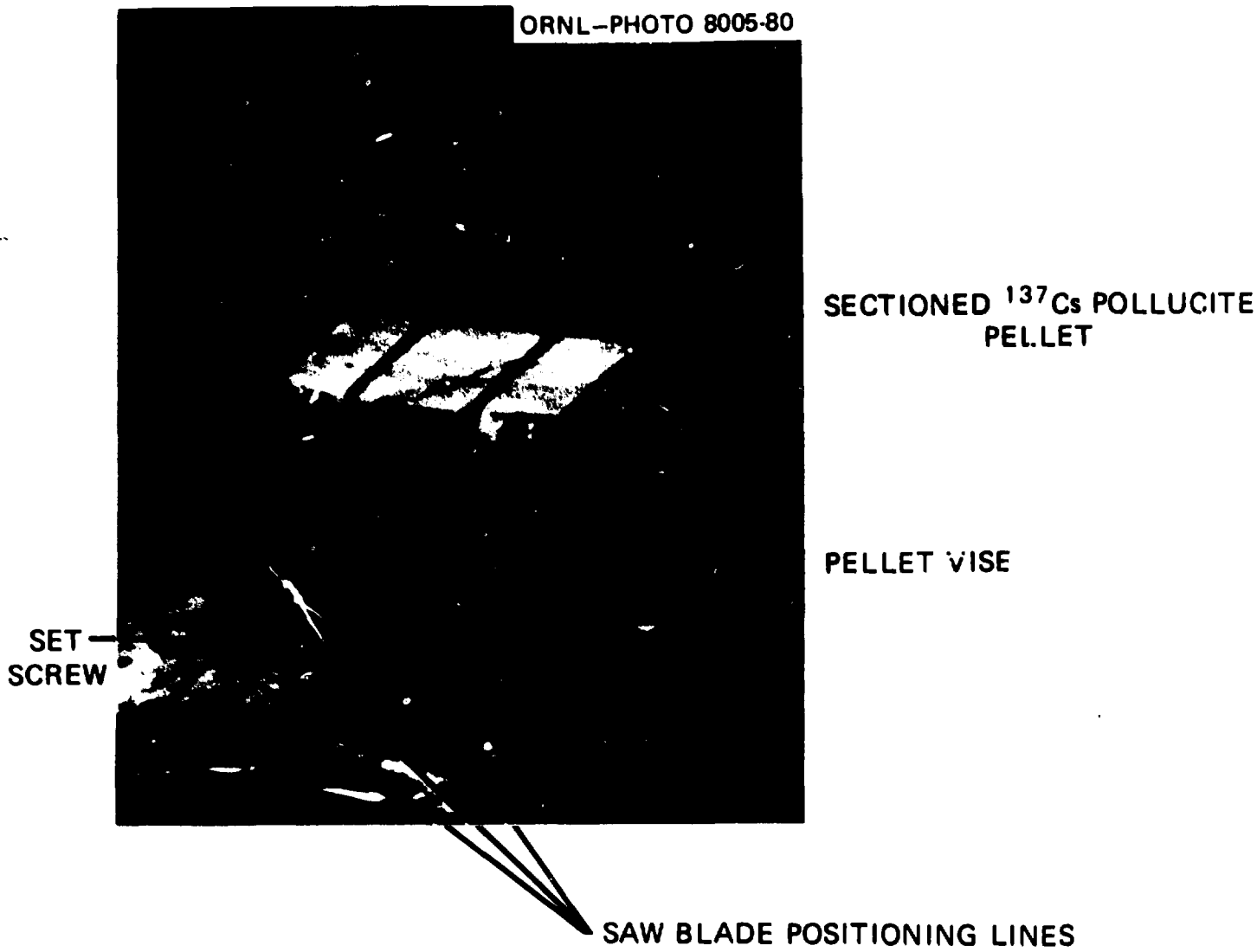

Fig. 22. A Partially Sectioned Cesium-137 Aluminosilicate Pellet and Pellet Vise

boiling flask. The temperature in the leach sample cup is approximately 94°C (367K). Removal of the leachant for analysis is accomplished by a syphon tube located at the bottom of the reservoir. Fresh leachate is added to the extractor through the top of the reflux condenser.

The unsectioned fully loaded ^{137}Cs aluminosilicate pellets [1 in. (2.54 cm) diam by 1 1/8 in. (2.86 cm) high], each with a geometric surface area of approximately 13 cm^2 were leached in approximately 400 ml of distilled water at a temperature of approximately 32°C. This static leach test approaches a dynamic experiment by employing frequent sampling periods wherein fresh distilled water is substituted at short time intervals. The pellet was suspended in a 500-ml Erlenmeyer flask by a stainless steel rod and cage.

The leach rates (kg $m^{-2}s^{-1}$) were calculated based upon measurements of the ^{137}Cs content of the recovered leachant samples. The quantity of cesium in the sample was determined from the assaying of the ^{137}Cs 661.64 keV gamma ray signature. From the known ratio of ^{137}Cs and the remaining cesium isotopes (^{133}Cs and ^{135}Cs), both stable and radioactive, the known activity contained in the original pellet sectioned, as well as the measured geometric surface area of the sectioned piece, one could then calculate the leach rate of cesium ion out of pollucite.

Fick's first and second laws of diffusion were applied to the tracer level ^{137}Cs pollucite leach rate data for the determination of the cesium diffusion coefficient. The diffusion coefficient is considered to be independent of time, position, and the concentration of the diffusing species. If we assume that the rate of diffusion is so small that the test specimen may be considered to be infinitely long in the direction of negative x with the exposed face in the plane $x = 0$, the following differential equations and accompanying boundary conditions describe the diffusion process.[21]

$$D \frac{\partial^2 C}{\partial x^2} = \frac{\partial C}{\partial t} + \lambda C \qquad (3)$$

with boundary conditions of

$$C(x,0) = C_0,$$

$$C(0,t) = 0,$$

$$\frac{\partial C}{\partial x} = 0 \text{ at } x = -\infty,$$

where

D = diffusion coefficient, cm^2/day,

C = atomic concentration, atoms/cc,

t = time, sec,

λ = radioactive disintegration constant, $\ell n2/t^1/_2$, sec^{-1},

$t^1/_2$ = radioactive half-life, sec.

Solving Eq. (3) by separation of variables yields Eq. (4).

$$C(x,t) = C_0 e^{-\lambda t} erf\left(\frac{-x}{2\sqrt{Dt}}\right). \tag{4}$$

Computing the flux across the interface at $x = 0$ and using the fact that the product, λt, for ^{137}Cs is $\ll 1$ ($\sim 0.00006\ t$) gives the following expression for the total amount of activity, a, accumulated in the leachant over N sampling periods with total elapsed time, T.

$$a = \sum_{n=1}^{N} a_n = \int_0^T \lambda F j_0(t)dt \ . \tag{5}$$

$$= \frac{\lambda FDC_0}{\sqrt{\pi D}} \int_0^T \frac{dt}{t^1{}_2} \ . \tag{6}$$

$$= \frac{2FA_0}{V}\sqrt{\frac{DT}{\pi}} \ . \tag{7}$$

where

a = total amount of radioactivity lost, Σa_n, curies,

a_n = radioactivity leached during the leachant renewal period, m, curies,

A_0 = initial radioactivity present in specimen, curies,

F = surface area, cm^2,

V = volume, cm^3,

D = diffusion coefficient, cm^2/day,

j = atom flux, atoms/cm^2-sec, and

T = total elapsed time, Σt_n, sec.

The equation below expresses the leach rate in units having the dimensions of grams of solid/cm^2-day.[22]

$$\text{Leach rate} = \left[\frac{\text{(activity of isotope leached)/day/}\dfrac{\text{initial activity of}}{\text{isotope in solid}}}{\text{[(sample area, cm}^2\text{)/(sample weight,g)]}}\right]$$

$$= \frac{\text{Fraction leached/day}}{\text{cm}^2/\text{g}}$$

$$= \text{g/cm}^2\text{-day} \; . \tag{8}$$

Leaching experiments with several types of glasses, asphalts, and polyethylenes[20] containing waste solids, have shown that the elution of ions is reasonably approximated by Fick's law of diffusion. This statement can be verified for the case of cesium in pollucite by rearrangement of Eq. (7) and plotting $\Sigma a_n/A_0$ vs $(\Sigma t_n)^{1/2}$ to determine if the resulting plot yields a straight line.[21] For the case of a semi-infinite slab the diffusion coefficient, D, is obtained from the slope of the line given by Eq. (7), which is in the form, $y = mx + b$.

$$a = \frac{2FA_0}{V}\sqrt{\frac{DT}{\pi}}$$

$$a/A_0 = \left\{2\left(\frac{F}{V}\right)\sqrt{\frac{D}{\pi}}\right\}T^{1/2} \tag{9}$$

$$m = 2\left(\frac{F}{V}\right)\sqrt{\frac{D}{\pi}} \; .$$

Solving for D

$$m^2 = 4\left(\frac{F}{V}\right)^2\frac{D}{\pi}$$

$$D = \frac{\pi}{4}\left(\frac{V}{F}\right)^2 m^2 \tag{10}$$

where

m = slope of the straight line from a plot of a/A_0 vs $T^{1/2}$.

The results of this analysis are presented in the following section.

Phase 1: Quasi-static Leaching of Tracer Level ^{137}Cs Pollucite Pellet Sections in Distilled Water [T = 94°C (367K)]

Three tracer level pellets recovered from VHP experimental runs 39, 40, and 41, were sectioned and a suitable piece from each was selected for leachability measurements. After the surface area of each test section was measured they were placed in their respective Soxhlet extractor sample cups and leaching was initiated. Each pellet section was leached with distilled water at a temperature of approximately 94°C (367K) with varying leachant renewal periods for an accumulated leaching period of 368 days. The leach rates calculated from the measured radioactivity of ^{137}Cs for each pellet are given in Table 20.

Table 20. Tracer Level Cesium-137 Aluminosilicate Pellet Cesium Leach Rates

Leachant Renewal Period (days)	Accumulated Leaching Period (days)	Leach Rate ($kgm^{-2}s^{-1}$)		
		Pellet 39	Pellet 40	Pellet 41
1	1	4.20×10^{-9}	4.76×10^{-9}	5.12×10^{-9}
3	4	4.11×10^{-9}	3.54×10^{-9}	5.01×10^{-9}
3	7	1.16×10^{-9}	2.43×10^{-9}	6.31×10^{-9}
3	10	1.27×10^{-8}	2.49×10^{-9}	6.25×10^{-9}
11	21	1.15×10^{-8}	3.45×10^{-9}	4.54×10^{-9}
9	30	2.24×10^{-8}	4.79×10^{-9}	5.32×10^{-9}
6	36	3.12×10^{-8}	6.38×10^{-9}	1.15×10^{-8}
16	52	3.14×10^{-8}	6.91×10^{-9}	1.06×10^{-8}
40	92	3.98×10^{-8}	1.04×10^{-8}	1.68×10^{-8}
21	113	5.29×10^{-8}	2.29×10^{-8}	2.80×10^{-8}
15	128	6.27×10^{-8}	1.42×10^{-8}	3.60×10^{-8}
16	144	5.56×10^{-8}	1.56×10^{-8}	2.91×10^{-8}
25	169	4.61×10^{-8}	6.97×10^{-9}	2.93×10^{-8}
23	192	4.96×10^{-8}	1.69×10^{-8}	3.10×10^{-8}
18	210	5.15×10^{-8}	1.59×10^{-8}	3.09×10^{-8}
14	224	8.47×10^{-8}	1.58×10^{-8}	2.94×10^{-8}
30	254	3.95×10^{-8}	1.30×10^{-8}	2.41×10^{-8}
62	316	3.30×10^{-8}	1.11×10^{-8}	2.70×10^{-8}
52	368	2.65×10^{-8}	1.02×10^{-8}	2.34×10^{-8}

Plots of the data, that is leach rate vs time, are shown in Figs. 23 through 25.

The diffusion coefficients for the elution of the cesium ion out of the pollucite pellet was calculated assuming a semi-infinite slab and applying Fick's law of diffusion as discussed earlier. The diffusion coefficients for each pellet, as well as the equation of the straight line and the sample correlation coefficient, r (the expression of the

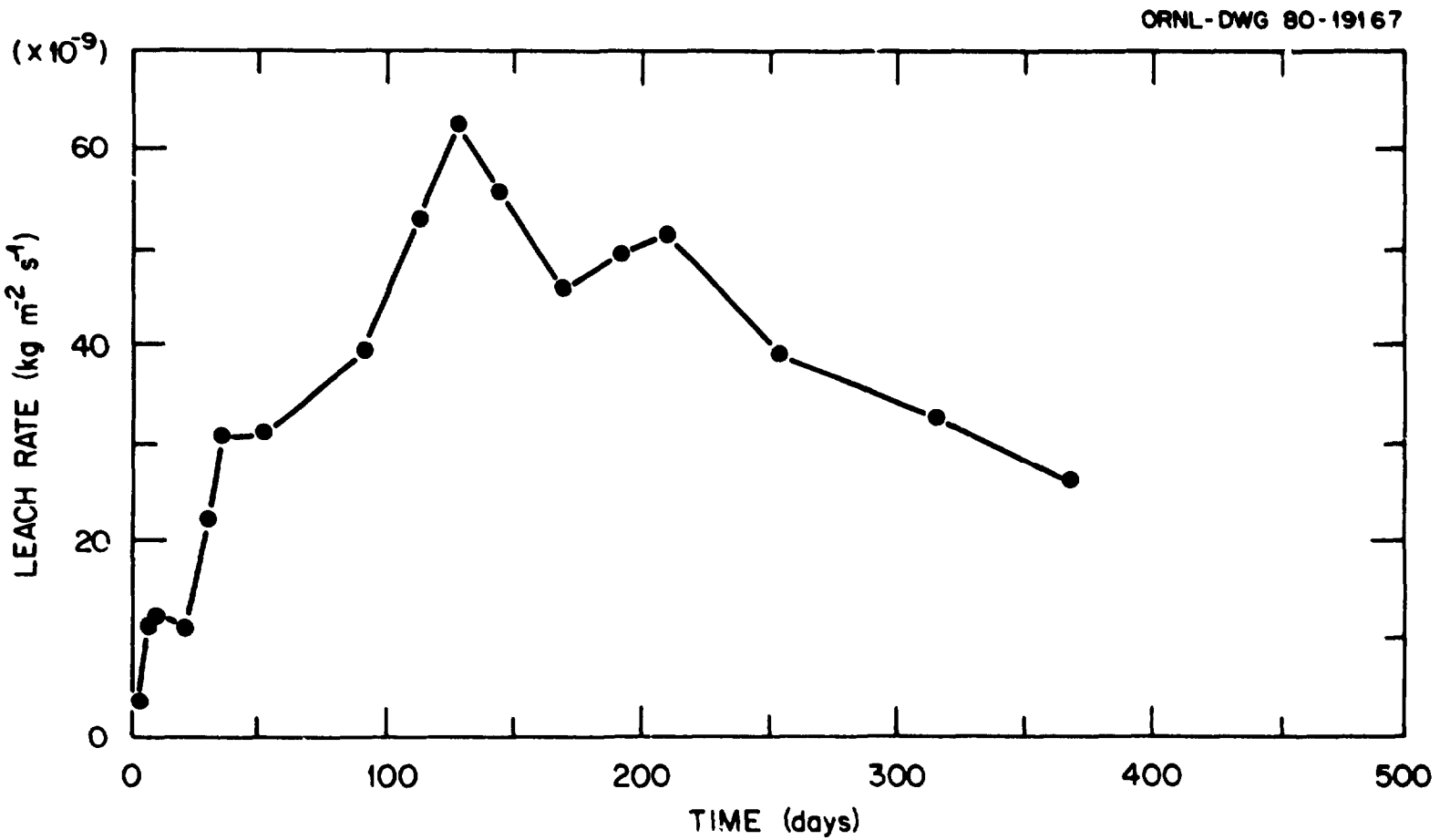

Fig. 23. A Graph of Cesium Leach Rate vs Time for Pellet 39

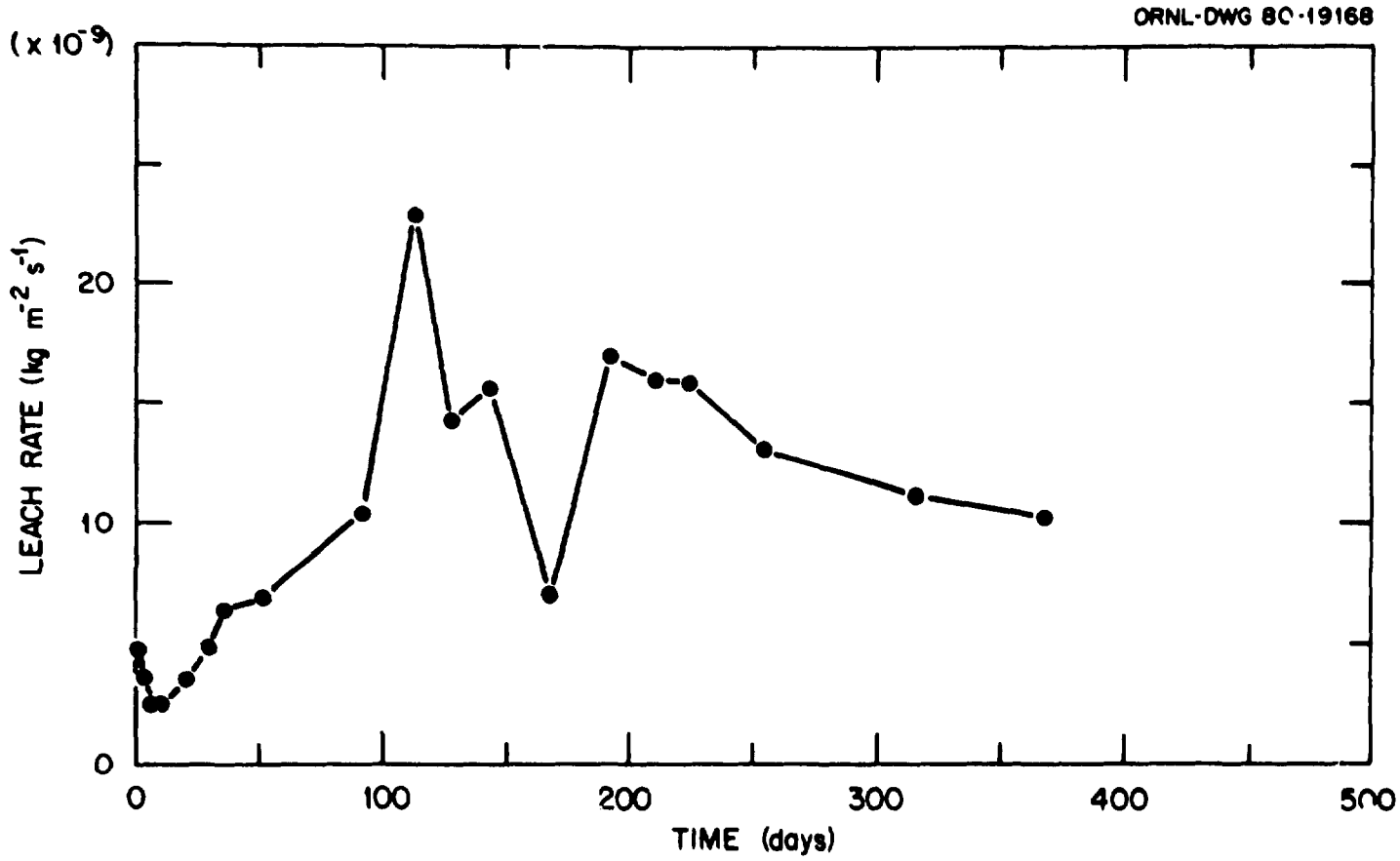

Fig. 24. A Graph of Cesium Leach Rate vs Time for Pellet 40

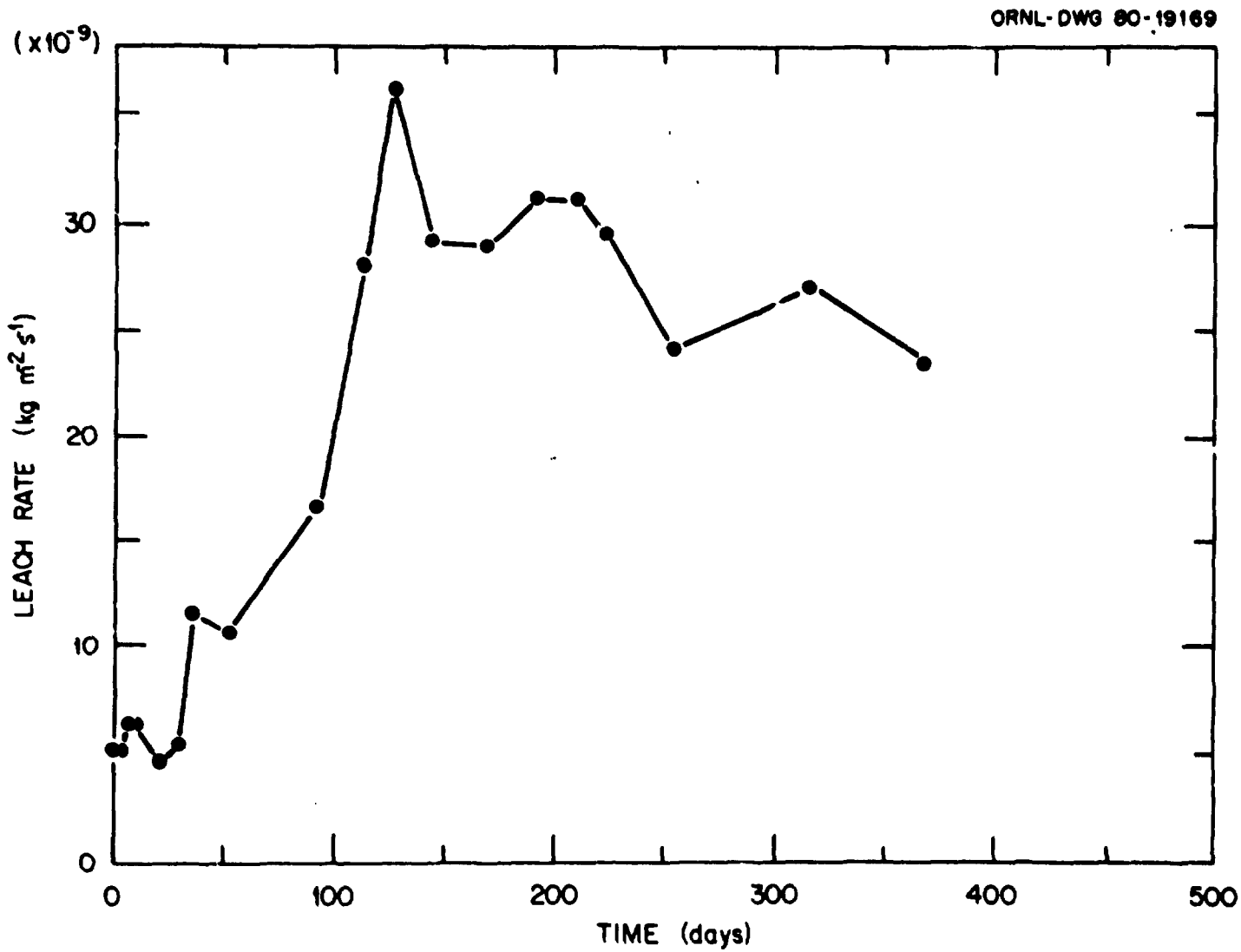

Fig. 25. A Graph of Cesium Leach Rate vs Time for Pellet 41

tendency for two variables to be linearly related; perfect linearity being defined as 1.00000), are presented in Table 21. Figures 26 through 28 show the plots of $\Sigma a_n/A_0$ vs $\sqrt{\Sigma t_n}$ and the diffusion controlled region used in calculating the diffusion coefficients.

Table 21. Cesium Ion Diffusion Coefficients for Tracer Level Cesium-137 Aluminosilicate Pellets

Pellet No.	Fick's Law Straight Line Eq. $[E(y) = \beta_0 + \beta_1 x]$	Sample Correlation Coefficient (r)	Cesium Ion Diffusion Coefficient (m^2s^{-1})
39	$y = (-2705.28\pm66.65)\times10^{-5} + [(379.07\pm4.70)\times10^{-5}]x$	0.99931	1.29×10^{-16}
40	$y = (-997.96\pm31.49)\times10^{-5} + [(127.99\pm2.22)\times10^{-5}]x$	0.99916	6.88×10^{-17}
41	$y = (-2348.50\pm56.56)\times10^{-5} + [(267.87\pm3.88)\times10^{-5}]x$	0.99865	1.35×10^{-17}

The above diffusion coefficient values can be compared with that for the diffusion of sodium in a soft crystal such as silver chloride, where the coefficient is approximately $4\times10^{-15}m^2s^{-1}$. (Ref. 23)

The leach rates measured for the tracer level pellets compare favorably with the leach rates of 5.8 to 11.6×10^{-8} $kgm^{-2}s^{-1}$ for non-radioactive pellets reported by Sandia, which were performed under identical leaching conditions.

Phase II: Quasi-static Leaching of Gamma-irradiated Tracer Level Cesium-137 Pollucite Pellet Sections in Distilled Water [T = 94°C (367K)]

The tracer level ^{137}Cs aluminosilicate pellet sections, which had been leached for 368 days in Soxhlet extractors, were removed, dried, and then exposed to an intense, high energy (^{60}Co:γ_1 = 1.3325 Mev; γ_2 = 1.1732 Mev) gamma-ray field (206,000 R/hr) for 100 hours. The total dose of 2.06×10^7 R simulated the environment into which the pellets would be positioned in a sludge irradiator.

After the irradiation the tracer level pellet sections were reweighed and placed in their respective Soxhlet extractor sample cups and releached

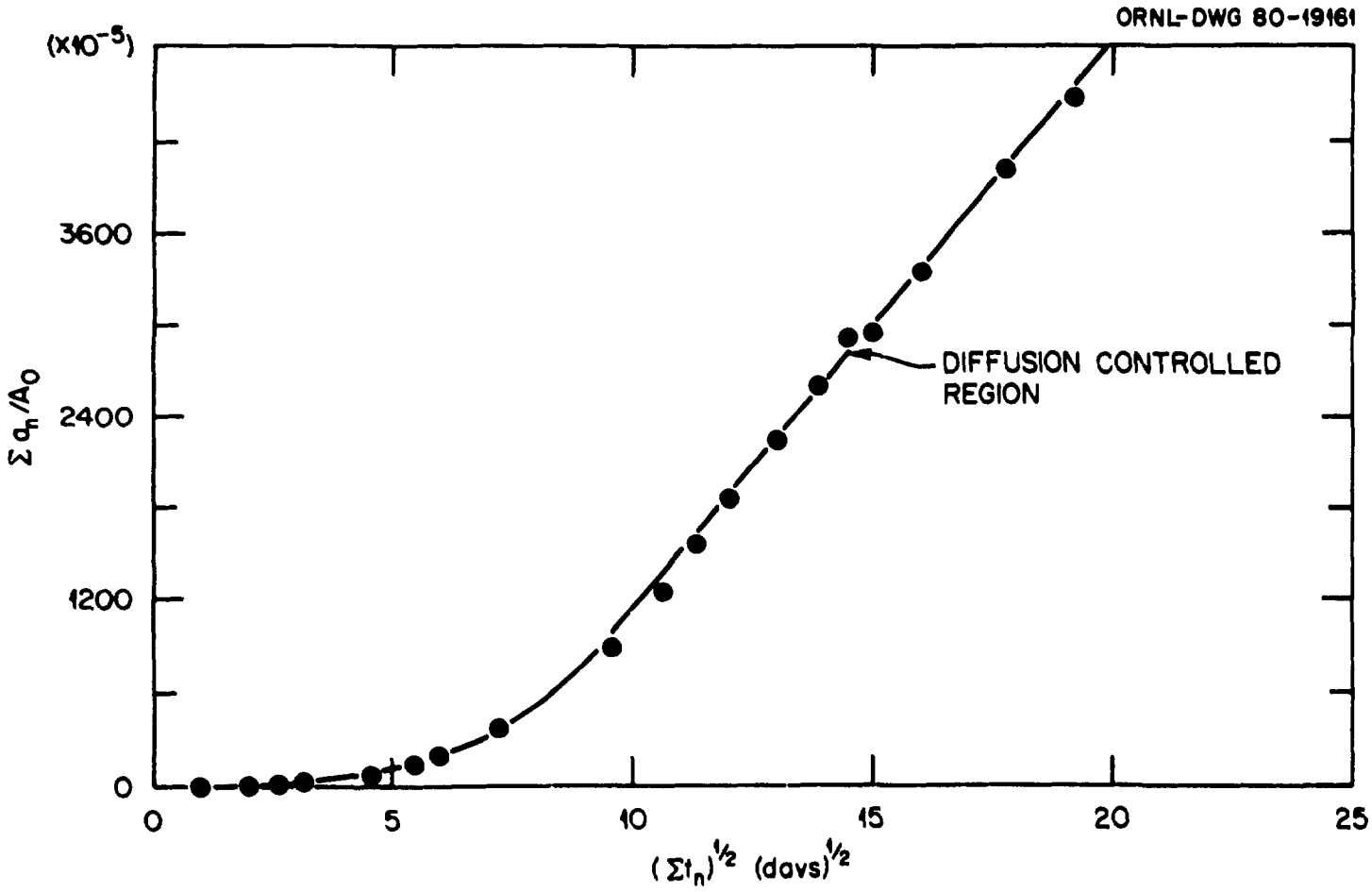

Fig. 26. Graph of $\Sigma a_n/A_0$ vs $\sqrt{t_n}$ for Pellet 39

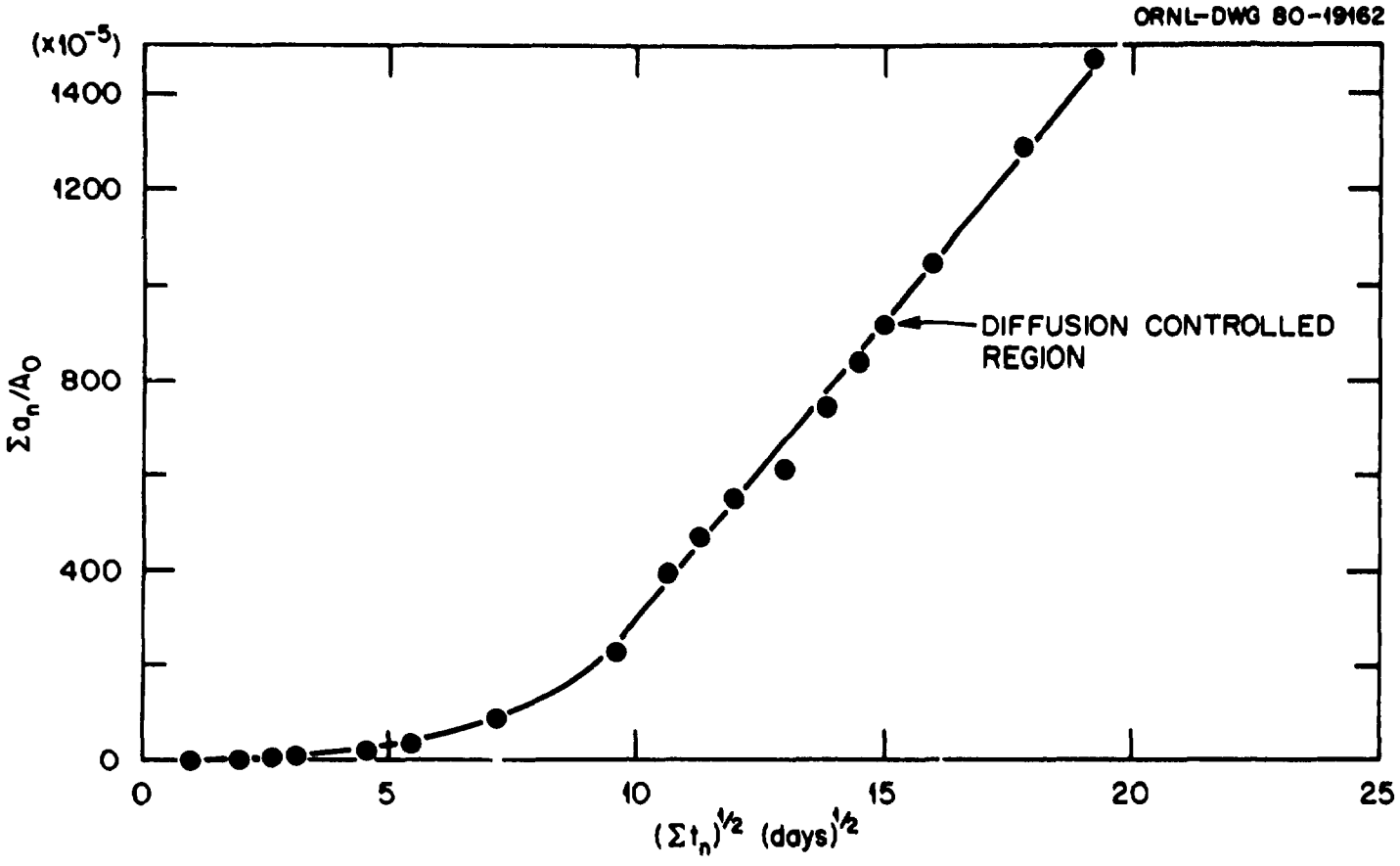

Fig. 27. Graph of $\Sigma a_n/A_0$ vs $\sqrt{t_n}$ for Pellet 40

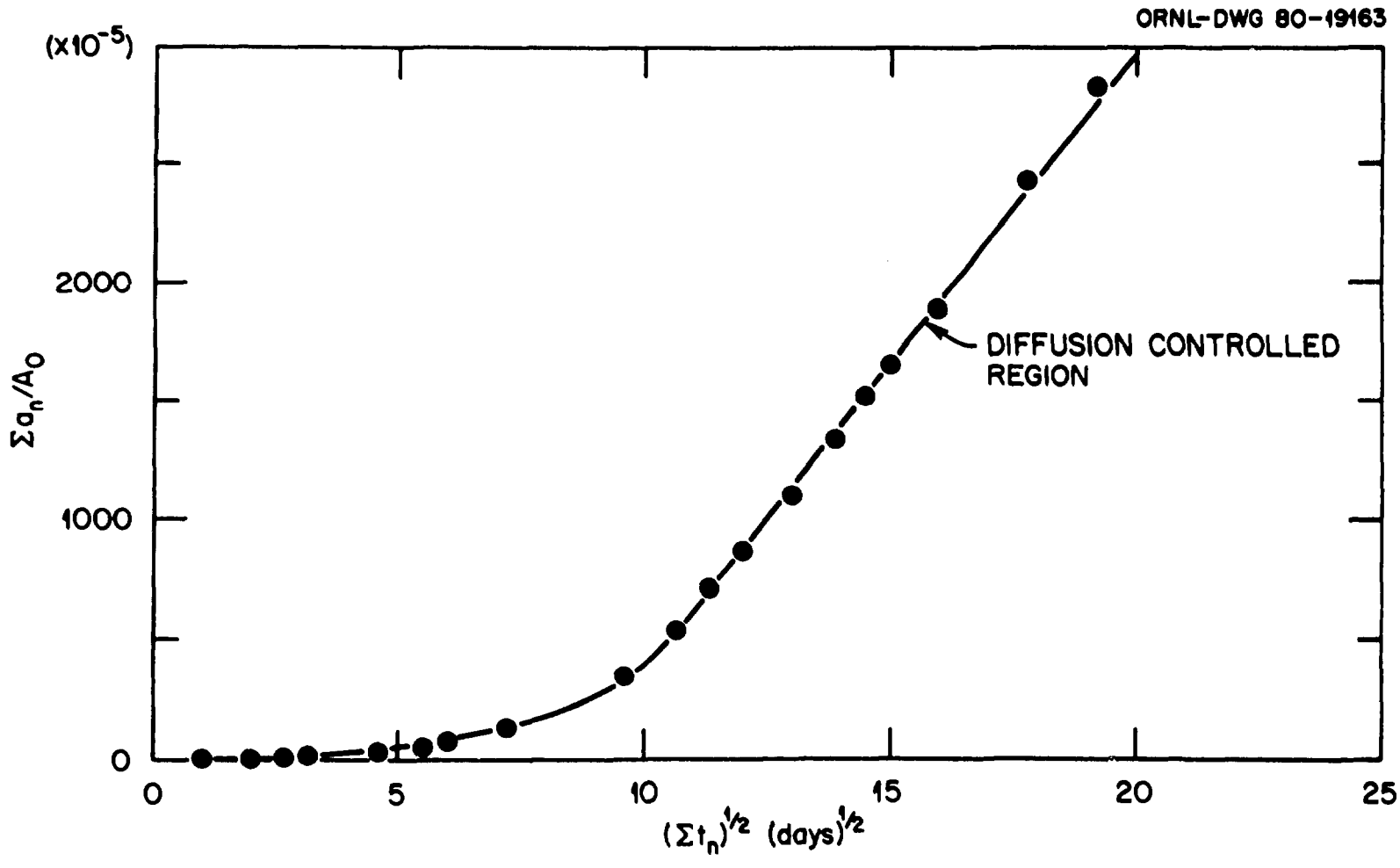

Fig. 28. Graph of $\Sigma a_n/A_0$ vs $\sqrt{t_n}$ for Pellet 41

under conditions idential to those which were employed before irradiation. The initial leach rates calculated for the pellet sections are given in Table 22. Plots of leach rates vs time for each irradiated pellet are shown in Figs. 29 through 31.

Table 22. Cesium Ion Leach Rates of Irradiated Tracer Level Cesium-137 Aluminosilicate Pellets

Leachant Renewal Period (days)	Accumulated Leaching Period (days)	Leach Rate ($kgm^{-2}s^{-1}$)		
		Pellet 39	Pellet 40	Pellet 41
0.980	0.980	4.05×10^{-8}	1.28×10^{-8}	2.24×10^{-8}
0.953	1.933	3.63×10^{-8}	1.36×10^{-8}	3.08×10^{-8}
1.008	2.941	3.77×10^{-8}	1.41×10^{-8}	3.19×10^{-8}
0.950	3.891	3.24×10^{-8}	1.50×10^{-8}	3.28×10^{-8}
3.024	6.915	3.19×10^{-8}	1.17×10^{-8}	2.47×10^{-8}
2.978	9.713	3.07×10^{-8}	1.09×10^{-8}	2.63×10^{-8}
4.979	14.692	2.74×10^{-8}	3.13×10^{-9}	2.32×10^{-8}

A comparison of the leach rates of the tracer level pellets before and after irradiation in the high energy gamma-ray field is shown in Table 23. The comparison to date reveals essentially no difference (within experimental error) between the leach rates of the non-irradiated and irradiated pellet sections. This suggests that the high energy gamma-ray field had little or no effect on the cesium leachability of the aluminosilicate pellet. Leaching of the irradiated pellet sections is continuing and more conclusive results will become available.

Table 23. Cesium Ion Leach Rates of Non-Irradiated and Irradiated Tracer Level Cesium-137 Aluminosilicate Pellets

Pellet No.	Accumulated Leaching Period (days)	Leach Rate ($kgm^{-2}s^{-1}$)
39, non-irradiated	368	2.65×10^{-8}
39, irradiated	15	2.74×10^{-8}
40, non-irradiated	368	1.02×10^{-8}
40, irradiated	10	1.09×10^{-8}
41, non-irradiated	368	2.34×10^{-8}
41, irradiated	15	2.32×10^{-8}

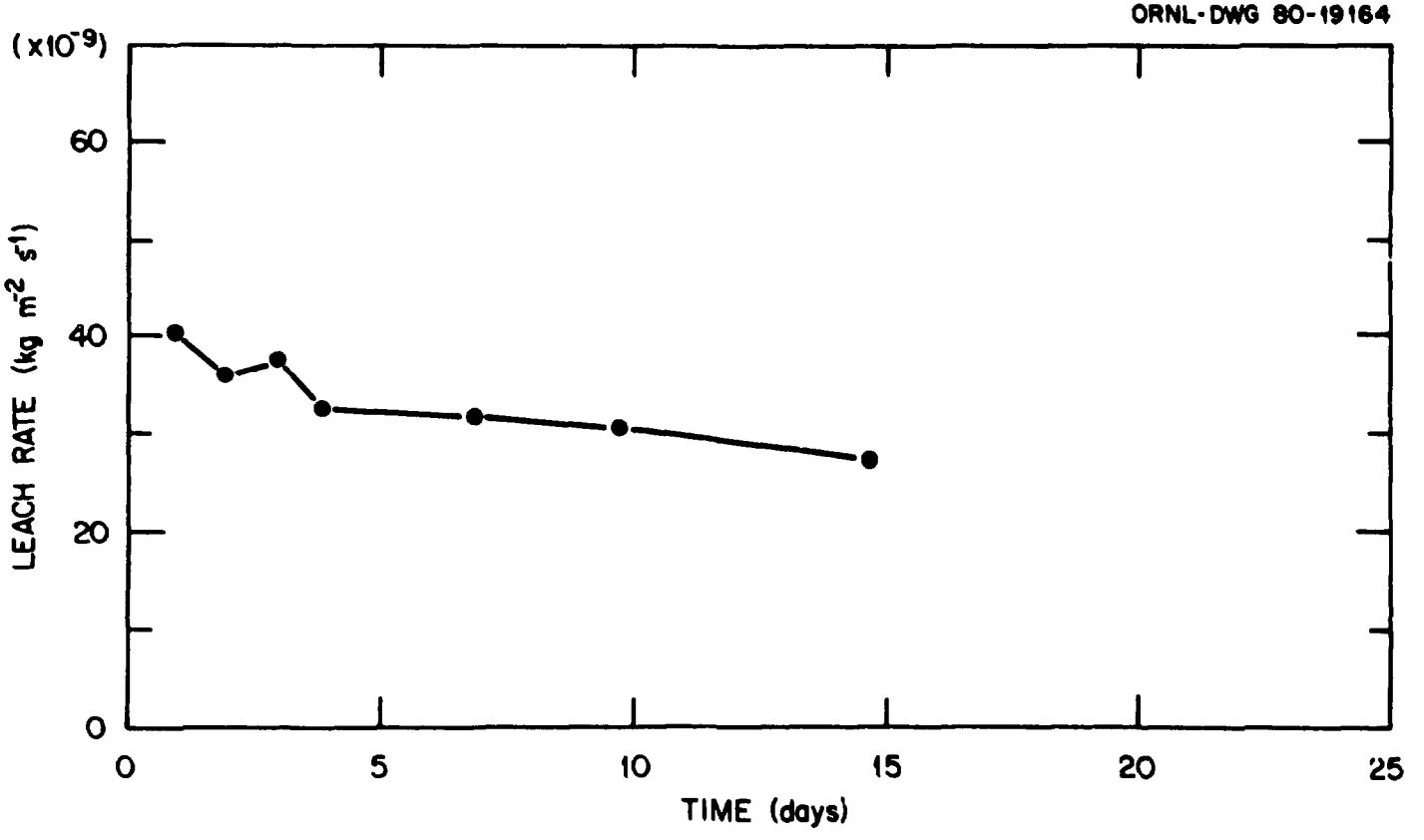

Fig. 29. Graph of Cesium Leach Rate vs Time for Irradiated Pellet 39

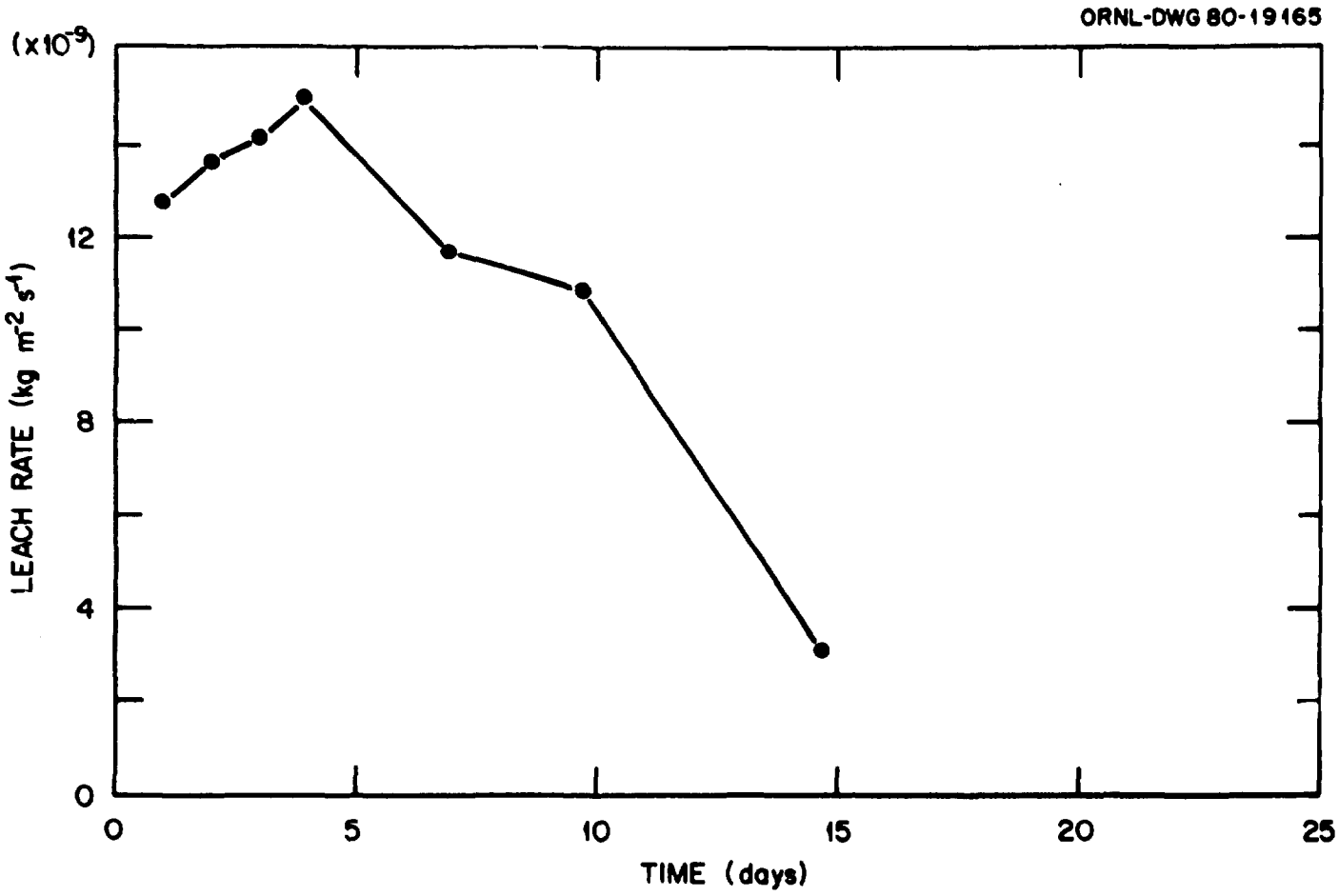

Fig. 30. Graph of Cesium Leach Rate vs Time for Irradiated Pellet 40

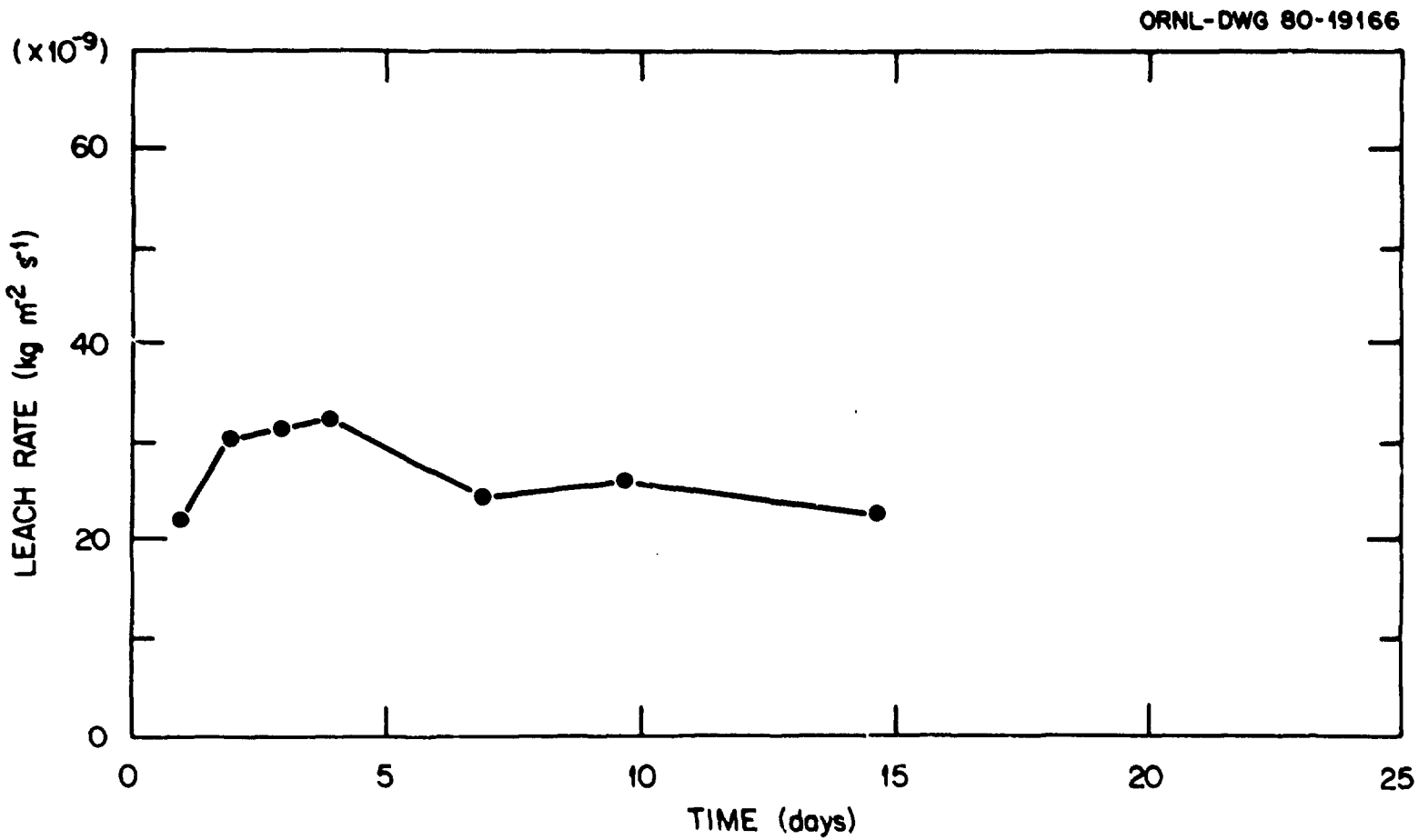

Fig. 31. Graph of Cesium Leach Rate vs Time for Irradiated Pellet 41

Phase III: Quasi-static Leaching of Full Level Cesium-137 Pollucite Pellet Sections in Distilled Water [T = 94°C (367K)]

The sections of the four test pellets which had been selected for cesium leachability measurements were leached in Soxhlet extractors containing 250 ml of distilled water at a temperature of approximately 94°C (367K). The leachability measurements are continuing and the leach rates calculated to date are given in Table 24. Plots of leach rate vs time for each pellet are presented in Figs. 32 through 35.

Table 24. Fully Loaded Cesium-137 Aluminosilicate Pellet Soxhlet Cesium Ion Leach Rates

Leachant Renewal Period (days)	Accumulated Leaching Period (days)	Leach Rate ($kgm^{-2}s^{-1}$)			
		Pellet C1	Pellet C2	Pellet C3	Pellet C4
1.007	1.007	9.96×10^{-10}	1.01×10^{-9}	3.81×10^{-10}	1.22×10^{-9}
2.948	3.955	8.65×10^{-10}	1.40×10^{-9}	4.91×10^{-10}	1.78×10^{-9}
2.906	6.861	9.41×10^{-10}	1.67×10^{-9}	6.15×10^{-10}	2.96×10^{-9}
4.905	11.766	2.33×10^{-9}	2.04×10^{-9}	7.35×10^{-10}	3.63×10^{-9}
2.913	14.679	2.49×10^{-9}	2.34×10^{-9}	1.01×10^{-9}	3.38×10^{-9}
4.905	19.584	2.81×10^{-9}	2.03×10^{-9}	7.27×10^{-10}	3.41×10^{-9}
7.911	27.495	1.80×10^{-11}	2.65×10^{-9}	1.02×10^{-9}	3.30×10^{-9}
5.898	33.393	1.35×10^{-10}		1.34×10^{-9}	3.48×10^{-9}
6.932	40.325	1.54×10^{-8}	3.66×10^{-9}	1.07×10^{-9}	2.99×10^{-9}
6.901	47.226	4.18×10^{-9}	3.15×10^{-9}	5.64×10^{-10}	3.23×10^{-9}
12.974	60.200	4.61×10^{-10}	1.10×10^{-9}	7.16×10^{-10}	3.44×10^{-9}

The leach rate reported for pellet C4 is higher by a factor of approximately 4 to 10 than those reported for the remaining three pellets. This discrepancy can be explained by the increased porosity inherited by pellet C4 (see Fig. 13). The higher porosity of the pellet provides additional exit pathways for the cesium ion out of the pollucite pellet. As can be seen from a comparison of the leach rates reported in Tables 23 and 24 the cesium ion leach rates for the fully loaded ^{137}Cs production pellets range from approximately 10 to 100 times lower than those for the experimental tracer level pellets. This indicates that the production pellets have incorporated the cesium more tightly into the crystal lattice structure. One must keep in mind that the tracer level pollucite pellets selected for cesium leachability measurements were not of the highest quality experimental pellets produced, but were selected based upon availability.

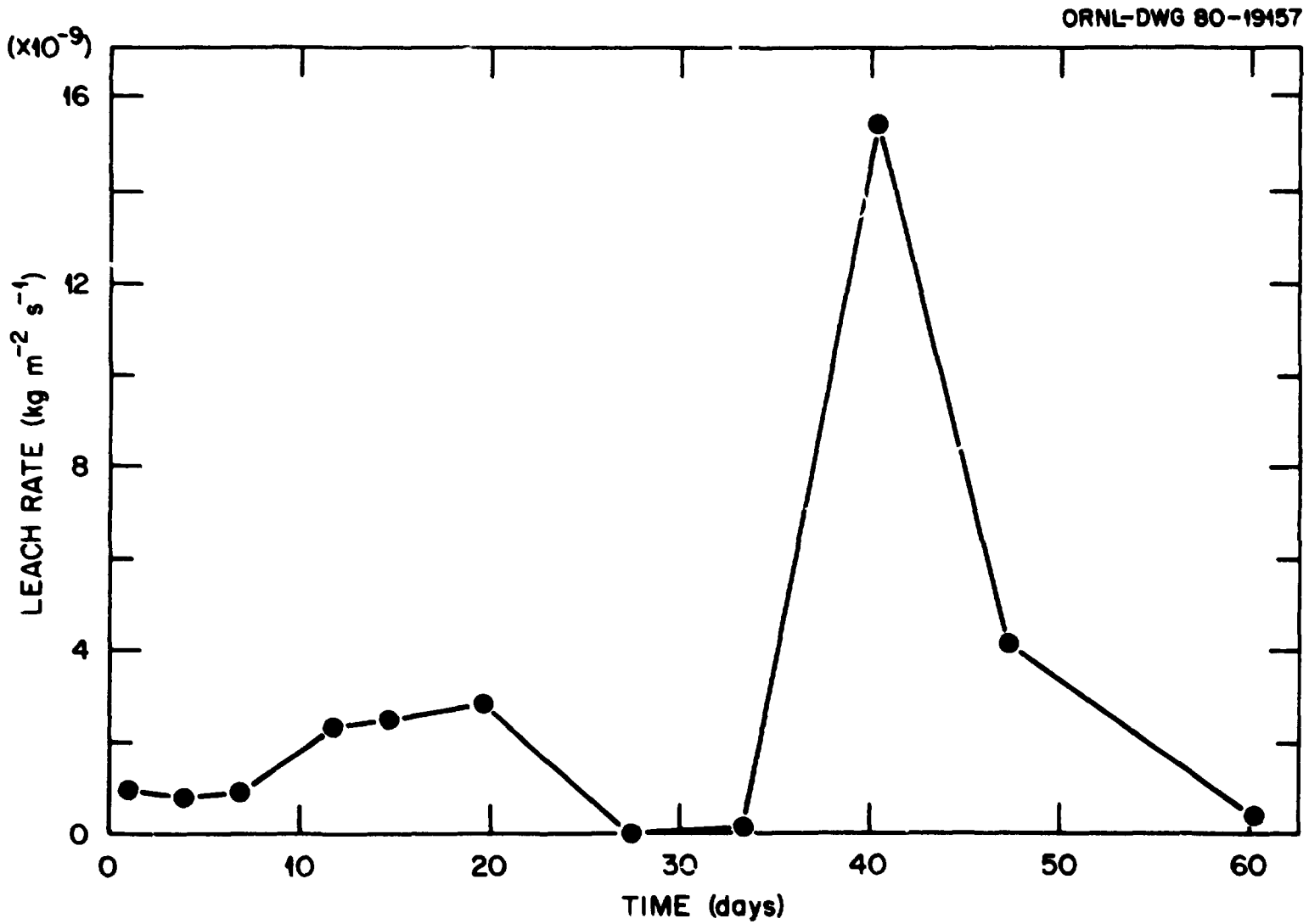

Fig. 32. Graph of Cesium Leach Rate vs Time for Pellet C1

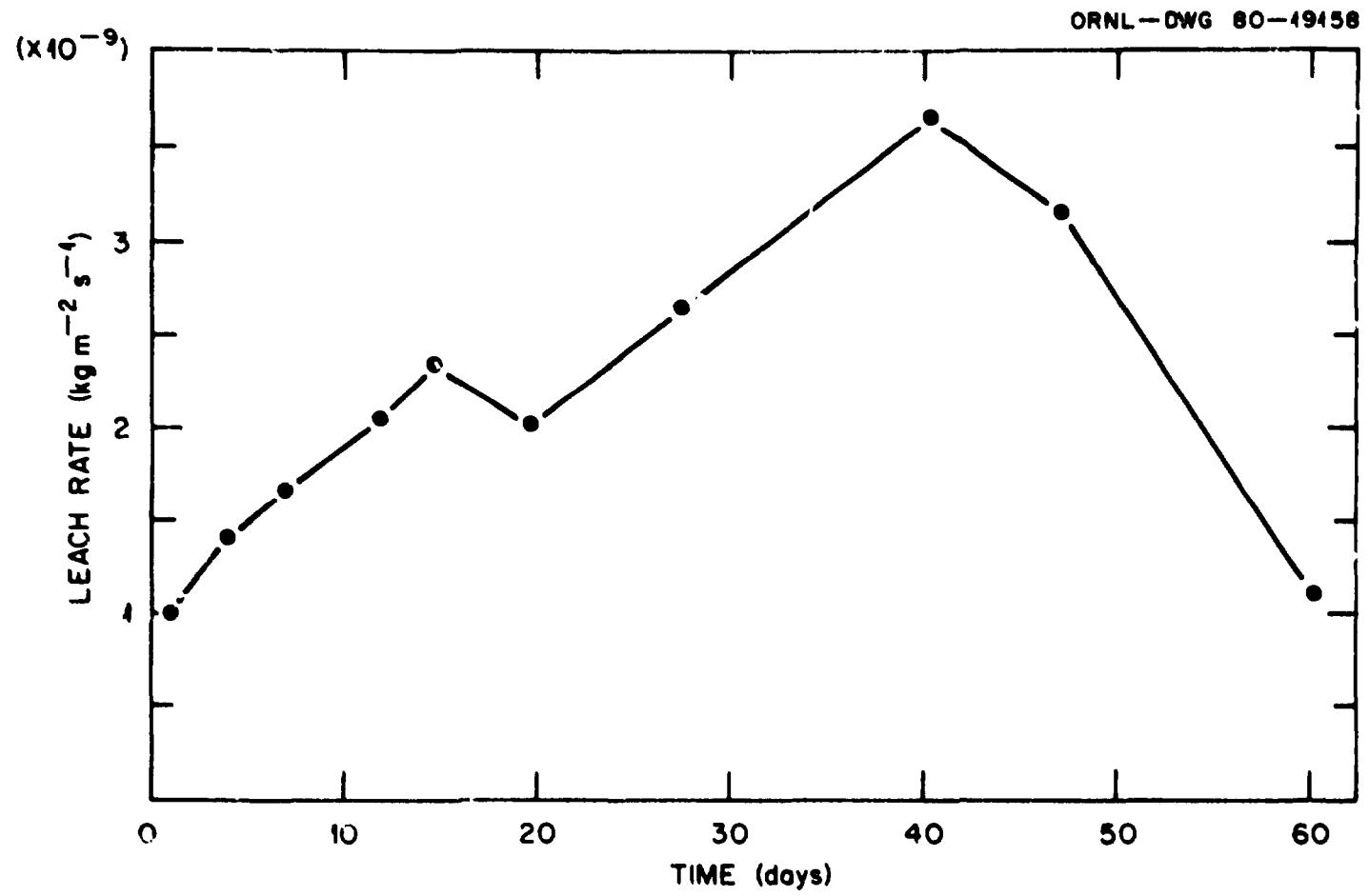

Fig. 33. Graph of Cesium Leach Rate vs Time for Pellet C2

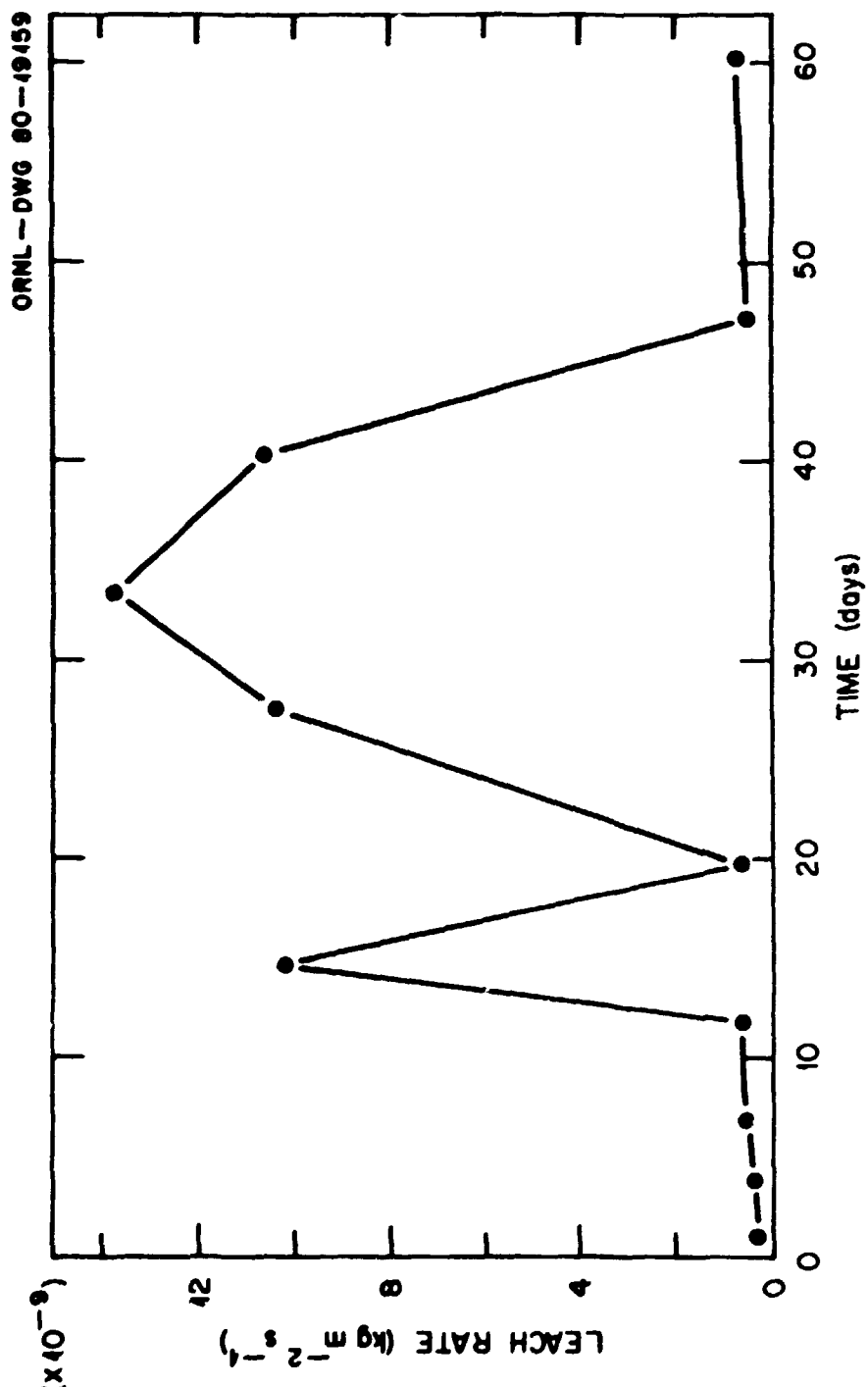

Fig. 34. Graph of Cesium Leach Rate vs Time for Pellet C3

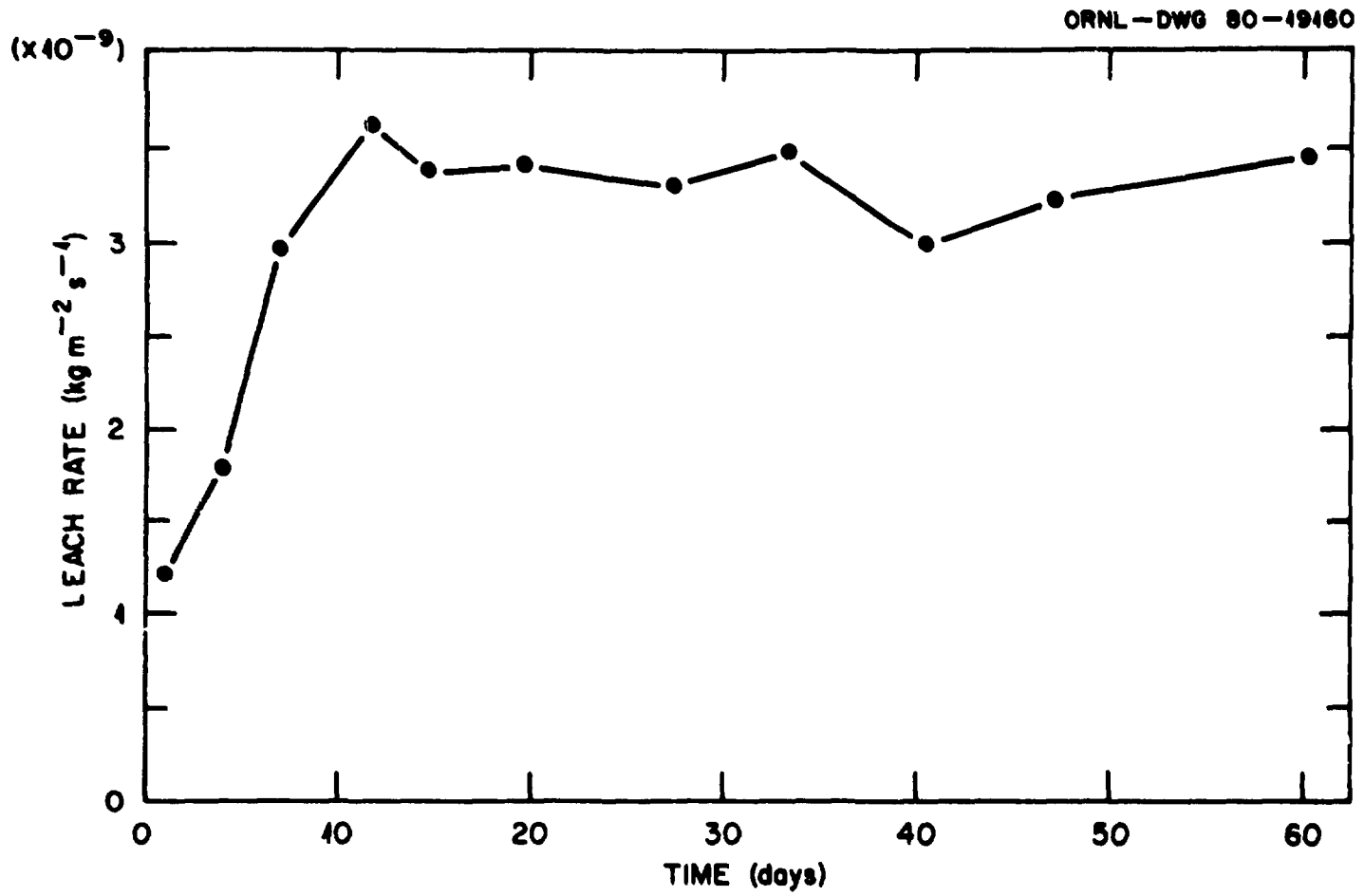

Fig. 35. Graph of Cesium Leach Rate vs Time for Pellet C4

A comparison of the fully loaded pellets' leach rates with the leach rates of stable (non-radioactive) pollucite pellets reported by Sandia is presented in Table 25.

Table 25. Comparison of Cesium Ion Leach Rates of Stable and Fully Loaded Aluminosilicate Pellets

Leachability Measurements	Accumulated Leaching Period (days)	Range of Leach Rates ($kgm^{-2}s^{-1}$)
Tracer level	368	$1.02 - 2.65 \times 10^{-8}$
Fully loaded	60.2	$4.61 - 34.4 \times 10^{-10}$
Stable		$5.8 - 11.6 \times 10^{-8}$

The leachability measurements of cesium out of the fully loaded ^{137}Cs pollucite reveal a leach rate which ranges from 33 to 125 times lower than that measured for the stable (non-radioactive) cesium pollucite pellets, while the leach rates obtained for the tracer level pellets range from approximately 4 to 6 times lower than those obtained for the stable pellets. This comparison indicates that the cesium ion is bound more tightly in the fully loaded pellet than in the other two types of pellets examined and, therefore, presents a substantial improvement in pellet quality.

Phase IV: Static Leaching of Full Level, Unsectioned Cesium-137 Pollucite Pellets in Distilled Water [T = 90°F (305K)]

Two unsectioned, fully loaded ^{137}Cs aluminosilicate pellets were selected for static cesium ion leachability measurements and were leached under the conditions discussed earlier. The leach rates obtained for pellets F1 and F2 are given in Tables 26 and 27, respectively. Plots of leach rates vs time for both pellets are given in Figs. 36 and 37.

The leach rates after initial surface decontamination are approximately 100 times lower than those for the fully loaded sectioned pellets exposed to refluxing distilled water in a Soxhlet extractor. The grafoil sheath surrounding the unsectioned pellets may, at least partially, account for the lower leach rates observed thus far. A final comparison of the cesium ion leach rates for all four phases and those reported for the non-radioactive pollucite are found in Table 28.

Table 26. *Unsectioned, Fully Loaded Cesium-137* Aluminosilicate Pellet Static Cesium Ion Leach Rates — Pellet F1

Leachant Renewal Period (days)	Accumulated Leaching Period (days)	Leach Rate ($kgm^{-2}s^{-1}$)
0.118	0.118	6.79×10^{-9}
0.110	0.228	3.09×10^{-9}
0.799	1.027	3.66×10^{-10}
0.196	1.223	1.35×10^{-10}
0.756	1.979	4.07×10^{-11}
0.237	2.216	2.92×10^{-11}
0.730	2.946	1.07×10^{-11}
0.210	3.156	1.29×10^{-11}
0.784	3.940	8.22×10^{-12}
0.270	4.210	9.95×10^{-12}
2.719	6.929	3.41×10^{-12}
1.000	7.929	1.82×10^{-12}
1.033	8.962	3.10×10^{-12}
0.969	9.931	2.92×10^{-12}
0.994	10.925	3.27×10^{-12}
3.043	13.968	2.19×10^{-12}
3.026	16.994	1.55×10^{-12}
4.926	21.920	3.81×10^{-12}
3.050	24.970	2.48×10^{-12}
6.988	31.958	2.25×10^{-12}

Table 27. Unsectioned, Fully Loaded Cesium-137 Aluminosilicate Pellet Static Cesium Ion Leach Rates — Pellet F2

Leachant Renewal Period (days)	Accumulated Leaching Period (days)	Leach Rate ($kgm^{-2}s^{-1}$)
0.113	0.113	7.16×10^{-9}
0.108	0.221	2.61×10^{-9}
0.797	1.018	4.93×10^{-10}
0.197	1.215	3.94×10^{-10}
0.756	1.971	7.63×10^{-11}
0.237	2.208	3.60×10^{-11}
0.731	2.939	2.00×10^{-11}
0.208	3.147	2.91×10^{-11}
0.788	3.935	1.91×10^{-11}
0.267	4.202	2.60×10^{-11}
2.763	6.965	9.90×10^{-12}
0.958	7.923	1.20×10^{-12}
1.031	8.954	7.09×10^{-12}
0.972	9.926	4.29×10^{-12}
0.950	10.876	5.17×10^{-12}
3.052	13.928	6.54×10^{-12}
3.024	16.952	1.81×10^{-12}
4.927	21.879	3.58×10^{-12}
3.050	24.929	2.66×10^{-12}

Table 28. Cesium Pollucite Static and Quasi-Static Cesium Ion Leach Rates

Leachability Measurement	Accumulated Leaching Period (days)	Leach Rates ($kgm^{-2}s^{-1}$)
Stable — Soxhlet		$5.8 - 11.6\times10^{-8}$
Tracer Level — Soxhlet (Phase I)	368	$1.02 - 2.65\times10^{-6}$
Gamma-Irradiated Tracer Level — Soxhlet (Phase II)	15	$3.13 - 27.4\times10^{-9}$
Fully Loaded — Soxhlet (Phase III)	60.2	$4.61 - 34.4\times10^{-10}$
Fully Loaded — Static (Phase IV)	25	$2.48 - 2.66\times10^{-12}$

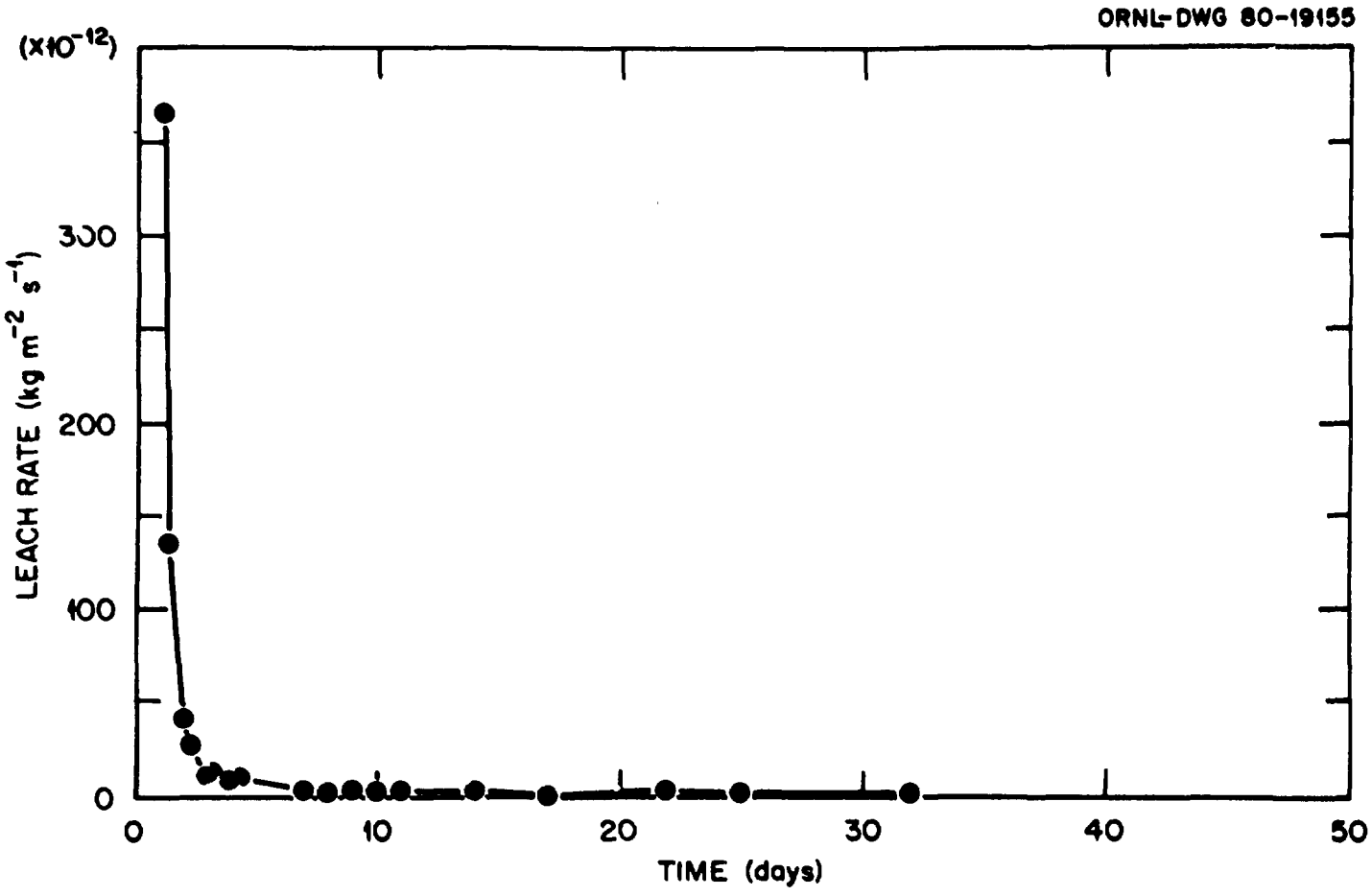

Fig. 36. Graph of Cesium Leach Rate vs Time for Pellet F1

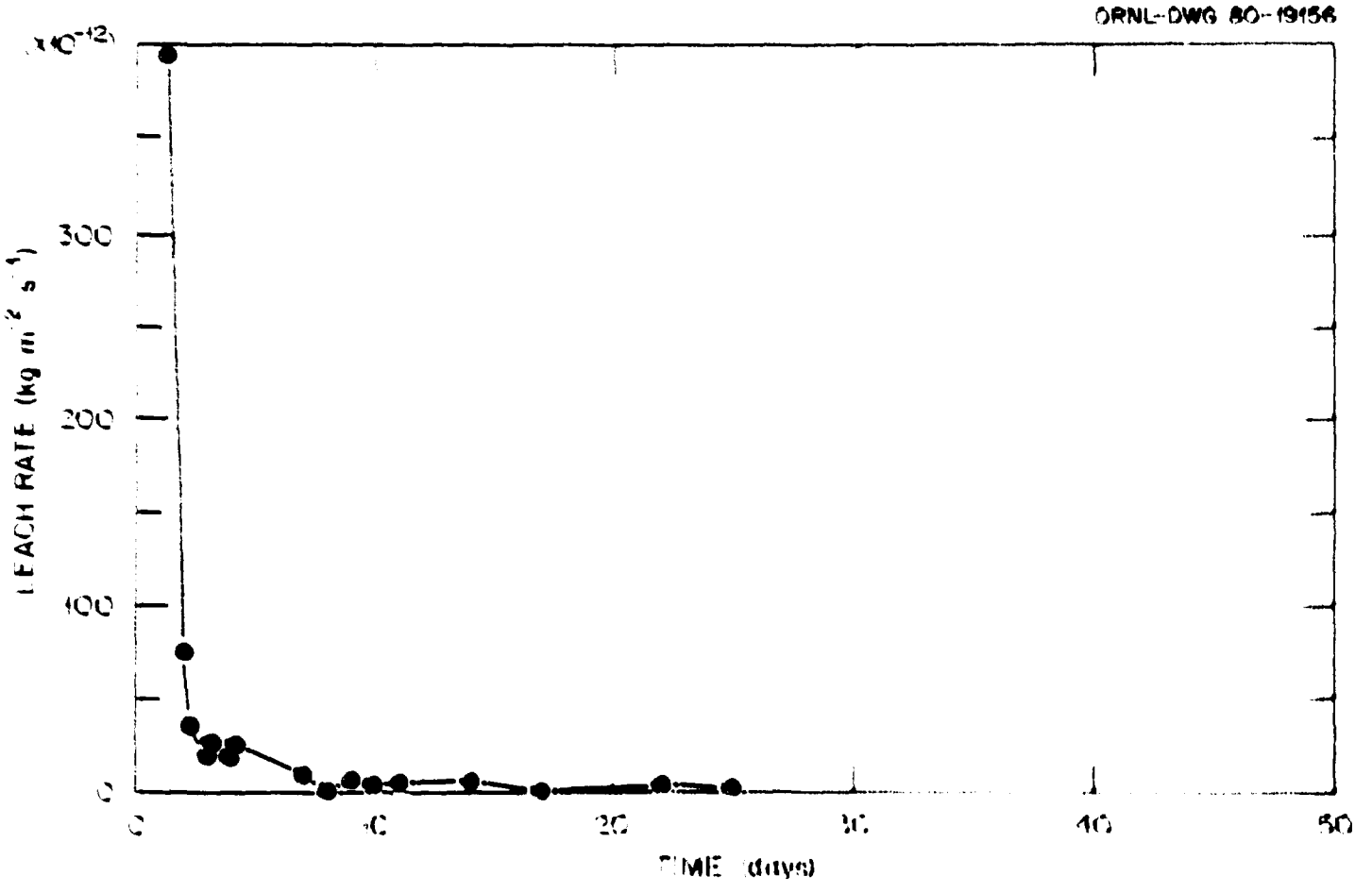
ORNL-DWG 80-19156
300
200
100
0
0
10
20
30
40
50
TIME (days)

SUMMARY

In all 27 fully loaded ^{137}Cs aluminosilicate pellets were fabricated in the hot cell using the large vacuum hot press under the production run conditions listed in Table 10. Each pellet, having dimensions 1 1/8 in. (2.86 cm) height by 1 in. (2.54 cm) diameter, and weighing 40 to 42 grams, contained 437 to 450 curies of ^{137}Cs as determined by calorimetric measurements. The uncorrected (not corrected for weight and volume of surrounding grafoil sheath) densities of the recovered full level ^{137}Cs pollucite pellets ranged from 2.75 to 3.00 g/cm^3 (2750 to 3000 kg/m^3).

The full level ^{137}Cs pollucite production pellets were characterized by calorimetry, metallography, SEM-BSE and electron microprobe, X-ray diffraction, and cesium ion leachability measurements for the purposes and objectives outlined in Table 14.

Calorimetric measurements performed on the four selected full level test pellets provided the ^{137}Cs curie content of each pellet (Table 16). From this data and the weights and densities of the four test pellets, Table 29, containing some useful pollucite pellet radioisotopic characteristics was constructed.

Table 29. Fully Loaded Cesium-137 Pollucite Pellet Data Sheet

	Pollucite Pellet			
	C1	C2	C3	C4
Corrected weight (g)[a]	41.24	40.40	40.35	39.00[b]
Content (Ci)	450	444	444	437
Curies ^{137}Cs/g of pollucite	10.9	11.0	11.0	11.2
Curies ^{137}Cs/cm^3 of pollucite	33.1	32.6	32.6	32.1
Curies ^{137}Cs/g of cesium	29.1	29.3	29.3	29.9
Specific activity (Ci ^{137}Cs/g ^{137}Cs)	84.3	85.0	85.0	86.6
Grams ^{137}Cs/g pollucite	5.34	5.23	5.22	5.04
Percent of Theoretical specific activity	96.9	97.6	97.7	99.5

[a]Corrected for weight and volume of surrounding grafoil sheath.

[b]Grafoil sheath was removed during the pellet extraction process.

A comparison of radioisotopic characteristics between the process starting material, CsCl, and the final product, $CsAlSi_2O_6 \cdot nH_2O$, is given in Table 30.

Table 30. Equivalence Table
(Comparison of $^{137}CsCl$ and ^{137}Cs-pollucite)

Chemical compound	^{137}Cs/g compound (Ci/g)	$^{137}Cs/cm^3$ compound (Ci/cm^3)	Specific activity (Ci ^{137}Cs/g ^{137}Cs)	Percent of theoretical specific activity[a]
CsCl	23.4	93.3	85.4	98.1
$CsAlSi_2O_6 \cdot nH_2O$[b]	11.0	32.6	85.2	97.9

[a]Theoretical specific activity of elemental ^{137}Cs is 87.06 Ci/g. Percent cesium in CsCl is 79.44%.

[b]Average values are reported.

Metallographic measurements of the four test pellets revealed a two-phase system. The primary, granular, gray matrix phase contained large and small pores and some small pore agglomerations, while the secondary, fused phase was sparsely interspersed throughout the gray matrix. A density gradient was also detected wherein an increase in pore (void) occurrence was noted as one scanned from the edge to the center of the pellet.

SEM-BSE (scanning electron microscope and electron backscattering) examinations of the full level pollucite production pellets showed cesium and silicon to be homogeneously distributed throughout the primary and secondary phases. Aluminum homogeneity was unconfirmed due to the high background noise associated with the inherent radioactivity of the test specimens. These results indicate that the cesium/silicon reaction went to completion during the vacuum hot pressing process step.

X-ray diffraction analysis of solid test specimens confirmed the crystal lattice structure to be pollucite ($CsAlSi_2O_6 \cdot nH_2O$)(Table 18).

Cesium ion leachability measurements were conducted to determine the leach rates of the cesium ion out of the aluminosilicate pellets. The analysis was divided into four phases (Table 19). The leach rates were calculated based on the assaying of the 661.64 keV gamma-ray of ^{137}Cs.

The leach rates obtained from each phase of the leachability measurements are given in Tables 20, 22, 24, 26, and 27. A comparison of the cesium ion leach rates is presented in Table 28.

The cesium ion diffusion coefficients through three tracer level pellets were calculated using Fick's first and second laws of diffusion. The diffusion coefficients obtained from a plot of the total amount of radioactivity lost from the specimen, divided by initial radioactivity present in specimen vs the square root of the total elapsed leaching time are given in Table 21. These values can be compared with that for the diffusion of sodium in a soft crystal such as silver chloride, where the diffusion coefficient for the sodium ion is approximately 4×10^{-15} $m^2 s^{-1}$.

REFERENCES

1. *Sandia Irradiator for Dried Sewage Solids*, Seminar Proc. and Dedication, Sandia Laboratory, SAND 79-0182 (Feb. 1979).

2. M. E. Morris, *Sandia Irradiator for Dried Sewage Solids*, Final Safety Analysis Report, SAND 79-2240 (July 1980).

3. M. C. Reynolds, R. L. Hagengruber, and A. C. Zuppero, *Thermoradiation Treatment of Sewage Sludge Using Reactor Waste Fission Products*, Sandia Laboratory, SAND 74-0001 (June 1974).

4. F. R. Fisher, E. S. Josephson, "Radiation Preservation of Foods Program", *Proc. Eighth Contractors' Meeting*, U.S. Army Natick Laboratory, Natick, Massachusetts, Oct. 7-9, 1963 (1964).

5. W. E. Sande and R. A. Libby, *Potential Sources for the Radiation Treatment of Food*, Battelle Northwest Laboratory, BNWL-SA-5850 (1976).

6. E. S. Josephson, "Health Aspects of Food Irradiation", paper presented at seminar held at Oak Ridge National Laboratory, July 24, 1980.

7. Final Report, "The Cesium-137 Power Program", AEC Research and Development Report SAN-366-1 (May 1964).

8. "Cesium-137 Purification Procedure", Oak Ridge National Laboratory, Operations Division, Radioisotope Department, Building 3517, Mar. 7, 1978.

9. "Preparation of Cesium-137 Carbonate for Use in the Fabrication of Pollucite Pellets", Oak Ridge National Laboratory, Operations Division, Radioisotope Department, Building 3517, Apr. 9, 1979.

10. "GK Technical Data Sheets", TD-40, Georgia Kaolin Co., Elizabeth, New Jersey.

11. A. B. Searle and R. W. Grimshaw, *The Chemistry and Physics of Clays and Other Ceramic Materials*, 3rd ed., Interscience Publishers, Inc., New York, 1959.

12. Personal communication, L. D. Hulett and F. L. Ball, Oak Ridge National Laboratory, Chemical Technology Division, to F. J. Schultz, Oak Ridge National Laboratory, Operations Division, "SEM-EDX Analysis of Cs-Al-Si Pellet," June 18, 1979.

13. Personal communication L. R. Walker, Oak Ridge National Laboratory, Chemical Technology Division to F. J. Schultz, Oak Ridge National Laboratory, Operations Division, Nov. 7, 1978.

14. T. C. Quinby, E. E. Pierce, R. C. McHenry, *Hot Press for Glove Box and Manipulator Cell Use*, ORNL-TM-1900 (Aug. 1967).

15. C. O. Fairchild and M. F. Peters, "Characteristics of Pyrometric Cones", *Journal of the American Ceramic Society*, Vol. 9, No. 11, Nov. 1926.

16. J. C. Posey, "Calorimetry for Measuring Radioactivity", *Isotopes and Radiation Technology*, Vol. 1, No. 1, 1963.

17. S. J. Rimshaw and E. E. Ketchen, *Cesium-137 Data Sheets*, ORNL-4186 (Dec. 1967).

18. Joint Committee on Powder Diffraction Standards, card file No. 25-193 and 25-194, 1975.

19. M. J. Kupfer and W. W. Schulz, *Fixation of Hanford Sludge by Conversion to Glass*, ARH-SA-285 (Mar. 1977).

20. R. C. Rastogi, et al., *Investigation of Materials and Methods for Fixation of Low and Medium Level Radioactive Waste in Stable Solid Media, Final Report*, BARC-400 (1969).

21. M. J. Bell, *An Analysis of the Diffusion of Radioactivity from Encapsulated Waste*, ORNL/TM-3232 (Feb. 1971).

22. J. E. Mendel, *A Review of Leaching Test Methods and the Leachability of Various Solid Media Containing Radioactive Wastes*, BNWL-1765 (July 1973).

23. "Fixation of Radioactivity in Stable, Solid Media", paper presented at meeting held at Johns Hopkins University, June 19-21, 1957.

24. Personal communication, J. Keith Johnstone, Geological Projects, Division 4537, Sandia Laboratory, Albuquerque, New Mexico to F. N. Case, Oak Ridge National Laboratory, Operations Division, Dec. 5, 1978.

APPENDIX A

Preforming Pre-Pollucite (Cesium Carbonate/Clay) Mixtures by "Cold Forming" and "Centrifuging" Methods

Method 1: "Cold Forming" Pre-Pollucite Paste

1. Add 30 ml distilled water to 49 g of dry pre-pollucite powder.
2. Load into a 1 in. steel die and press using 11,600 psig. Allow to air dry for approximately 1 hour.
3. Press out the cylinder and dry in an oven at 100°C for 8 hours.

A comparison between the dried and undried cylinders obtained using the above procedure is presented in Table A1.

Table A1. Dried and Wet Pre-Pollucite Cylinder Dimensions

	Weight (g)	Height (cm)	Diameter (cm)
Wet Cylinder	59.5	6.5	2.5
Dry Cylinder	41.5	6.0	2.2

Method 2: Centrifuging Pre-Pollucite Paste

1. Add 30 ml distilled water to 49 g of dry pre-pollucite powder.
2. Place 49.0 g of pre-pollucite paste in a centrifuge tube.
3. Centrifuge the paste for two minutes at medium setting. Decant excess water.

A table giving some typical centrifuged cylinders (or rods) dimensions is presented in Table A2. The length of each rod is approximately 7.6 cm (3 in.).

Table A2. Dimensions of Some Typical Centrifuged Cylinders

Cylinder No.	Dry Weight (g)	Diameter [in. (cm)]
1	35.5	27/32 (2.14)
2	35.7	7/8 (2.22)
3	36.0	7/8 (2.22)
4	36.0	29/32 (2.30)

The advantages of the paste techniques over loading dry powder into the die are listed below.

1. Facilitates loading of the pre-pollucite mixture into the die.
2. Prevents any powder from lodging in between the grafoil liner and the bore hole of the die causing pellet extraction difficulties.
3. Minimizes cell contamination.
4. Less likely of mixture loss due to spillage.

APPENDIX B

Discussion and Derivation of Cesium Carbonate-Aluminosilicate Clay Ratio Calculation

The optimum quantity of Cs^+ desired in the final pollucite product pellet is weight factor 0.375. This value was reported by Sandia Laboratories[24] as one which would produce a pollucite pellet with the desired characteristics. The general chemical formula for pollucite is $CsAlSi_2O_6 \cdot nH_2O$ (an aluminosilicate hydrate). In the unhydrated (no waters of hydration, n = 0) the weight percent of cesium is 42.6%. However, pellets fabricated incorporating this weight percent of cesium (40% – 43%) tended to be brittle, easily fractured, white in color, and the cesium (as hydroxide) easily leached out of the pellet by contact with water. If one considers that the pollucite crystal lattice structure contains two waters of hydration (i.e., n = 2), the weight percent of cesium contained in the pollucite is reduced to 38.2%. Therefore, the optimum 37.5 wt % reported by Sandia for producing high quality pollucite pellets takes into account the waters of hydration and thus results in little excess cesium which would be subject to the action of leaching agents.

From the above discussion an equation for the correct quantity of montmorillonite clay (GWL) to be added to the cesium carbonate can now be formulated.

$$\frac{\text{grams of } Cs^+}{\text{grams of GWL + grams of } Cs^+} = 0.375 \qquad \text{(B1)}$$

But,

$$\text{grams of } Cs^+ = (\text{weight fraction } Cs^+ \text{ in } Cs_2CO_3)(\text{grams of } Cs_2CO_3) \qquad \text{(B2)}$$

Substituting Eq. (2) into Eq. (1) yields

$$\frac{(\text{weight fraction } Cs^+ \text{ in } Cs_2CO_3)(\text{g } Cs_2CO_3)}{\text{g GWL} + (\text{weight fraction } Cs^+ \text{ in } Cs_2CO_3)(\text{g } Cs_2CO_3)} = 0.375 \qquad \text{(B3)}$$

Expanding the above expression gives

$$(\text{g GWL})(0.375) + (0.375)(\text{weight fraction } Cs^+ \text{ in } Cs_2CO_3)(\text{g } Cs_2CO_3) =$$

$$= (\text{weight fraction } Cs^+ \text{ in } Cs_2CO_3) \times (\text{g } Cs_2CO_3) \; . \qquad \text{(B4)}$$

Rearranging and combining similar terms gives the final expression

$$\text{g GWL} = \left[\left(\frac{1}{0.375}\right)(\text{weight fraction } Cs^+ \text{ in } Cs_2CO_3)(\text{g } Cs_2CO_3)\right] - \left[\left(\frac{0.375}{0.375}\right)(\text{weight fraction } Cs^+ \text{ in } Cs_2CO_3) \times (\text{g } Cs_2CO_3)\right]$$

$$= \left(\frac{1}{0.375} - 1\right)(\text{weight fraction } Cs^+ \text{ in } Cs_2CO_3)(\text{g } Cs_2CO_3)$$

$$\boxed{\text{g GWL} = (1.667)(\text{weight fraction } Cs^+ \text{ in } Cs_2CO_3)(\text{g } Cs_2CO_3)} \qquad \text{(B5)}$$